

A MOBILE 3D PRINTER FOR LARGE-SCALE COLLABORATIVE ADDITIVE MANUFACTURING

by

Yun Chai

A Thesis Submitted in Partial Fulfillment of the Requirements for the Degree of
Master of Engineering in Industrial and Manufacturing Engineering

Examination Committee: Dr. Pisut Koomsap(Chairperson)
Prof. Huynh Trung Luong
Dr. Mongkol Ekpanyapong

Nationality: Chinese

Previous Degree: Bachelor of Engineering
Shanghai Ocean University
Shanghai, China

Scholarship Donor: China Scholarship Council(CSC)

Asian Institute of Technology
School of Engineering and Technology
Thailand

December 2022

AUTHOR'S DECLARATION

I, Yun Chai, declare that the research work carried out for this thesis was in accordance with the regulations of the Asian Institute of Technology. The work presented in it are my own and has been generated by me as the result of my own original research, and if external sources were used, such sources have been cited. It is original and has not been submitted to any other institution to obtain another degree or qualification. This is a true copy of the thesis, including final revisions.

Date: 06. 12. 2022

Name (in printed letters): Yun Chai

Signature: Yun Chai

ACKNOWLEDGMENTS

First and foremost, I would like to express my deep and sincere gratitude to my research advisor, Dr. Pisut Koomsap. Studying for a master degree in a foreign country is novel but not easy, especially in the past two years when the pace of everybody's life was disrupted by the epidemic. During this period, my advisor kept giving me unique inspiration, positive encouragement and careful guidance, which enabled me to grow in life and work, not just limited to course study and project research.

I would also like to express my gratitude to my committee members Dr. Huynh Trung Luong and Dr. Mongkol Ekpanyapong. They have continued to supervise and guide me at the beginning of my research, until a complete ending is reached.

I would like to express my gratitude to the China Scholarship Council and Erasmus+ Programme of the European Union for providing me with tuition and research funding. Without their financial support, my research and thesis would not have been completed, and my life journey would have been missing such an important part. It was they who gave me valuable opportunities and wealth and guided me to the next stage of my life.

I would also like to be grateful to all the professors, secretaries, staff in the ISE department and all the members of the A-Cube team I am part of. They provided me the pleasant research environment to be creative in the lab. In addition, their help, advice, and encouragement to me are constantly motivating me to move forward.

Endless gratitude goes also to my family and friends who have always supported me in my home country. Their comfort is my sweet medicine, and their encouragement is my driving force. It is because of their concern that I have the courage to stand up quickly after a fall and continue to face any difficulties.

ABSTRACT

Over the past few decades, additive manufacturing (AM) has grown rapidly as a latecomer and is now an integral part of modern manufacturing industry. While additive manufacturing takes advantage of the incomparable advantages of traditional manufacturing methods, it always suffers from poor efficiency and scalability. Mobility and collaboration were introduced and validated by researchers to increase the flexibility of AM devices, effectively increasing the efficiency and scalability of this technology. Since then, it has become possible to conduct large-scale collaborative additive manufacturing with mobile AM devices. However, the combination of mobility and collaboration also places higher requirements on the positioning accuracy of AM devices. In large-scale collaborative additive manufacturing processes, more errors of all causes are more likely to arise than ever and lead to manufacturing failures, especially under uneven fabrication conditions. This research proposes some certain technical solutions, and analyzes in detail the causes and effects of various errors in large-scale collaborative additive manufacturing in three-dimensional space. According to the source of error formation, two error control concepts, "positioning error correction" and "leveling error correction", are proposed. To verify the validity of the two concepts and corresponding strategies for large-scale collaborative additive manufacturing, a modular mobile 3D printer equipped with technical methods corresponding to the concepts was designed and developed. A set of experiments based on the laboratory environment was carried out to verify the error reduction effect of the developed device. The inspiration for the concept, the process of development, the design of the experiment and the result are described in detail in this paper. Ultimately, the developed device was shown to greatly reduce all of the potential errors during operation. This also means that the proposed concepts can be further generalized to various additive manufacturing technologies and better serve large-scale collaborative additive manufacturing.

CONTENTS

| | Page |
|--|-------------|
| ACKNOWLEDGMENTS | iii |
| ABSTRACT | iv |
| LIST OF TABLES | viii |
| LIST OF FIGURES | ix |
| LIST OF ABBREVIATIONS | xii |
| CHAPTER 1 INTRODUCTION | 1 |
| 1.1 Background of the Study | 1 |
| 1.2 Problem Statement | 3 |
| 1.3 Objective of the Study | 7 |
| 1.4 Scope and Limitation | 7 |
| CHAPTER 2 LITERATURE REVIEW | 8 |
| 2.1 Additive Manufacturing | 8 |
| 2.1.1 Current Status of Large-scale Additive Manufacturing | 9 |
| 2.1.2 Applications of Large-scale Additive Manufacturing | 13 |
| 2.2 Collaboration | 17 |
| 2.2.1 The Role of Collaboration in Manufacturing | 18 |
| 2.2.2 Collaboration in Additive Manufacturing | 19 |
| 2.3 Mobility | 21 |
| 2.3.1 The Role of Mobility in Manufacturing | 21 |
| 2.3.2 Mobility in Additive Manufacturing | 23 |
| CHAPTER 3 METHODOLOGY | 26 |
| 3.1 Idea Generation | 26 |
| 3.2 Technical Solutions | 29 |
| 3.2.1 Position Control Solutions | 29 |
| 3.2.2 Attitude Control Solutions | 30 |
| 3.3 Error Source and Reflection Analysis | 34 |
| 3.3.1 Distance Error Classification and Analysis | 35 |

| | Page |
|---|-------------|
| 3.3.2 Angle Error Classification and Analysis | 37 |
| 3.3.3 Summary of Error Types and Causes | 39 |
| 3.4 Positioning Error Correction | 40 |
| 3.4.1 Distance Error Control | 41 |
| 3.4.2 Angle Error Control | 43 |
| 3.5 Leveling Error Correction | 44 |
| 3.5.1 Distance Error Control | 45 |
| 3.5.2 Angle Error Control | 47 |
| CHAPTER 4 SYSTEM DEVELOPMENT | 50 |
| 4.1 Modular Mobile Platform: Automated Guided Vehicle (AGV) | 50 |
| 4.1.1 Track-Stop Strategy | 51 |
| 4.1.2 Development of AGV Prototype Structure | 53 |
| 4.1.3 Development of AGV Control System | 55 |
| 4.2 Modular AM Unit: Outstretched 3D Printer | 57 |
| 4.2.1 Zero Value Unifying Strategy | 57 |
| 4.2.2 Development of 3D Printer Prototype Structure | 59 |
| 4.2.3 Development of 3D Printer Control System | 64 |
| 4.3 Modular Angle Adjustment System (AAS) | 66 |
| 4.3.1 Angle Adjustment Strategy | 67 |
| 4.3.2 Development of AAS Prototype Structure | 67 |
| 4.3.3 Development of AAS Control System | 70 |
| CHAPTER 5 IMPLAMENTATION AND RESULT | 74 |
| 5.1 Operation Process | 74 |
| 5.2 Experiment Method and Implementation | 76 |
| 5.2.1 Experimental Inspiration | 76 |
| 5.2.2 Standard Printed Object | 81 |
| 5.2.3 Judgment of “Positioning Errors” | 84 |
| 5.2.4 Judgment of “Leveling Errors” | 84 |
| 5.2.5 Potential Radom Error | 85 |

| | Page |
|---|-------------|
| 5.2.6 Experimental Condition Setting | 87 |
| 5.2.7 Experimental Variable Setting | 88 |
| 5.3 Result | 89 |
| CHAPTER 6 CONCLUSION AND RECOMMENDATIONS | 100 |
| 6.1 Conclusion | 100 |
| 6.2 Recommendations | 100 |
| REFERENCES | 102 |

LIST OF TABLES

| Tables | Page |
|--|-------------|
| Table 3.1 Comparison of Two Leveling Solutions | 33 |
| Table 5.1 Results of the Random Error Tests | 86 |
| Table 5.2 Results of Slopes Being Placed at the Bottom of the Left Front Wheel and Right Front Wheel of the Mobile 3D Printer | 91 |
| Table 5.3 Results of Slopes Being Placed at the Bottom of the Left Rear Wheel and Right Rear Wheel of the Mobile 3D Printer | 92 |
| Table 5.4 Results of Slopes Being Placed at the Bottom of the Left Front Wheel and Left Rear Wheel of the Mobile 3D Printer | 93 |
| Table 5.5 Results of Slopes Being Placed at the Bottom of the Right Front Wheel and Right Rear Wheel of the Mobile 3D Printer | 94 |
| Table 5.6 Results of Slopes Being Placed at the Bottom of the Left Front Wheel and Right Rear Wheel of the Mobile 3D Printer | 95 |
| Table 5.7 Results of Slopes Being Placed at the Bottom of the Right Front Wheel and Left Rear Wheel of the Mobile 3D Printer | 96 |
| Table 5.8 Average Values of Printing Result | 98 |

LIST OF FIGURES

| Figures | Page |
|--|-------------|
| Figure 2.1 Classification of Different AM Devices (Gao et al., 2015) | 10 |
| Figure 2.2 Two Kinds of Gantry-Based AM Devices and Their Printable Space (Shen et al., 2019) | 12 |
| Figure 2.3 A Kind of Gantry 3D Printer (Zuo et al., 2019) | 14 |
| Figure 2.4 The World's First 3D Printed Power Distribution Station | 14 |
| Figure 2.5 A 2.16-m-high Statue of Sir Wilfrid Laurier (Barnett and Gosselin, 2015) | 15 |
| Figure 2.6 A Delta-Type AM Device Developed by Company WASP | 16 |
| Figure 2.7 The Process of 3D Printing Some Large Concrete Parts (Gosselin et al., 2016) | 16 |
| Figure 2.8 Large-Scale Robotic Arm AM Device Developed at the TU Dresden (Mechtcherine et al., 2019) | 17 |
| Figure 2.9 Concurrent Printing of One Large-Scale Structure by Two Mobile Robot Printers (Zhang et al., 2018) | 20 |
| Figure 2.10 Printing Sequence Planning for Large-Size Parts (Shen et al., 2019) | 20 |
| Figure 2.11 Printing Sequence Planning for Small-to-Medium Parts (Shen et al., 2019) | 21 |
| Figure 2.12 Different Types of Mobile Platform in Manufacturing (Keating et al., 2017) | 22 |
| Figure 2.13 Aerial 3D Printer (Hunt et al., 2014) | 23 |
| Figure 2.14 Mobile 3D Printer Based on A Mecanum Wheel Mobile Platform (Marques et al., 2017) | 24 |
| Figure 2.15 A Large Single-Piece Concrete Structure with Obvious Error in the Joint (Zhang et al., 2018) | 25 |
| Figure 3.1 Methodology Flow Chart | 28 |
| Figure 3.2 Interrelationship Between Mobile Platform and Uneven Ground | 30 |

| | Page |
|---|-------------|
| Figure 3.3 Two Different Leveling Solutions | 31 |
| Figure 3.4 Maximum Fabrication Size Reduction | 33 |
| Figure 3.5 Six Degrees of Freedom in Three-Dimensional Space | 34 |
| Figure 3.6 Effect of Distance Error on Collaboration | 36 |
| Figure 3.7 Effect of Angle Error on Collaboration | 38 |
| Figure 3.8 Error Classification | 39 |
| Figure 3.9 Errors Produced by Internal Causes | 41 |
| Figure 3.10 “Track-Stop” Strategy | 43 |
| Figure 3.11 Errors Produced by External Causes | 45 |
| Figure 3.12 Zero Value Unifying Strategy | 47 |
| Figure 3.13 Angle Adjustment Strategy | 48 |
| Figure 4.1 CAD Models of Mobile 3D Printers | 50 |
| Figure 4.2 Specification and Accuracy of Magnetic Tape Following Sensor | 51 |
| Figure 4.3 Magnetic Tape Setting Method | 52 |
| Figure 4.4 Components of the Modular AGV Prototype | 53 |
| Figure 4.5 Magnetic Tape Detection Code | 56 |
| Figure 4.6 Code for PID Control of AGV | 57 |
| Figure 4.7 Positional Relationship Between BLTouch and Nozzle | 58 |
| Figure 4.8 Comparison of the Characteristics of Commonly Used Sensors for 3D Printer | 59 |
| Figure 4.9 CAD Model of the Developed Outstretched 3D Printer | 60 |
| Figure 4.10 Three-Axis Series Structure | 61 |
| Figure 4.11 3D Printer Driver Components | 62 |
| Figure 4.12 Maximum Stroke of the X-Axis of the Outstretched 3D Printer | 63 |
| Figure 4.13 The Structure of the End of the Outstretched Arm | 64 |
| Figure 4.14 Core Parameters of the Outstretched 3D Printer's Firmware Code | 65 |
| Figure 4.15 UI of the Outstretched 3D Printer's Display | 65 |
| Figure 4.16 Slicing and Printing Parameters of Outstretched 3D Printer | 66 |
| Figure 4.17 CAD Model of the Angle Adjustment System | 68 |

| | Page |
|---|-------------|
| Figure 4.18 Practical Assembly of the Angle Adjustment System | 68 |
| Figure 4.19 Actuator Layout | 69 |
| Figure 4.20 Core Code of the AAS Program | 71 |
| Figure 4.21 UI of the AAS's Display | 72 |
| Figure 4.22 Control Schematic Diagram of the Angle Adjustment System | 72 |
| Figure 4.23 Response Time Domain Diagram of Angle Adjustment System | 73 |
| Figure 5.1 Physical Construction of Mobile 3D Printer | 74 |
| Figure 5.2 Operation Process Flow Chart | 75 |
| Figure 5.3 Standard Printed "R" Shape 3D Icon | 77 |
| Figure 5.4 Printed "R" Shape 3D Icon with 1° Pitch Angle | 78 |
| Figure 5.5 Thickness Comparison Between Two Printed Icons | 79 |
| Figure 5.6 Bottom Comparison Between Two Printed Icons | 80 |
| Figure 5.7 Printed "R" Shape 3D Icon with -10° Yaw Angle | 80 |
| Figure 5.8 Printed "R" Shape 3D Icon with Certain Distance Error | 81 |
| Figure 5.9 Sliced Model of the Printed Object for Experiment | 82 |
| Figure 5.10 Physical Fabrication Setting | 83 |
| Figure 5.11 Standard Experimental Printed Object | 83 |
| Figure 5.12 Measurement of Positioning Errors Produced by "Internal Causes" | 84 |
| Figure 5.13 Measurement of Leveling Errors Produced by "External Causes" | 85 |
| Figure 5.14 Artificial Slopes | 87 |
| Figure 5.15 Six Different Ground Conditions Created by Slope Placement | 88 |
| Figure 5.16 Printing and Measurement Results Under Ground Condition without "Positioning Error Correction" and "Leveling Error Correction" | 89 |
| Figure 5.17 Printing and Measurement Results Under Ground Condition with "Positioning Error Correction" and "Leveling Error Correction" | 90 |
| Figure 5.18 Error Reduction Ratio | 99 |

LIST OF ABBREVIATIONS

| | |
|-------|---|
| AM | = Additive Manufacturing |
| RP | = Rapid Prototyping |
| FDM | = Fused Deposition Modeling |
| SLM | = Selective Laser Melting |
| SLA | = Stereolithography |
| DLP | = Digital Light Processing |
| 3DP | = Inkjet head 3D Printing |
| SLAM | = Simultaneous Localization and Mapping |
| CAD | = Computer-Aided Design |
| AGV | = Automated Guided Vehicle |
| PID | = Proportional-Integral-Derivative |
| AAS | = Angle Adjustment System |
| LCD | = Liquid-Crystal Display |
| UI | = User Interface |
| OLED | = Organic Light-Emitting Diode |
| ANOVA | = Analysis of Variance |

CHAPTER 1

INTRODUCTION

1.1 Background of the Study

Additive manufacturing (AM) is very popular in modern manufacturing. It evolved from rapid prototyping (RP) developed in the 1980s. It is a technology which can build three-dimensional parts by depositing material layer upon layer directly from a digital model (Guo and Leu, 2013). In the past few decades, additive manufacturing is often used to manufacture molds and prototypes in the field of industrial design. Now, with the rapid development of this technology, it has gradually penetrated into various fields. From aerospace to essential household items, we can see its various applications.

As the name suggests, additive manufacturing is obviously different from the principle of traditional subtractive manufacturing. Compared with traditional manufacturing, additive manufacturing has many advantages, including its higher material utilization rate, lower manufacturing cost, its ability to manufacture products with complex shapes and to quickly produce prototypes. However, additive manufacturing also has some shortcomings that make it unable to replace traditional manufacturing methods. These shortcomings include its low manufacturing efficiency, poor scalability, limited materials, limited accuracy and poor quality, and so on.

The increasing position of additive manufacturing in the manufacturing industry is the trend of the times. Researchers have been working to overcome the shortcomings of additive manufacturing, but it is clear that it is not so easy to break through these existing technical barriers. Among these shortcomings, some must be overcome through core technological innovation. Limited material is a typical example of such shortcomings. Only through the advancement of materials science can more new materials be invented. On the contrary, it has been proven that there are some shortcomings that can be overcome by optimizing technical solutions, such as low

efficiency and poor scalability. Efficiency is related to time, and scalability is related to space. Therefore, theoretically optimizing time and space technical solutions for additive manufacturing can improve these two shortcomings. Take the most common Fused Deposition Modeling (FDM) additive manufacturing process as an example. There is usually a fixed size device. It is of gantry structure or robotic arm structure. And there is a nozzle that ejects the printing material, which can move in the three-dimensional space inside the device. The nozzle moves along the cross-sectional contour and filling trajectory of the manufactured part layer by layer. The nozzle has a fixed moving speed and limited moving space, so the efficiency of manufacturing is limited. The so-called scalability refers to the maximum size of object that can be produced. Also due to the special structure, this kind of devices can produce objects whose sizes are limited by the structure of themselves. When large-scale or complex parts need to be printed, situations like insufficient manufacturing space or too long manufacturing time can easily occur.

A multi-nozzle 3D printing teaching aid (Sun et al., 2019) is designed to improve the efficiency of additive manufacturing. Unlike conventional 3D printers, there are two nozzles installed on this printer in a single printing space. These two nozzles can print at the same time in their respective areas without interfering with each other. In theory, the printing efficiency is doubled. As for Agranoff and McGuire (2003), a process that simplifies and executes in multi-organizational arrangements to solve a problem that cannot be solved or solved easily by a single organization, can be called as collaboration. This concept has been noticed by researchers in recent years. They hope to make multiple additive manufacturing devices work collaboratively, and to improve the efficiency and scalability of this technology. Based on the concept of collaboration, a prototype composed of multiple AM units was developed (Ranaweera, 2019). This equipment realized multi-material collaborative additive manufacturing which is impossible with conventional single-nozzle technology. Under the same concept, a large-scale 3D printing system composed of multiple robots was proposed (Shen et al., 2019). The research discussed the influence of the layout of the robots on the maximum

printing area and geometric adaptability. At the same time, it also proposed algorithms to optimize printing efficiency and strategies to avoid multi-robot interference. Unlike the previous study, this study proves that collaboration can improve the efficiency and scalability of additive manufacturing.

As mentioned before, researchers have introduced some innovative concepts into additive manufacturing. They designed and completed experiments to prove that optimizing technical solutions is effective for improving some of the disadvantages. But in fact, they have not improved enough due to various restrictions, and some additional problems have also been exposed. It can be said that this field is still a blue ocean. Therefore, it is of great significance and research value to overcome the disadvantages of low flexibility, low efficiency and poor scalability of additive manufacturing by optimizing technical solutions.

1.2 Problem Statement

Researchers have realized that simultaneously improving the efficiency and scalability of additive manufacturing is not an easy task. Using traditional methods to improve one of the shortcomings tends to worsen the other shortcomings. When facing poor scalability, designing a device large enough to fabricate the needed models has been proven to work. But in most cases, scaling up the device is costly and time-consuming. A large-scale 3D printing method with a cable-suspended robot (Eric and Clement, 2015) was developed to improve the scalability of additive manufacturing. Although the system has many innovative features, the actual printing accuracy and printing efficiency seem to be worse. The aforementioned research that introduced the concept of collaboration (Shen et al., 2019) has indeed been proven to effectively improve the efficiency of additive manufacturing. However, it has little effect on improving manufacturing scalability. Since these devices are still fixed, their flexibility is severely limited. When a larger object needs to be manufactured, this system will be helpless. At this point, it might be a good way to introduce some new concepts.

In order to realize the printing of filling materials in some extreme environments, flying robots were combined with additive manufacturing technology (Hunt et al., 2014). This research introduces the concept of “mobility”, breaking the routine of fixed additive manufacturing work. Although the experimental results were not particularly ideal, this innovative concept inspired other researchers.

Later, a few researchers have introduced the two concepts of “collaboration” and “mobility” into additive manufacturing technology at the same time. In order to improve the scalability of additive manufacturing, a mobile 3D printer with an extrusion print head and four omnidirectional wheels was designed (Marques et al., 2017). Multiple such printers can move to print at the same time. However, the researchers did not show whether these mobile printers can collaborate to print the same part. Another thing is that due to the large movement error of the printer, the accuracy of the printed parts has yet to be verified.

On the basis of the previous research, a generation method for automatic block and scheduling of large-scale parts was developed (Poudel et al., 2020). This method is suitable for multiple printers to collaboratively print the same large-scale part. It can avoid collisions and generate a large number of different printing schemes. However, the researchers did not verify by printing the actual product.

A 3D printing system that uses multiple mobile robots was demonstrated to print a large single-piece structure at the same time (Zhang et al., 2018). However, because the positioning accuracy of the mobile robot is not very high, and the researchers did not consider other influences that may be caused by the external environment, the printed parts have large errors in the joints.

Mobile and collaborative solutions were also used to build a large house through additive manufacturing technology (Kevin et al., 2018). Different from the previous cases, this experiment took into account the flatness defects of the manufacturing

platform and made corrections. However, the method of measurement and correction is too complicated and time-consuming.

From the examples mentioned above, we can find that mobility seems to be an ideal solution to improve the scalability of additive manufacturing. The size of an additive manufacturing device is limited, but since the object to be produced can be manufactured in “blocks”, so constantly changing the working position of the device can increase its scalability infinitely. However, the continuous movement of a single device to print large-scale part is extremely inefficient. This is why researchers always combine “collaboration” and “mobility” together in this work. “Collaboration” is mainly used to improve efficiency, and “mobility” is mainly used to improve scalability. In addition, the benefits of these two concepts to additive manufacturing can complement and gain each other, achieving the effect of “one plus one is greater than two”.

It can be seen from the above researches that the introduction of new concepts has brought both positive and negative effects. Researchers tried their best to gain positive effects. However, it is not negligible to propose solutions to those new and additional problems. These problems include how to allocate work to multiple devices, how to avoid collisions between devices, how to arrange the location of the devices, how to control the accurate positioning of the devices, etc. One of the common problems is that mobile devices have more or less inaccurate positioning. This problem deeply affects the accuracy and completeness of the manufactured objects. In the study of 3D printing system with multiple mobile robots (Zhang et al., 2018), we can clearly see that there is a big error at the joint point of the part printed by the two mobile AM devices. Regardless of the accuracy of the additive manufacturing device itself, it is obvious that the error is caused by the inaccurate calibration of the coordinate origin of the two AM units. In three-dimensional space, each mobile AM device itself has a three-axis coordinate. Each axis includes a translational degree of freedom and a rotational degree of freedom. In the manufacturing space, when positioning is complete, all six degrees

of freedom of each device should be fully constrained. In addition, the positional relationship of the coordinate origins between every device needs to be accurately controlled. Only after these two conditions are met, the AM unit starts to work and the fabricated “blocks” can be accurately combined. Positioning fails when any of the degrees of freedom is not fully constrained or the relative position relationship is inaccurate. Inaccurate positioning introduces errors that can lead to gaps or interference between “blocks”. There are many factors that cause positioning inaccuracy, including sensor accuracy, mark recognition, parameter settings, etc. These factors usually determine the level of positioning accuracy in the horizontal direction. In addition, since this kind of mobile additive manufacturing usually needs to be operated on a wide table or ground, the flatness of the operation table or the ground also needs to be considered. If there is an inclination or drop on the operating table or the ground, the attitude of the device will also be affected. If the attitudes of multiple devices are not calibrated, errors will occur in the vertical direction, which will affect the positioning accuracy. As in the study of mobile robot location dedicated for habitable house construction (Kevin et al., 2018), they measured the flatness of the operating ground and manually calibrated the attitudes of the devices in different positions. But obviously this manual adjustment method is time-consuming and laborious.

The benefits of collaboration and mobility to additive manufacturing are obvious to all. Of course, there is also a lot of space for improvement in this technical solution. However, the problems brought about by these concepts to the manufacturing process must not be ignored, especially the inaccurate positioning of mobile devices which includes translational and rotational degrees of freedom in any axis. If there is a small error in positioning, defects or even failures in the manufacturing process may occur. At present, most of the researches on mobile collaborative additive manufacturing has not proposed a systematic solution for device positioning or error collection. A few studies that have noticed this problem have only dealt with it through traditional labor-intensive solutions. Therefore, an efficient and accurate positioning solution designed for mobile collaborative additive manufacturing is urgently needed.

1.3 Objective of the Study

The objective of this study is to design and develop a mobile 3D printer, which is towards supporting large-scale collaborative additive manufacturing in practical fabrication environments.

1.4 Scope and Limitation

- Any category of reduced error will only be minimized to meet the tolerance range of large-scale additive manufacturing, not guaranteed to be completely eliminated.
- All of the designated location points and transfer paths have been given before any experiment.
- All mobility and positioning tests and experiments will be conducted on existing or simulated ground in the department's laboratory.
- The proposed mobile platform will be equipped with a specific Fused Deposition Modeling (FDM) AM unit, which is not necessarily suitable for other types of AM devices.

CHAPTER 2

LITERATURE REVIEW

In order to adopt reasonable and effective technical methods to build a mobile 3D printer suitable for large-scale collaborative additive manufacturing, this literature review is dedicated to summarizing the current development level of large-scale additive manufacturing and related technologies, including engineering collaboration and mobility technology. This paper takes these existing achievements as references and combines technical methods in various fields to achieve the research objective.

2.1 Additive Manufacturing

Additive manufacturing (AM) is an advanced technology in the field of manufacturing, which was also called additive fabrication, additive processes, additive techniques, additive layer manufacturing, layer manufacturing, solid freeform fabrication, freeform fabrication, and 3D printing in the past (ISO, 2015). It refers to the technologies used to manufacture 3D objects, in which materials are accumulated layer by layer via specific techniques such as extrusion, sintering, melting, photopolymerisation, jetting, lamination, and deposition (Gibson et al., 2015). Modern AM technologies firstly emerged with stereolithography in the 1980s, and it has gradually derived a variety of manufacturing methods.

Compared with the traditional manufacturing method of subtractive manufacturing, AM technology does not require tools, fixtures and complex processing procedures. An AM device can quickly and accurately manufacture parts of any complex shape, which greatly reduces the manufacturing difficulty and cost, and shortens the processing cycle. Since this technology was invented, it has been mostly used for prototype production purposes (Kruth et al., 1998). However, in recent years, people have realized that the advantages of AM can be used to a greater extent. As a result, the products of additive

manufacturing appear in a variety of fields, including medical, biological, construction, automotive, aviation and so on.

2.1.1 Current Status of Large-scale Additive Manufacturing

Technology serves mankind. It is undeniable that AM technology has been integrated into various industries and fields, bringing people a convenient and innovative experience. However, as an emerging manufacturing technology, it still has many disadvantages that make it unable to shake the status of traditional manufacturing technology. Part of the disadvantages can be seen through the scale of the mainstream commercial additive manufacturing devices currently on the market and their applications. Figure 2.1 shows the classification of different additive manufacturing devices according to the build volume in different usage scenarios.

Figure 2.1

Classification of Different AM Devices (Gao et al., 2015)

| | Small Printers Desktop-size | Medium Printers Fridge-size | Large Printers Wardrobe-size |
|---------------------------------------|--|--|--|
| Home and hobbyist use printers | UP series; (3D Systems) Cube®; CubePro™; (Afinia) H480; (Aleph Objects) LulzBot™; (Deezmaker) Bukobot; (Envision TEC) Perfactory®; Fablicator; (FELIXprinters) Felix; (Formlabs) Form 1+; HYREL 3D; (MakerGear) M Series; (MakerBot) Replicator; (Mcor Technologies) IRIS; MiiCraft; Portabee; Printrbot; Printxel, Pwdr; (RepRapPro) Ormerod; Prusa; RoBo3D; SandBox; Orion Delta™; Solido3D; Solidoodle; (Tinkerine) Ditto™ Pro; (Type A Machines) Series 1; Newton 3D | (Stratasys) Mojo, (3D Systems) ProJet® 1200; Deltamaker™; (Makerbot) Replicator 2X | (Stratasys) uPrint |
| Professional use printers | (3D Systems) ProJet® 1200; (Asiga) Freeform; (Envision TEC) Perfactory®; (Nanoscribe) Photonic Professional GT; | (3D Systems) ProJet® 3500, 3510, 6000, 7000; (EOS) Precious; ExOne™ X1-Lab; (Stratasys) Dimension; Objet Eden, 260, 350, 500; (Envision TEC) ULTRA®; (SLM Solutions) SLM 125 | (3D Systems) ProJet® 660, 4500, 5000, 5500; Optomec® LENS 450; Aerosol Jet 300; (EOS) EOS M; (ExOne™) M-Flex |
| Industrial use printers | Optomec® Aerosol Jet 200; (Nanoscribe) Photonic Professional; | (Stratasys) Fortus 360, 400; (Envision TEC) Xede®; Xtreme® | (Voxeljet) VX series; Optomec® Aerosol Jet 5X, LENS 850-R, MR-7; (EOS) EOSINT; (Acram AB) Q series; (ExOne™) S Print, M Print; (Stratasys) Fortus 900; Objet 1000; |

Obviously, the build volume of most current additive manufacturing devices is small-scale, which means that these devices can eventually be used to manufacture small size

parts. Medium and large-scale additive manufacturing devices mainly serve professional and industrial uses. The main reason for this differentiation is the cost difference, which includes device cost, technical cost, time cost and so on (Winkless, 2015). Generally, additive manufacturing requires a fixed-size device/printer with limited printing space. The volume of these manufactured parts is limited by the size of the device/printer itself (Hunt et al., 2014). To use AM technology to manufacture a large part, a larger device must be introduced. However, devices of different sizes and their use costs are not simply proportional. Large-scale device is more difficult to ensure manufacturing accuracy and increase manufacturing speed, so the development costs will inevitably increase greatly. In addition, large-scale device has additional requirements for the use environment and operator skills. These costs are often unaffordable by individuals and small-scale groups. Even in professional and industrial applications, large-scale additive manufacturing suffers from low accuracy, low flexibility, and low efficiency. This situation greatly limits the development of large-scale additive manufacturing technology.

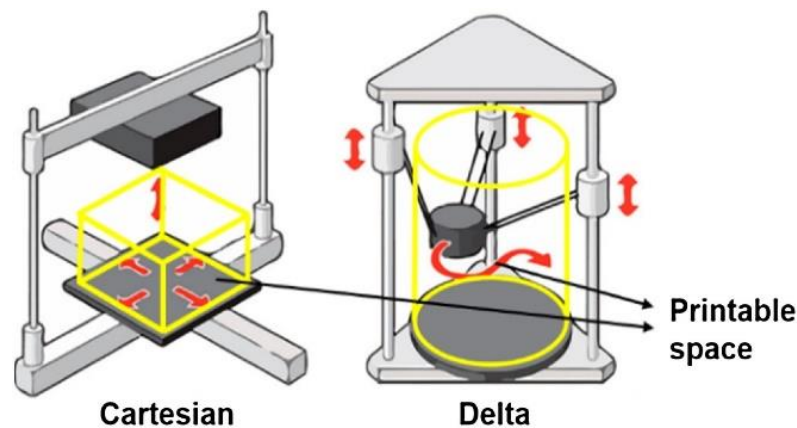
Several AM technology methods, including fused deposition modeling (FDM), selective laser melting (SLM), Stereolithography (SLA), and digital light processing (DLP) have been adopted (Petrovic, 2011). On the other hand, according to different types of additive manufacturing processes, many different types of materials have been proven to be used in this technology, including some polymers, metals, composite materials, and ceramics. Generally speaking, the existing large-scale additive manufacturing technologies are mostly based on fused deposition modeling (FDM) technology and inkjet head 3D printing (3DP) technology of various materials (Albar et al., 2020). The application of large-scale additive manufacturing in the construction field most clearly reflects this law.

AM equipment that serves large-scale additive manufacturing usually has two types, which are gantry-based and robotic arm-based. The two types of devices are significantly different in structure. The device with gantry structure is the most widely

used. It has a visible external frame, which limits the volume of the manufacturing chamber. Therefore, this type of device can only manufacture parts whose size is not larger than the volume of its own chamber (Shen et al., 2019). The gantry-based device mainly includes Cartesian printers and Delta printers. Cartesian printers are often box-shaped. The motor controls the printing nozzle to move along the track in the Cartesian coordinate system. Delta printers often have a columnar structure. The printing nozzle is connected to the track by three arms. These arms can move up and down independently to control the position of the nozzle. Figure 2.2 shows the dimensions of the manufacturing chamber for two gantry-based devices, Cartesian and Delta. Although these two chambers have different shapes, they both strictly limit the size of the manufactured parts.

Figure 2.2

Two Kinds of Gantry-Based AM Devices and Their Printable Space (Shen et al., 2019)



Robotic arm-based AM devices have no visible external frame. The size of the parts manufactured with this device depends on the movable space of the robot arm. Due to the higher degree of freedom of the robotic arm, the manufacturing process of this device is more flexible than that of the device based on the gantry. Additional roll, pitch and yaw controls are provided to the print nozzle, allowing it to perform more articulate print designs, such as printing with the tangential continuity method (Gosselin et al.,

2016). This method can make the transition between the printed layers smoother, thereby improving the processing quality.

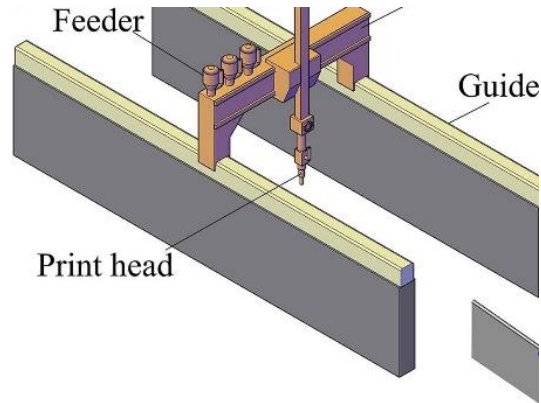
In general, large-scale additive manufacturing is often associated with the words high cost, low accuracy, and low efficiency. The limitations of traditional manufacturing concepts have also hindered the development of this technology to a certain extent. Subject to various disadvantages, it is difficult for large-scale additive manufacturing to demonstrate its value and gain recognition in various fields. Therefore, researchers have begun to seek innovative methods to overcome the disadvantages of large-scale additive manufacturing.

2.1.2 Applications of Large-scale Additive Manufacturing

Nowadays, large-scale additive manufacturing projects of many companies and teams have been proven feasible, and some of the mature AM devices have also been put into use in engineering projects. A method for evaluating the rationality of the models and optimizing the parameters of the full-size additive manufacturing was proposed (Zuo et al., 2019). Researchers believe that the trend of additive manufacturing must shift from manufacturing reduced-size models to manufacturing corresponding full-size objects. To verify this point, they verified the feasibility of using additive manufacturing technology to print a 15-meter-long bridge. The researchers used two artesian gantry structure additive manufacturing devices based on FDM to manufacture the bridge model and its full-scale structure, respectively. By comparing the errors of the two manufactured objects, they confirmed the feasibility of this manufacturing method and proposed the best parameters for full-scale additive manufacturing. Figure 2.3 shows the gantry structure AM device proposed by the researchers for large-scale additive manufacturing. Although this study did not really put their large-scale additive manufacturing method into practice, it provided theoretical support for the feasibility of this technology.

Figure 2.3

A Kind of Gantry 3D Printer (Zuo et al., 2019)



Gantry 3D printer

Figure 2.4 shows a large-scale AM device based on Cartesian gantry jointly developed by Tongji University and company Green Print in China. The device can theoretically complete the manufacture of houses independently. At the same time, it can save a lot of building materials and shorten the manufacturing time. This device built the world's first 3D printed power distribution station using commercial ready-mixed concrete, and its reliable manufacturing effect has been proven.

Figure 2.4

The World's First 3D Printed Power Distribution Station



In addition to gantry-based Cartesian AM devices, another delta-type devices have also developed some applications. Researchers have developed a large-scale 3D printer based on the Delta Gantry AM device. It uses a six-degree-of-freedom cable-suspended robot for positioning, with polyurethane foam as the object material and shaving foam as the support material (Barnett and Gosselin, 2015). The researchers used this device to build the construction of a 2.16-m-high statue of Sir Wilfrid Laurier, the seventh Prime Minister of Canada, as shown in Figure 2.5. Generally speaking, the equipment successfully completed the manufacture of large-scale parts. However, the accuracy and speed of this large-scale additive manufacturing device needs to be improved.

Figure 2.5

A 2.16-m-high Statue of Sir Wilfrid Laurier (Barnett and Gosselin, 2015)



Figure 2.6 shows a large delta-type AM device based on gantry structure developed by company WASP. This device became the world's largest 3D printer when it was launched. It is 12 meters high and used to build houses. Nevertheless, the restricted mobility seems to be a clear disadvantage of this 3D printer, because disassembly and assembly are required for each on-site building construction (Xiao et al., 2021).

Figure 2.6

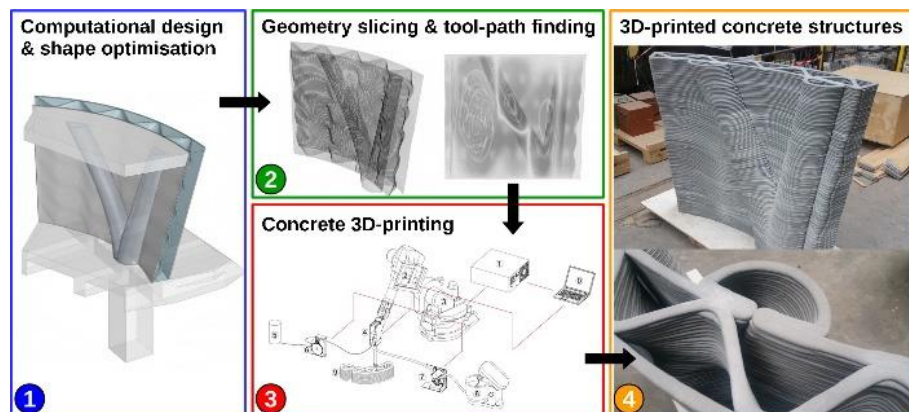
A Delta-Type AM Device Developed by Company WASP



Some large-scale AM devices based on robotic arms have also been developed. Based on a technology similar to FDM, researchers have developed a new additive manufacturing processing route for ultra-high performance concrete (Gosselin et al., 2016). The AM device involved is based on an industrial ABB 6620 6-axis robotic arm. This device produced some large 3D printed concrete parts, as shown in Figure 2.7. It can produce large-scale parts with complex geometries without providing support.

Figure 2.7

The Process of 3D Printing Some Large Concrete Parts (Gosselin et al., 2016)



A large-scale robotic arm-based AM device has been developed at the TU Dresden, as shown in Figure 2.8. It has a long, foldable boom whose range (total lengths of up to 70m) is large enough to print multi-story buildings (Mechtcherine et al., 2019). This technology provides a mobile on-site monolithic printing solution for pumping and printing coarse-aggregate concrete, but it is still in the development stage. Due to the large size of the device and the long robotic arm, it is difficult to precisely control the position of the printing nozzle. Researchers have been adjusting the driving system of the robotic arm to optimize the positioning accuracy of this device.

Figure 2.8

Large-Scale Robotic Arm AM Device Developed at the TU Dresden (Mechtcherine et al., 2019)



2.2 Collaboration

In recent years, the word collaboration has been frequently mentioned. With the advancement of science and technology, people realize that collaboration is no longer limited to individuals. In today's highly connected technology-driven economy, the production industry must rely on the best practices of collaborative engineering to stay

competitive when designing, manufacturing and operating complex machines, processes, and systems on a global scale (Lu et al., 2007).

2.2.1 The Role of Collaboration in Manufacturing

In the manufacturing industry, collaboration is showing unprecedented value. Some researchers have declared that collaboration is the heart of Industry 4.0 (Agranoff and McGuire, 2003). In fact, collaborative manufacturing can be categorized into three sections, which are human-human collaboration, human-device collaboration, and device-device collaboration (3D-Proto, 2014).

The collaboration between humans is the most primitive and simplest. Large-scale assembly line production after the second industrial revolution promoted this type of collaboration. People realize that communication, sharing, and cooperation between people can improve production efficiency.

The collaboration between human and device is also prevalent in the manufacturing industry of assembly line production. This type of collaboration has been widely recognized and used. The most common collaborative application in manufacturing is collaborative robot. The term collaborative robot was proposed in 1996 by scientists Colgate, Peshkin, and Wannasuphoprasit (1996) for passive mechanical devices used to aid humans in solving industrial tasks. The main objectives reported by manufacturing companies to introduce collaborative robots in the manufacturing processes are fundamentally to improve productivity, flexibility and quality (Simoes et al., 2020).

The collaboration between device and device is currently the most promising type of collaboration in the manufacturing industry. It refers to two or more devices that automatically cooperate to complete a work without human intervention. The difficulty of this kind of collaboration is often uncertain, and it depends on many factors such as the environment, the task, and even the device itself. Researchers are working to

overcome the disadvantages of device-device collaboration so that this highly automated manufacturing method can be used more widely.

2.2.2 Collaboration in Additive Manufacturing

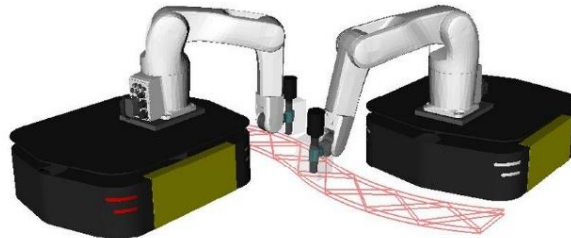
Some additive manufacturing researches have introduced the concept of collaboration. Although these collaboration methods are different, they generally show a lot of advantages, especially in the manufacture of large-scale parts. However, these researches also exposed some disadvantages and room for improvement of collaborative additive manufacturing.

In order to achieve the deposition of multiple materials, a concept of collaborative additive manufacturing was successfully developed, which consist with identification of layer attributes, toolpath generation and communication among computer and additive manufacturing units (Ranaweera, 2019). Researchers have developed an algorithm to avoid collisions of multiple AM devices, and used multiple AM units to co-manufacture to demonstrate. Although this research has proved that collaborative additive manufacturing can be applied to deposit a variety of materials, the manufacturing quality and efficiency of this system have yet to be verified.

In addition to achieving multi-material deposition, some researchers are more concerned about the impact of collaborative additive manufacturing on the scalability and efficiency of manufacturing. The researchers designed an AM system for manufacturing large-scale concrete structures. As shown in Figure 2.9, two robot printers were required to build a large-scale structure whose size is beyond the printing volume of one single robot printer (Zhang et al., 2018). Compared with a single manufacturing device, this collaborative approach greatly improves manufacturing efficiency. More importantly, it breaks through the strict print size limitation of conventional AM devices, making it possible for small AM devices to manufacture large-scale parts.

Figure 2.9

Concurrent Printing of One Large-Scale Structure by Two Mobile Robot Printers
(Zhang et al., 2018)



Similarly, an extensible large-scale 3D printing system composed of multiple robots working in collaboration was developed. This set of device is based on the research and development of the ordinary robotic arm AM unit and does not require additional hardware facilities. The number and placement of AM devices can be adjusted according to the printing requirements, and this system has more flexibility than other large-scale AM devices (Shen et al., 2019). In order to avoid device collisions during collaboration, the researchers designed interference solutions for parts of different sizes. Taking the collaborative additive manufacturing process involving four devices as an example, Figure 2.10 and Figure 2.11 respectively show the printing sequence rules applicable to large and small to medium-sized parts.

Figure 2.10

Printing Sequence Planning for Large-Size Parts (Shen et al., 2019)

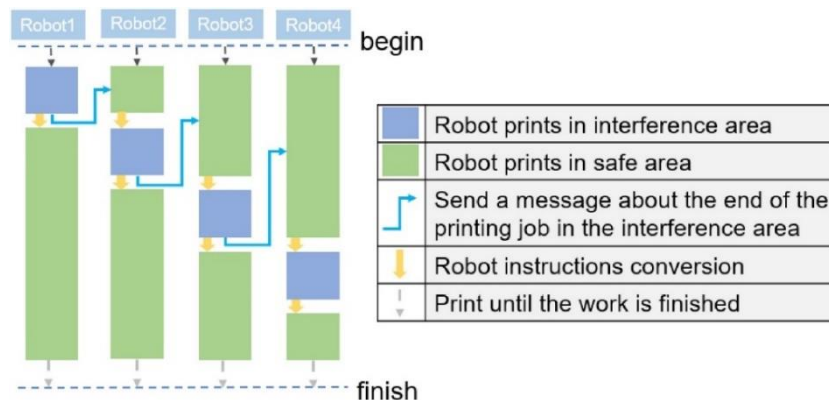
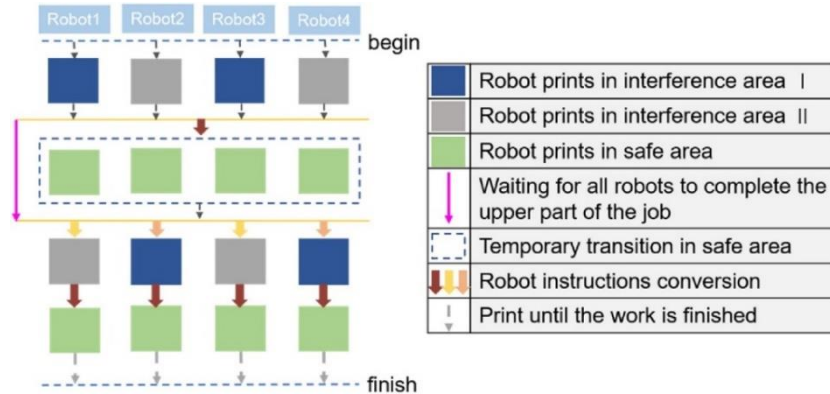


Figure 2.11

Printing Sequence Planning for Small-to-Medium Parts (Shen et al., 2019)



The above research also pointed out some key difficulties of collaborative additive manufacturing today. First, reliable collaborative additive manufacturing requires a complex group control system responsible for the coordination and monitoring of multiple devices. Second, reasonable manufacturing tasks assignment and mutual collision avoidance are difficult issues in real-time manufacturing processes. In this regard, some researchers have also proposed some theoretical methods for collaborative additive manufacturing, including task allocation (Poudel et al., 2020), multi-tool path planning, etc. (Bui et al., 2020).

2.3 Mobility

The word mobility is often associated with high degree of freedom, high flexibility and high efficiency. It has great value in the current rapid development of science and technology. Various carriers and vehicles have been created to improve mobility in various fields.

2.3.1 The Role of Mobility in Manufacturing

The value of mobility in manufacturing can be divided into two categories. Whether the manufacturing device itself has mobility is the key to distinguish these two categories. Mobility is often directly involved in the manufacturing process when a manufacturing device has it. Conversely, mobility is defined as the ability to change

between geographically different places with little penalty in time, effort, cost, or performance (Stillstrom and Jackson, 2007).

Manufacturing device with its own mobility is often built on a mobile platform. This mobile platform can be any movable mechanism such as guide rails, robotic arms, mobile robots, vehicles, etc., as shown in Figure 2.12. According to different manufacturing principles, these mobile platforms provide different functions to assist in the manufacturing process.

Figure 2.12

Different Types of Mobile Platform in Manufacturing (Keating et al., 2017)



When discussing the other type of mobility that is not attached to manufacturing device, information processing capabilities, material management capabilities, and transportation capabilities are the objects to be studied, not the manufacturing process itself. These mobility issues often belong to the scope of supply chain and economic management (Kenger et al., 2021). However, it is undeniable that the focus on this mobility has also indirectly promoted the trend of modular development of manufacturing device. This paper does not discuss this type of mobility.

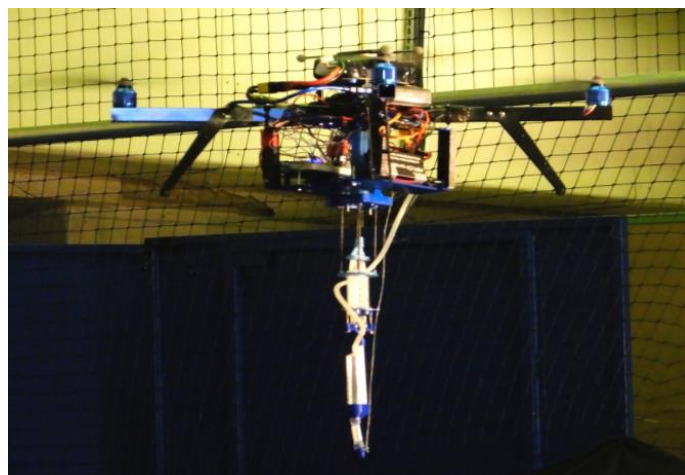
2.3.2 *Mobility in Additive Manufacturing*

In order to solve the problem that fixed-size AM devices have strict size restrictions on the objects to be manufactured, some researchers have improved the scalability and flexibility of the manufacturing process by giving AM devices mobility.

A set of aerial 3D printing robot was developed, as shown in Figure 2.13. The quadcopter is equipped with the entire printing system and controls the orderly deposition of materials through its own movement. This allows it to print three dimensional structures in areas normally inaccessible by ground or climbing robots with a variety of maintenance and repair applications (Hunt et al., 2014). Although this set of AM device based on flying robot proved to be feasible, the poor flight stability made the deposition inaccurate and the smoothness of the material was low.

Figure 2.13

Aerial 3D Printer (Hunt et al., 2014)

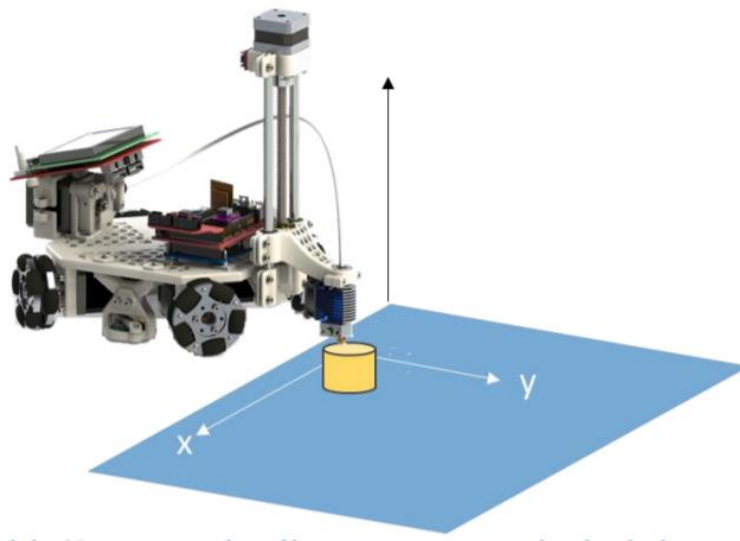


Compared with the previous research, more researchers are committed to combining AM devices with mobile robots used on the ground to create more possibilities. A group of researchers built a mobile 3D printer based on the mobile platform of four mecanum wheels, as shown in Figure 2.14. The nozzle of the printer is installed on a vertical rail. During the printing process, the mobile platform moves to control the nozzle path.

Although an additional feedback control system was used to improve the positioning accuracy of the mobile platform, slippage and imperfect alignment of the wheels still caused large errors in the printed results (Marques et al., 2017).

Figure 2.14

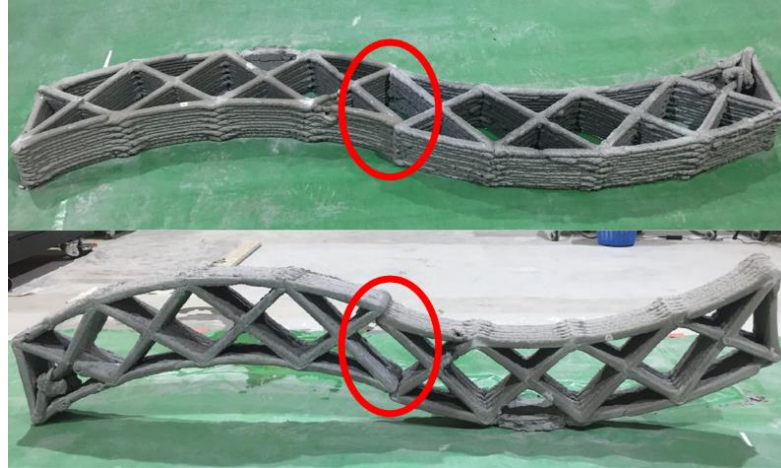
Mobile 3D Printer Based on A Mecanum Wheel Mobile Platform (Marques et al., 2017)



Another group of researchers also employed two mobile robots concurrently printing a large single-piece concrete structure (Zhang et al., 2018). This mobile robot uses simultaneous localization and mapping (SLAM) positioning technology. Different from the mobile platform studied above, this mobile robot only moves and positions once before the start of the manufacturing process. This method guarantees the quality of each AM device independently manufactured, but puts forward high requirements on the accuracy of the positioning of the mobile robot. Once the positioning is not accurate enough, errors will occur in the joints of the final manufactured parts, as shown in Figure 2.15.

Figure 2.15

A Large Single-Piece Concrete Structure with Obvious Error in the Joint (Zhang et al., 2018)



In view of the above-mentioned problem that the positioning of mobile robots affects manufacturing quality, researchers have proposed a process to improve the positioning accuracy of mobile robots. In an actual manufacturing case, the unevenness of the ground caused the mobile robot to correct an offset of 60mm. To solve the issue, a correction matrix has been implemented to relocate the industrial robot while ensuring the feasibility of the trajectory (Kevin et al., 2018). This method is effective, but obviously in the field of additive manufacturing, more automated and efficient methods are worth to be developed.

CHAPTER 3

METHODOLOGY

This chapter first presents two general technical solutions of "additional positioning assistance" and "automatic leveling mechanism" that can be applied to error control. In order to find the implementation method of these solutions from the source, all potential errors in large-scale collaborative additive manufacturing are specifically list out. By analyzing their causes, all errors are classified into two categories. Two innovative concepts of "positioning error correction" and "leveling error correction" and corresponding error control strategies are proposed to combine with the generated solutions. The implementation methods of solutions, concepts and strategies in large-scale collaborative additive manufacturing processes are presented in details in this chapter. Their feasibility will be verified by practical operations and experiments in subsequent chapters.

3.1 Idea Generation

Flexibility and scalability are the core advantages that mobility brings to large-scale collaborative additive manufacturing, taking the technology to a whole new level. In this technology, both the fabrication region and the object to be fabricated are divided into smaller pieces that meet the dimensions that a single AM unit can manufacture. It can be imagined that in an ideal environment, multiple mobile platforms can be equipped with AM unit to move to different designated positions in the fabrication region, and then the AM units start to collaboratively manufacture object piece in their corresponding region till the overall large-scale object is finished. In practice, however, the manufacturing environment and the positioning accuracy of the mobile platform are always far from ideal, especially for large-scale additive manufacturing, which is often conducted outdoors and has limited device accuracy. Inaccurate positioning and uneven ground will cause deviations in the position and attitude of mobile AM devices, and

then distance error and angle error are introduced into a collaboration process which requires extremely high precision.

According to Chapter 2, "mobility" and "collaboration" have already been introduced by some of researchers to large-scale additive manufacturing technology. However, there are still problems with how to deal with the cooperation between this two, especially in the case of error controlling. In terms of this field, there has not yet been a unified standard or breakthrough. It cannot be denied that unpredictable positioning misalignment and complicated fabrication environments often bring extra errors. This results in the AM devices having a different position and attitude than expected, and the parts it manufactures perpetuate these errors and fail to combine accurately. In previous researches, manual measurement and correction are often used as a conventional error correction method. However, this method is unadvanced, time-consuming and sacrifices the convenience and efficiency brought by mobility to a certain extent, which is not in line with Industry 4.0. development trend.

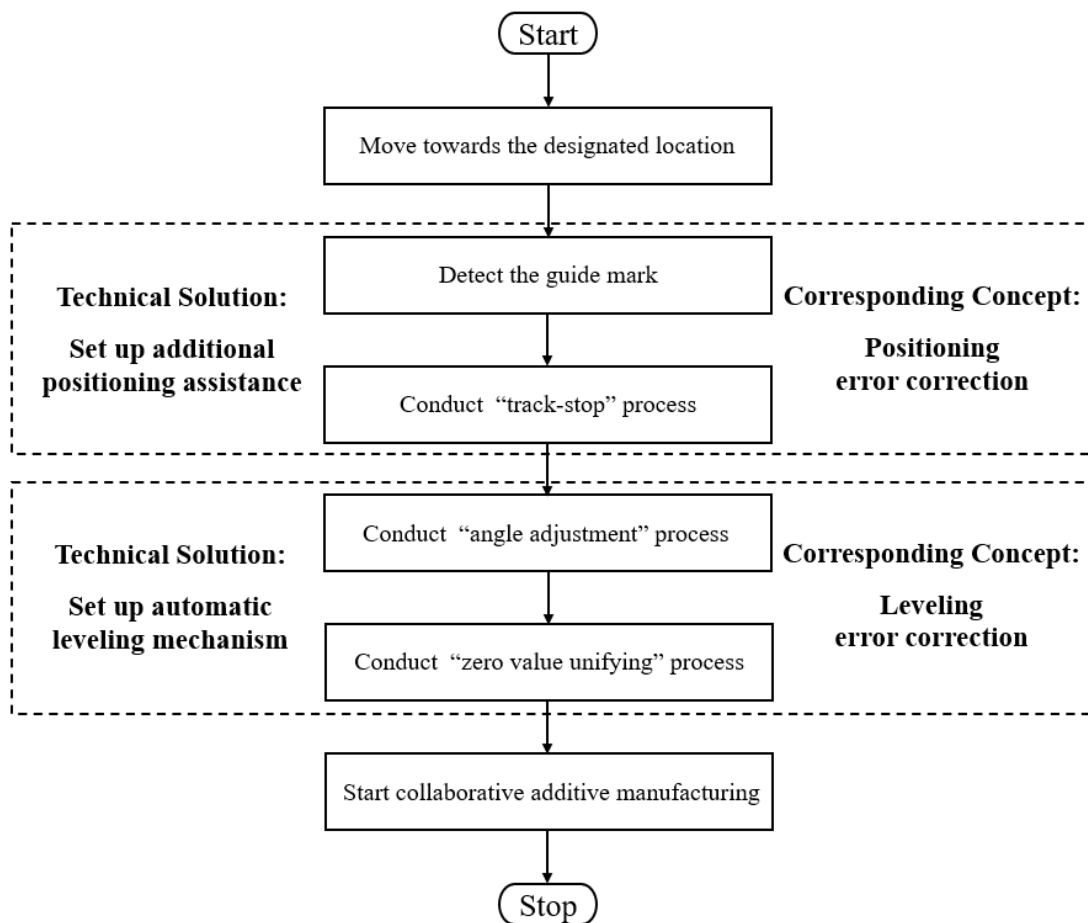
Therefore, the main idea of this research is to apply reliable and effective technical methods to minimize errors in the process of mobile positioning on the basis of a deep understanding of the causes of these errors of additive manufacturing devices before the collaborative process. Combined with the actual situation, it can be seen that the position and attitude of the mobile AM device are the key to the error. In this regard, the technical solutions of "additional positioning assistance" and "automatic leveling mechanism" are proposed respectively. Under the principle that objects in three-dimensional space have six degrees of freedom, three kinds of distance errors and three kinds of angle errors are divided into two categories according to whether they are spontaneously generated by the devices. The concepts of "positioning error correction" and "leveling error correction" are proposed to combine with the technical solutions and deal with these two categories of errors separately. Correspondingly, in the process of mobile AM device movement and positioning, a strategy of "track-stop" to assist positioning is implemented to reduce the first category of error spontaneously generated

by the device. After the positioning of the mobile AM device is completed, strategies of “zero value unifying” and “angle adjustment” are implemented to correct another category of error caused by external causes.

Figure 3.1 is a flow chart of the methodology of this chapter. This flow chart covers the entire process of mobile AM device from moving to implementing collaborative manufacturing. It shows how the proposed technical solutions and concepts can get involved in and gradually reduce various errors into tolerance range when potential distance and angle errors exist in large-scale collaborative additive manufacturing process.

Figure 3.1

Methodology Flow Chart



3.2 Technical Solutions

With the addition of mobility, the positions and attitudes of multiple AM devices are no longer fixed, which becomes a key factor that leads to errors in large-scale collaborative additive manufacturing. Only when the relative coordinates between devices are precisely constrained, can the collaborative manufacturing process be carried out accurately. Therefore, effective technical solutions need to be adopted to control and correct the positions and attitudes of mobile AM devices. Correspondingly, two technical solutions, "additional positioning assistance" and "automatic leveling mechanism", are proposed. As for the specific implementation strategies of these two schemes in the actual process, it needs to be analyzed in detail in the following sections based on the causes of all potential errors.

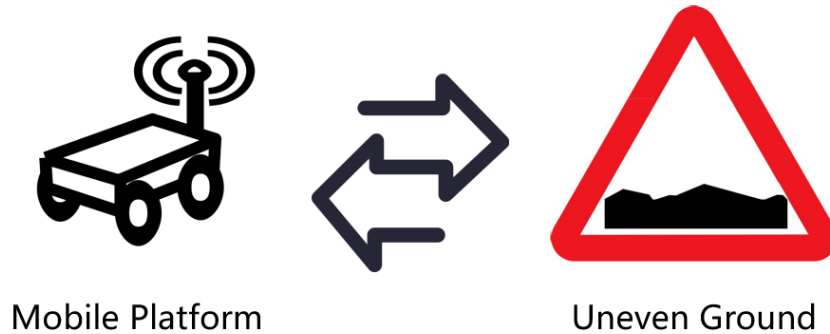
3.2.1 Position Control Solutions

For the mobile platform used to carry the AM unit, the accuracy of its original navigation and positioning method greatly determines the final position and orientation of the device. Once the final position and orientation of the device deviates from those planned ones, it means that errors are generated and the collaboration process cannot be completed accurately. The reality is that large-scale collaborative additive manufacturing often faces unknown and complex uneven ground conditions. This undoubtedly puts forward higher requirements for the positioning accuracy of the mobile platform.

As shown in Figure 3.2, when the mobile platform is under uneven ground conditions, its original navigation and positioning methods may not be able to adapt or match part or even all of the ground region, resulting in failure to operate properly, especially those that requiring to set reference markers precisely. In addition, complex ground conditions will further reduce the accuracy of mobile platform navigation and positioning, especially those with low sensor recognition sensitivity.

Figure 3.2

Interrelationship between Mobile Platform and Uneven Ground



Therefore, a position control solution of setting up "additional positioning assistance" is proposed. This technical solution aims to add an additional positioning assistance technique to achieve "hybrid positioning" according to specific ground conditions without changing the original navigation and positioning methods of the mobile platform. This positioning assistance will not affect the normal movement of the mobile platform, but it can replace or cooperate with the original navigation and positioning methods in the key positioning process to achieve more accurate positioning effects and minimize positioning errors. Depending on the actual ground conditions, different positioning assistance methods can be used. Since there is no need to change the original navigation and positioning methods as a whole, the positioning assistance added to achieve "hybrid positioning" can greatly save costs and effectively control the position of the device.

3.2.2 Attitude Control Solutions

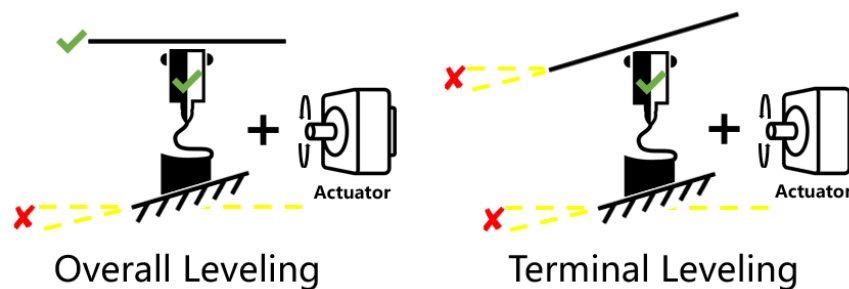
For the mobile AM device operating on uneven ground conditions, the height and attitude angle it assumes when reaching its final position is unpredictable. Once the final height and attitude angle of the device deviate from the planned ones, it means that errors are generated and the collaboration process cannot be completed accurately.

In the past large-scale collaborative additive manufacturing researches, researchers often manually measure and calibrate the attitude of the AM unit, which is very inefficient and time-consuming, especially for large-scale additive manufacturing processes that require multi-device collaboration. Therefore, an attitude control solution with an "automatic leveling mechanism" is proposed. This technical solution aims to introduce suitable sensors and actuators to automatically level the necessary structures on the AM unit. Depending on the actual accuracy requirements, leveling sensors and actuators with different precision can be used to control the cost reasonably.

For the leveling and calibration of the height, the corresponding mechanism is required to have the ability of active detection and identification. Therefore some special structures or sensors need to be used. However, for the leveling of the attitude angle, it will inevitably involve the cooperation of the sensor and the actuator. When the attitude angle of the AM unit does not match the planned angle, the actuator is used to output power and correct for these differences. To be clear, the inclination and unevenness of the ground cannot be corrected by the actuator. Only the attitude angle of the AM unit or its substructure can be corrected. As shown in Figure 3.3, two different specific technical solutions can be adopted, one is overall leveling and the other is terminal leveling.

Figure 3.3

Two Different Leveling Solutions



The overall leveling of the AM unit means that its main structure, including the extruder (nozzle), the actuator and the guide rail frame, have obtained the radial rotational degrees of freedom, and their posture is no longer fixed relative to the mobile platform. This kind of technical solution requires that the actuator used for leveling needs to have a large load capacity. After the adjustment by applying this kind of system, the AM units can quickly work on collaborative fabrication without other influences.

The terminal leveling of the AM unit means that only the extruder (nozzle) obtains the radial rotation degrees of freedom, and other main structures are still fixed relative to the mobile platform, and are always accompanied by angle errors. This kind of technical solution does not have high requirements on the load capacity of the actuator for leveling, but it will have an impact on the fabrication capacity and preparation for collaborative manufacturing. First, adding a mechanical structure to adjust the angle at the terminal of the AM unit would add weight and occupy on space there. This can reduce the maximum fabrication size and cause more unnecessary shakings during fabrication, which reduces manufacturing effectiveness. Second, since the angle error of the frame structure, which limits the fabrication size of the AM unit, is not corrected, the maximum fabrication size will change to affect the partition of subpart size and the cooperation between devices in large-scale collaborative additive manufacturing process, as shown in Figure 3.4. Last but not least, since the angle error of the main structure such as the guide rail is not corrected, the terminal will still move according to the original tool path with the angle error. Therefore, before starting fabrication, the parts to be manufactured by each AM unit must be re-sliced according to the correction data of the angle error, otherwise the manufactured parts will still carry angle errors. It can be predicted that running the device with the original tool path in the wrong coordinate system, the terminal extruder (nozzle) is very likely to interfere with the surface of the fabrication region and damage, or its gap with the surface is too large to cause manufacturing failure.

Figure 3.4

Maximum Fabrication Size Reduction

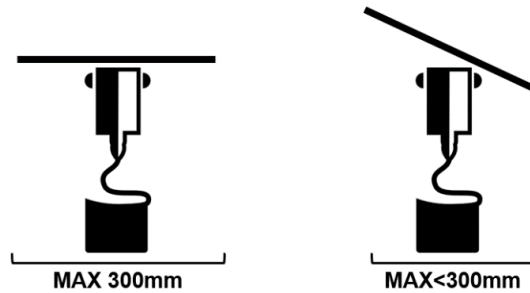


Table 3.1 lists and compares the sensitivities of two different leveling solutions to the associated requirements.

Table 3.1

Comparison of Two Leveling Solutions

| | Overall Leveling | Terminal Leveling |
|--|------------------|-------------------|
| Are high-performance actuators needed? | Yes | No |
| Will the terminal space be occupied? | No | Yes |
| Will stability be affected? | No | Yes |
| Will manufacturing size be changed? | No | Yes |
| Will the slice file need to be modified? | No | Yes |

To sum up, there are certain differences in the requirements of the actuator and the post-processing requirements of the two different leveling solutions. The technical solution that adjusts the overall unit angle requires the actuator with sufficient load capacity, and no longer requires any preprocessing steps for collaborative additive manufacturing; while the technical solution that only adjusts the angle of the terminal does not require high performance of the actuator, but a series of preprocessing steps must be added due

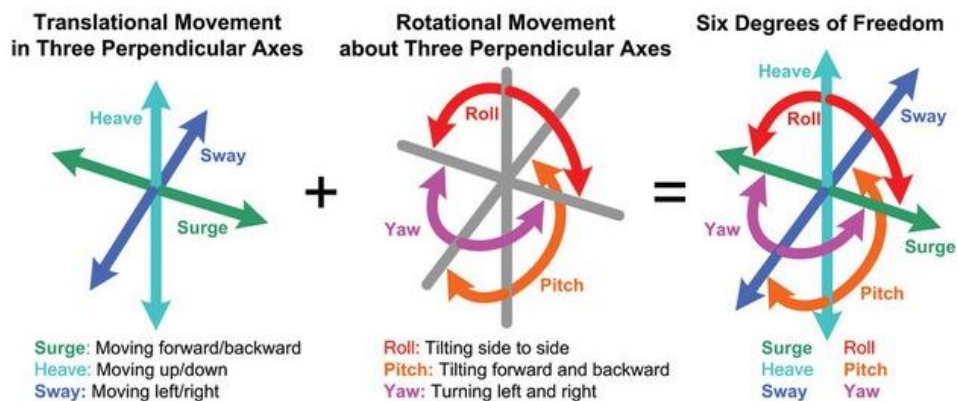
to changes in AM device setup, which complicates large-scale or multi-device collaborative additive manufacturing processes. Therefore, the technical solution of overall leveling of the AM unit is finally adopted.

3.3 Error Source and Reflection Analysis

In order to find suitable concepts and strategies to match the proposed technical solutions, sources and reflections of all potential errors need to be analyzed. In three-dimensional space, a common three-axis Cartesian coordinate system can be introduced to measure the positional relationship between objects. In this coordinate system, the object is given six degrees of freedom, including three translational degrees of freedom and three rotational degrees of freedom. Any position and angular attitude of an object in three-dimensional space can be measured by these six degrees of freedom, as shown in Figure 3.5. Once the variables of the six degrees of freedom of an object are fully defined, it means that its position and attitude in this space are confirmed.

Figure 3.5

Six Degrees of Freedom in Three-Dimensional Space



Collaborative additive manufacturing is extremely strict about the relative position and attitude control between multiple devices. In general, the collaborative AM devices should be precisely constrained in their respective three-degree-of-freedom variables

for translation, while the three-degree-of-freedom variables for rotation should remain consistent. Now due to the addition of mobility, more positioning errors are brought into the process, because the relative positions between devices are no longer maintained fixed, and complicated fabrication environments may also generate or gain errors. Part of the research in Chapter 2 has verified this. Therefore, potential errors in the positioning process of mobile AM devices in various fabrication environments need to be analyzed, and then some reasonable solutions to reduce or correct should be given.

3.3.1 Distance Error Classification and Analysis

In the three-dimensional space, there are three kinds of distance errors that can be defined, and they correspond one-to-one to the axial direction of each axis of the three-axis rectangular coordinate system. For the large-scale mobile collaborative additive manufacturing technology process, the device needs to move to a designated target position, and then start collaborative fabrication. After the moving process is over, the difference between the coordinate of the device's position and the coordinate of the target position due to various reasons is the distance error.

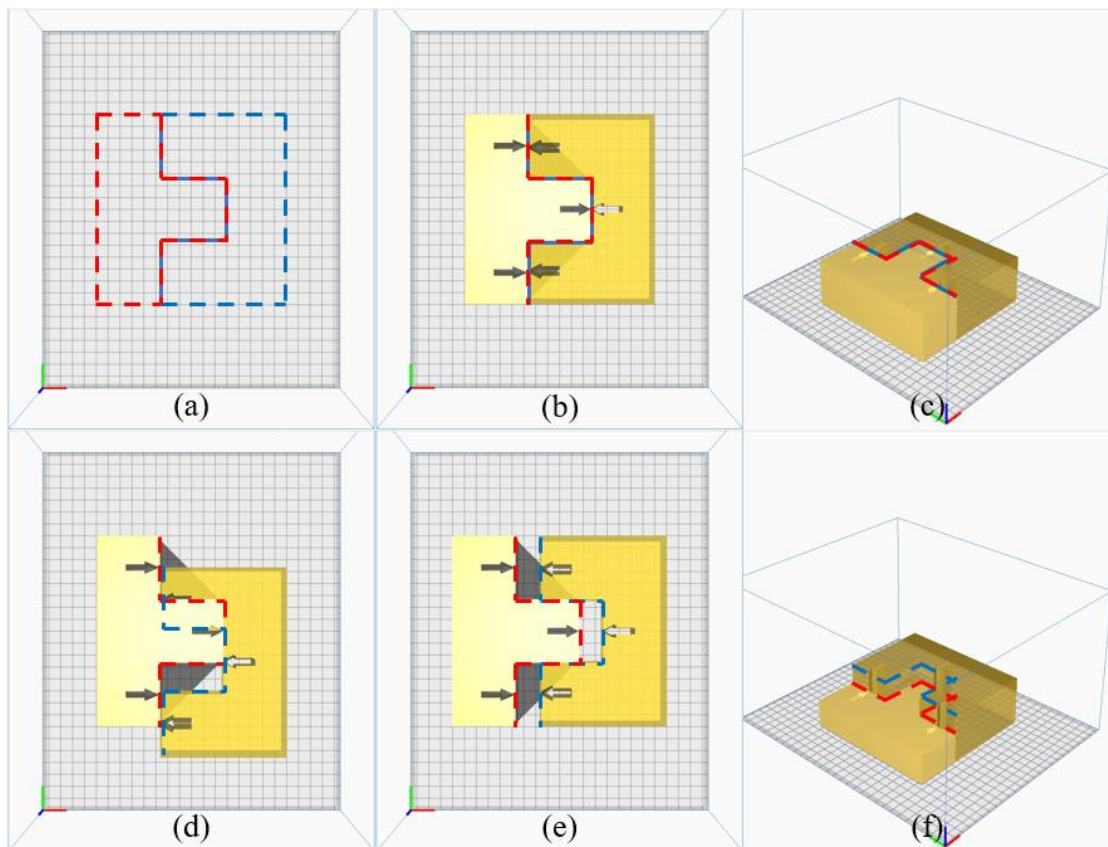
According to the characteristics of the AM device, the relative position of the manufactured part to the device never changes. In other words, in the same space, if the distance error exists in a certain AM device after positioning, then the parts manufactured by this device will also have the same amount of distance error. This kind of distance error is fatal for large-scale collaborative additive manufacturing, because the boundary of the part with this kind of error will shift and cause it to fail to meet other parts at the planned joint, then joint misalignment, gap or interference may appear because of this.

For mobile AM devices moving on the ground, there are two causes for distance errors in all directions. One is the positioning error caused by the insufficient positioning ability of the mobile platform itself or the misalignment of the movement process, and the other is the leveling error caused by the uneven ground or drop.

Now suppose that two mobile AM devices are in a Cartesian coordinate system in which the plane formed by the X-axis and the Y-axis is the horizontal plane, and the Z-axis is perpendicular to the horizontal plane. Figure 3.6(a) simulates two parts that are connected to each other manufactured by the two devices, respectively, and the connecting edge of each part is marked with arrows. Figure 3.6(b), Figure 3.6(c) shows the effect of splicing the two parts without any error, and it can be seen that the tips of the arrow marks on the two parts are in exact contact with each other. Figure 3.6(d) and Figure 3.6(e) show the effect of a certain distance error in the X-axis and Y-axis axial directions. It can be seen that the two sets of combinations appear interference and gaps respectively. Figure 3.6(f) shows the effect of certain distance error in the Z-axis axial direction, and it can be seen that the two parts are misaligned at the joint.

Figure 3.6

Effect of Distance Error on Collaboration



Note. (a) Outlines of the two objects; (b) Top view of two objects that have been accurately and collaboratively manufactured; (c) Orthographic view of two objects that have been accurately and collaboratively manufactured; (d) Top view of two objects that have been collaboratively manufactured with X-axis distance error; (e) Top view of two objects that have been collaboratively manufactured with Y-axis distance error; (f) Orthographic view of two objects that have been collaboratively manufactured with Z-axis distance error.

3.3.2 Angle Error Classification and Analysis

In three-dimensional space, there are three kinds of angle errors that can be defined, and they correspond one-to-one to the radial direction of each axis of the three-axis rectangular coordinate system. Similarly, for large-scale mobile collaborative additive manufacturing technology processes, the device needs to be moved to a designated target position before collaborative fabrication begins. However, after the moving process is over, the difference between the attitude formed by the device and the target attitude due to various reasons is the angle error.

According to the characteristics of the AM devices, the relative position of the manufactured part and the device will not change. In other words, in the same space, if the angle error exists in a certain AM device after positioning, then the parts produced by this device will also have the same amount of angle error. In the same way, for large-scale collaborative additive manufacturing, the existence of angle errors will cause the boundaries of sub-parts to deflect and make it impossible to meet other parts at the planned junction, resulting in gaps or interference.

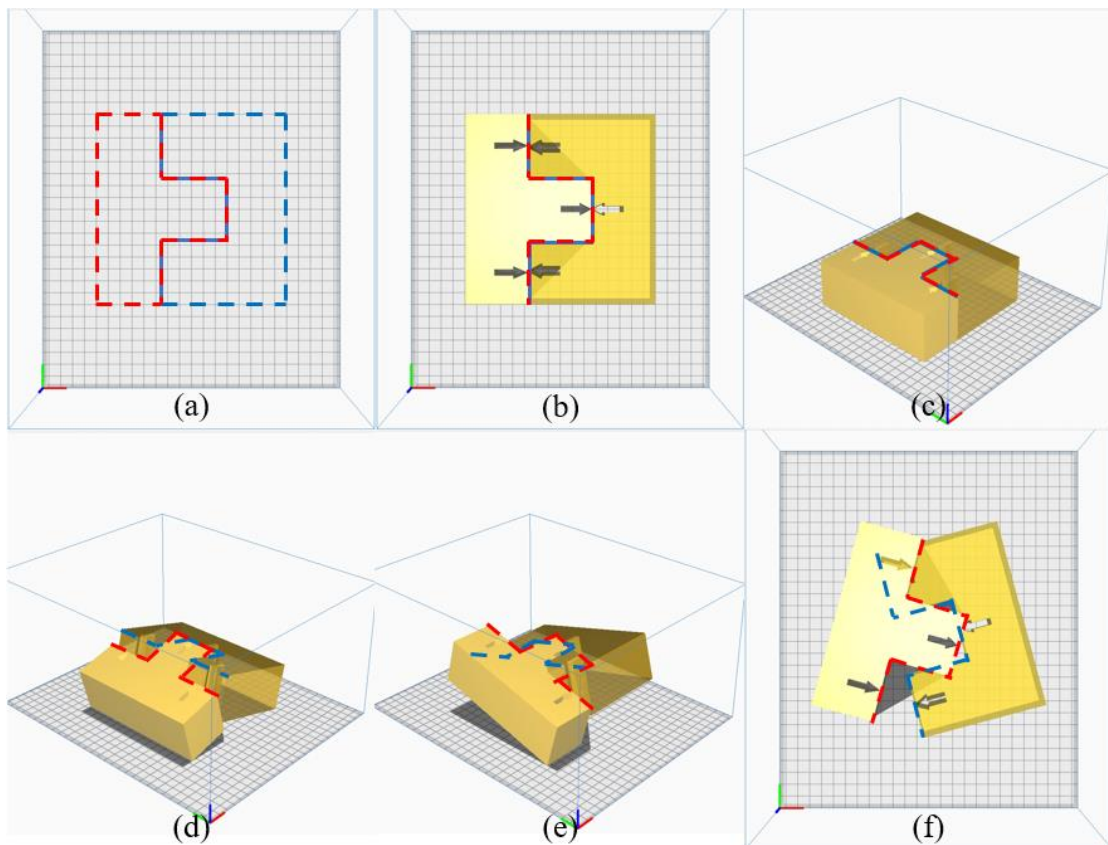
For mobile AM devices moving on the ground, there are two causes for angle errors in all directions. One is the declination angle caused by the insufficient positioning ability of the mobile platform itself or the misalignment of the movement process, and the other is the inclination angle caused by the uneven ground or drop.

Now suppose that two mobile AM devices are in a Cartesian coordinate system in which the plane formed by the X-axis and the Y-axis is the horizontal plane, and the Z-axis is

perpendicular to the horizontal plane. Figure 3.7(a) simulates two parts that are connected to each other manufactured by the two devices, respectively, and the connecting edge of each part is marked with arrows. Figure 3.7(b), Figure 3.7(c) shows the effect of splicing the two parts without any error, and it can be seen that the tips of the arrow marks on the two parts are in exact contact with each other. Figure 3.4(d), Figure 3.7(e) and Figure 3.7(f) show the effect of a certain angle error in the radial direction of the X axis, the radial direction of the Y axis and the radial direction of the Z axis. It can be seen that all sets of combinations appear interference and gaps to varying degrees.

Figure 3.7

Effect of Angle Error on Collaboration



Note. (a) Outlines of the two objects; (b) Top view of two objects that have been accurately and collaboratively manufactured; (c) Orthographic view of two objects that have been accurately

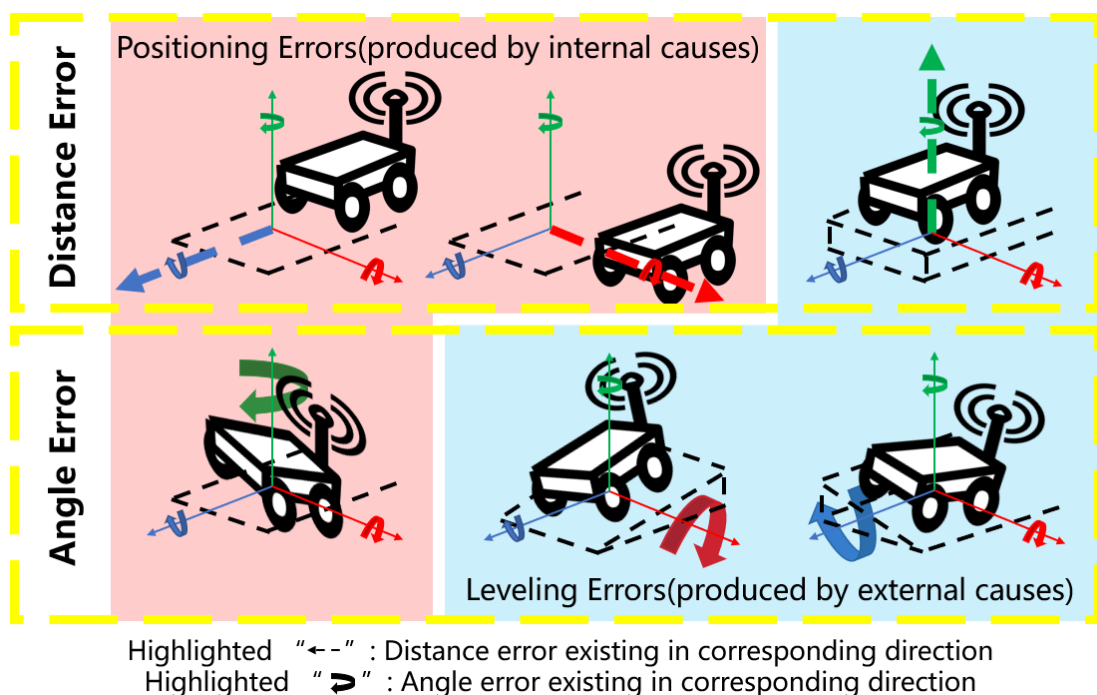
and collaboratively manufactured; (d) Top view of two objects that have been collaboratively manufactured with X-axis angle error; (e) Top view of two objects that have been collaboratively manufactured with Y-axis angle error; (f) Orthographic view of two objects that have been collaboratively manufactured with Z-axis angle error.

3.3.3 Summary of Error Types and Causes

In the first two subsections, all potential positioning errors before collaborative fabrication of mobile AM devices are analyzed. In general, all six types of errors can be divided into two categories in terms of their manifestations, and two other categories in terms of causes, as shown in Figure 3.8. From the perspective of the consequences caused by errors, the existence of any kind of error will lead to different degrees of gap, interference or dislocation between the two parts that need to be combined. It is also the core problem that must be avoided in the collaboration process before the implementation of large-scale collaborative additive manufacturing.

Figure 3.8

Error Classification



3.4 Positioning Error Correction

From the classification of errors caused by mobility and the analysis of the impact on collaborative additive manufacturing in the previous subsections, it was determined that controlling these errors to limit them within the tolerances range of large-scale collaborative additive manufacturing technology is necessary. However, considering the complexity of terminal errors in real situations, a variety of detection and correction methods of different error types and dimensions must be applied. The detection and control methods of these errors need to be properly classified and set up and can be carried out efficiently and orderly when errors appear.

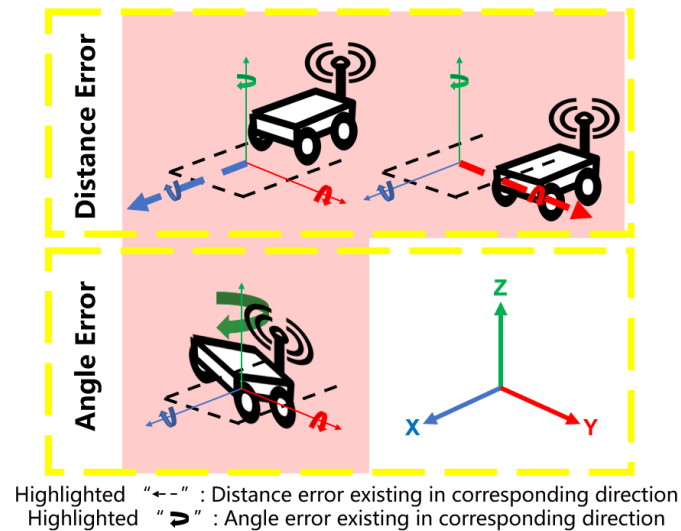
A scheme to control all kinds of errors introduced by mobility to large-scale collaborative additive manufacturing by classifying them into two categories which are "positioning error" and "leveling error", and applying correction technical solutions and strategies is proposed in this study. The difference between the two categories is when and how errors are reduced. Error correction implemented when mobile platform moving or positioning is defined as "positioning error correction" process, which emphasizes that errors of this category should be effectively contained before they occur. On the contrary, the error correction implemented after the movement and positioning of the mobile platform is defined as "leveling error correction" process, which emphasizes that various types of errors of this category need to be effectively detected and corrected after they are generated.

This section will be devoted to expounding the methodology for error reduction under the positioning error correction category. This category includes two distance errors and one angle error. Consistent with the previous sections, suppose that the mobile AM device is in a rectangular coordinate system in which the plane formed by the X-axis and the Y-axis is a horizontal plane, and the Z-axis is perpendicular to the horizontal plane, then the two distance errors exist in the axial direction of X-axis and Y-axis respectively, and an angle error exists in the radial direction of Z axis, as shown in Figure 3.9. The three types of errors are grouped together because they are entirely

caused by inaccurate movement or positioning of the mobile AM device. This kind of cause belongs to the "internal cause", which is completely irrelevant to the external environment. That is to say, if the movement and positioning capabilities of the AM device are properly controlled, such errors can be avoided at the source. This is the origin of the concept of "positioning error correction" in this section: using reasonable and effective methods to improve the positioning effect of mobile AM device so that the generated positioning errors are within the tolerance range. This solution is optimal in terms of cost and efficiency. The following subsections will introduce the corresponding feasible strategies according to the proposed technical solutions for each type of error.

Figure 3.9

Errors Produced by Internal Causes



3.4.1 Distance Error Control

Following the classification of the parent section, this subsection proposes a strategy to reduce two types of distance error for mobile AM devices serving large-scale collaborative additive manufacturing. It is known that the mobile AM device is in a Cartesian coordinate system in which the plane formed by the X-axis and the Y-axis is the horizontal plane, and the Z-axis is perpendicular to the horizontal plane, and the two

distance errors exist in the axial directions of the X-axis and the Y-axis respectively. That is to say, what needs to be controlled is the positioning error of the device. If the mobile AM device can move and locate the specified position with absolute accuracy, then the error is equal to zero. However, in practice, it is very difficult to achieve absolutely accurate positioning.

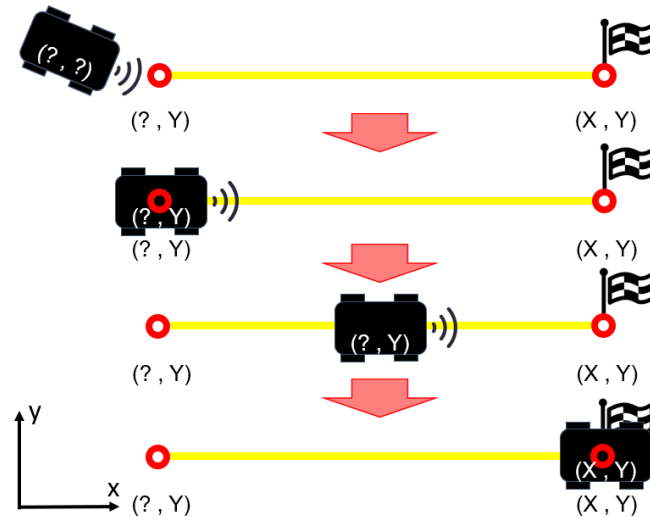
Among several common mobile platform positioning methods, most of them can achieve limited accuracy, which can only be accurate to the centimeter level or even decimeter level. The precision level of the sensor is usually the main cause for this. This level of positioning accuracy might not be sufficient for some of the specific large-scale collaborative additive manufacturing that to be implemented. In addition, the nature of emphasizing scalability for large-scale collaborative additive manufacturing dictates that the cost, flexibility, and reliability of any positioning method also need to be considered.

Therefore, a set of suitable positioning method and sensor need to be used for the proposed "additional positioning assistance". In addition, reasonable positioning paths can also be introduced to assist in further reducing positioning error. A strategy of setting travelling paths in a "track-stop" mode is proposed. The core of this strategy is that the mobile platform no longer follows the logic of "stop positioning as soon as the sensor detects the target location" like the conventional positioning method, but by extending the detection process, starts to compensate the error during the travelling process till the end.

To implement this strategy, a sensor-identifiable continuous tracking mark with start and end point is placed in advance on the navigation path near the end of the designated location. The mobile platform that detects the starting point triggers the tracking navigation, and then continues to move following the direction of the mark and corrects its travelling path, so that an axial positioning parameter is confirmed. When the sensor detects the end point, it will stop accurately, so that the positioning parameter of the other axis is confirmed, as shown in Figure 3.10.

Figure 3.10

“Track-Stop” Strategy



Through the above process, the axial distance error of the two axes on the horizontal plane can be effectively controlled. This strategy is applicable to almost all kinds of mobile platforms and can be flexibly adjusted to match different manufacturing environments. By optimizing the sensor and mobility accuracy of the mobile platform or the setting of the "track stop" mark, the distance error of the AM device in the X-axis and Y-axis can be minimized until the tolerance range requirements for large-scale collaborative additive manufacturing are met.

3.4.2 Angle Error Control

Following the classification of the parent section, this subsection proposes a strategy to reduce one type of angle error for mobile AM devices serving large-scale collaborative additive manufacturing. It is known that the mobile AM device is in a rectangular coordinate system in which the plane formed by the X axis and the Y axis is the horizontal plane, and the Z axis is perpendicular to the horizontal plane. This angle error exists in the radial direction of the Z axis, which means that what needs to be controlled is the orientation of the device. If the mobile AM device is oriented at the target angle after reaching the specified position, then the error is equal to zero.

In practice, the orientation of a mobile AM device is closely related to the positioning path, because the orientation at the moment when the device stops moving is often the final orientation. That is to say, as long as the orientation accuracy during the movement of the mobile AM device can be ensured, the angle error in the radial direction of the Z-axis can be well controlled.

In fact, the strategy used in the previous subsection to reduce the distance error on the two axes of the horizontal plane is also applicable to control the angle error in this subsection. It is known that during the positioning process the sensor no longer only detects a single final designated point, but can continuously detect to track the path as it travels. This means that as long as the tracking control logic is set up properly, the mobile AM device can adjust its orientation on the navigation path between the start and end point, and ensure that the orientation is accurate before stopping. In addition, the mark identification method of the end point can also be flexibly set as required to ensure the same orientation before and after stopping. As long as the accuracy of the “track stop” process is continuously calibrated, the angle error of the mobile AM device in the radial Z-axis can be minimized until the tolerance range of large-scale collaborative additive manufacturing is met.

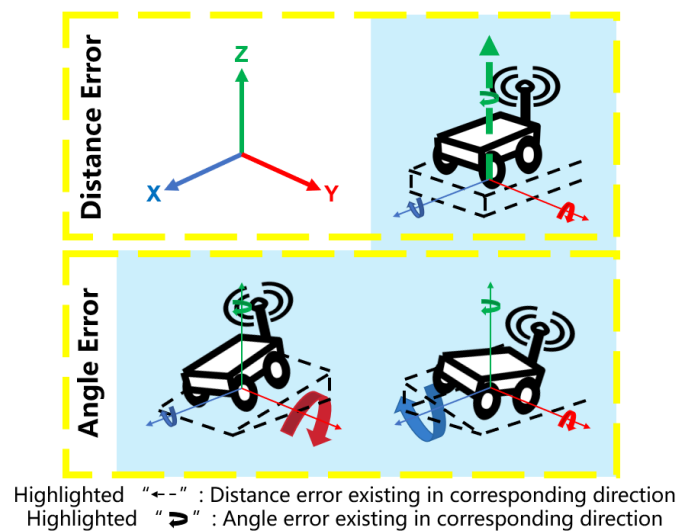
3.5 Leveling Error Correction

This section will be devoted to expounding the methodology for error correction under the leveling error correction category. This category includes one distance error and two angle errors. Consistent with the previous sections, suppose that the mobile AM device is in a rectangular coordinate system in which the plane formed by the X-axis and the Y-axis is a horizontal plane, and the Z-axis is perpendicular to the horizontal plane, then one single distance error exists in the axial direction of the Z-axis, and the two angle errors exist in the radial directions of the X-axis and the Y-axis, respectively, as shown in Figure 3.11. The three types of errors are grouped together because they are entirely caused by the external environment, such as ground flatness, inclinations, and drops. This kind of cause belongs to "external cause" and is not caused by the mobile AM

device itself. That is to say, regardless of the movement and positioning capabilities of the AM device, as long as there is any abnormality in the external environment, the positioning of the device is very easy to generate errors. Because the source of this category of errors is not spontaneous and cannot be corrected by any movement or adjustment of the mobile platform carrying the AM device itself, to achieve automatic error reduction, a concept of detecting and correcting errors must be introduced. This is the origin of the concept of "leveling error correction" in this section. The following subsections will introduce the corresponding feasible solutions according to the proposed technical solutions for each type of error.

Figure 3.11

Errors Produced by External Causes



3.5.1 Distance Error Control

Following the classification of the parent section, this section proposes a strategy to correct a distance error for mobile AM devices serving large-scale collaborative additive manufacturing. It is known that the mobile AM device is in a rectangular coordinate system in which the plane formed by the X-axis and the Y-axis is a horizontal plane, and the Z-axis is perpendicular to the horizontal plane, and this distance error exists in the axial direction of the Z-axis. In practice, the ground on which mobile AM

devices are located is usually not absolutely flat. And due to the different positions, there will inevitably be a certain height difference between the devices in the vertical direction, that is, in the axial direction of the Z-axis. Once consider about the flexibility and scalability given to the mobile AM device, it is not practical to measure and calibrate the surface of the fabrication region before every large-scale collaborative additive manufacturing process, as that would be extremely time-consuming and costly, and also there is no guarantee that the ground drop can be calibrated with absolute precision.

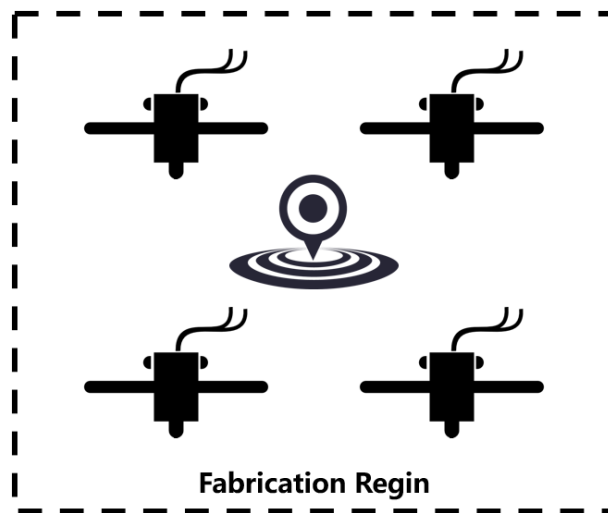
For large-scale collaborative additive manufacturing technology, the mobile platform used to carry the AM unit is only responsible for movement and positioning, and does not participate in the subsequent fabrication process. In other words, the height difference in the Z-axis will only affect the operating accuracy of the AM unit and cause errors in the collaboration process. This also means that the correction of this type of error can be carried out only for the AM unit without considering the mobile platform. In fact, almost all AM units calibrate the distance between their extruder (nozzle) and the plane of the fabrication region before running, and set the height value of this fabrication region as the zero value of the AM unit's Z-axis. Based on this reason, an idea comes out that there is no need to correct the height of each AM unit, but just make sure that their zero values on the Z axis are consistent, then the error can be corrected.

Therefore, a strategy for correcting the Z-axis axial distance error is proposed by allowing multiple AM units to conduct zero value calibration at the same height in the fabrication region. This strategy requires that after multiple mobile AM devices arrive at their respective designated locations, they need to conduct Z-axis zero value calibration at the same position or the same height reference in the collaborative manufacturing region, as shown in Figure 3.12. After calibration, multiple devices having the same zero value reference in the same space means that such distance errors have been corrected. Both conventional stroke limit sensor or endstop can be used to measure the stroke of the Z axis. In this strategy, the precision of the sensor used for

calibration almost determines the dimension of this distance error. Therefore, under different manufacturing environments and error tolerance ranges, sensors of different types and precisions can be flexibly selected to control cost.

Figure 3.12

Zero Value Unifying Strategy



3.5.2 Angle Error Control

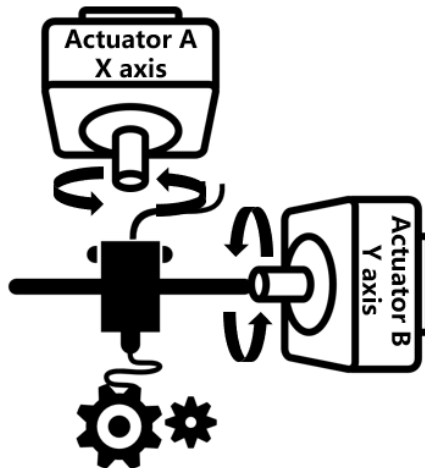
Following the classification of the parent section, this subsection proposes a strategy to correct two angle errors of mobile AM devices serving large-scale collaborative additive manufacturing. It is known that the mobile AM device is in a Cartesian coordinate system in which the plane formed by the X-axis and the Y-axis is a horizontal plane, and the Z-axis is perpendicular to the horizontal plane, and these two angle errors exist in the radial directions of the X-axis and the Y-axis, respectively. In practice, the ground on which mobile AM devices are located is usually not absolutely flat. This leads to possible differences in the attitude angles formed by each device, and the manufactured parts carry the corresponding angle differences, resulting in gaps or interference at the joints. When mobile AM devices work outdoors on uneven ground or build large objects that require multiple movements, this kind of angle error is more likely to accumulate and manifest. Consistent with the previous subsection, it is not

practical to measure and calibrate the surface of the fabrication region before each large-scale collaborative additive manufacturing process. This requires that the radial angle error of the two axes must be accurately detected and corrected according to the proposed technical solutions.

A strategy of releasing the rotational degrees of freedom of the X-axis and Y-axis of the AM unit and adding actuators to correct the angle error is proposed. Necessary sensor, controller and actuator make up the control system of this strategy. The sensor is used to detect the angle error value of the AM unit. The controller analyzes and calculates the error and outputs execution instructions. The actuator corrects the angle error existing in the AM unit by outputting rotating motion. Normally, two actuators are required. As shown in Figure 3.13, they should be placed vertically and control the rotational degrees of freedom for the X and Y axes, respectively.

Figure 3.13

Angle Adjustment Strategy



Similar to correcting the Z-axis distance error, the angle error only affects the collaboration between AM units and has nothing to do with the positioning of the mobile platform. Therefore, it is only necessary to perform angle error correction on the structure corresponding to the AM unit. In addition, according to the comparison

and selection of the proposed corresponding technical solution, the overall AM unit needs to be controlled and rotated by the actuators.

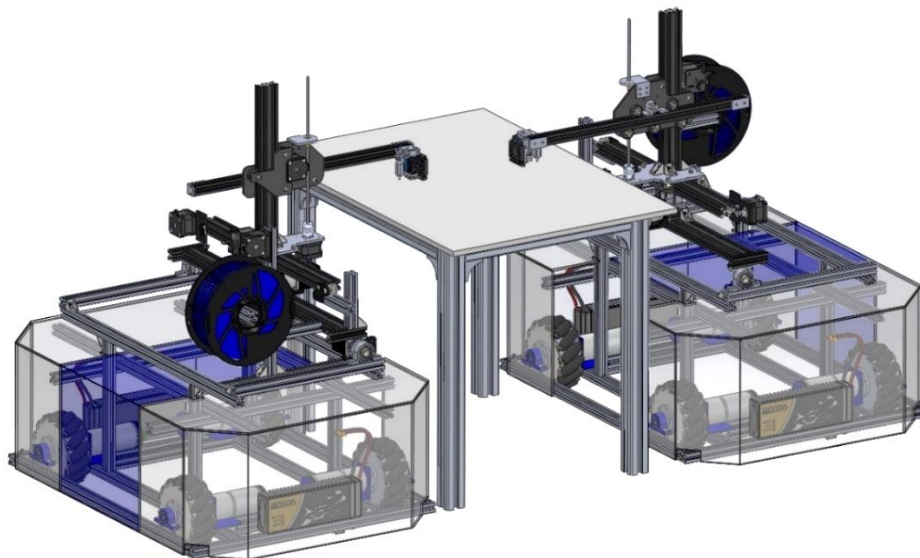
CHAPTER 4

SYSTEM DEVELOPMENT

To implement and validate those various concepts and technical solutions generated in the previous chapter, a prototype of a mobile 3D printer based on Fused Deposition Modeling (FDM) technology for large-scale collaborative additive manufacturing was developed, as shown in Figure 4.1. The prototype is mainly composed of three modular parts, including the mobile platform, the AM unit and the angle adjustment system (AAS). This chapter focuses on explaining which specific technical methods the mobile AM device uses to achieve "positioning error correction" and "leveling error correction". The developed mobile AM device will also be implemented in experiments under a laboratory environment to prove the feasibility of the concepts.

Figure 4.1

CAD Models of Mobile 3D Printers



4.1 Modular Mobile Platform: Automated Guided Vehicle (AGV)

In order to improve the flexibility of mobile AM device to match different manufacturing environments, a modular automated guided vehicle (AGV) was adopted

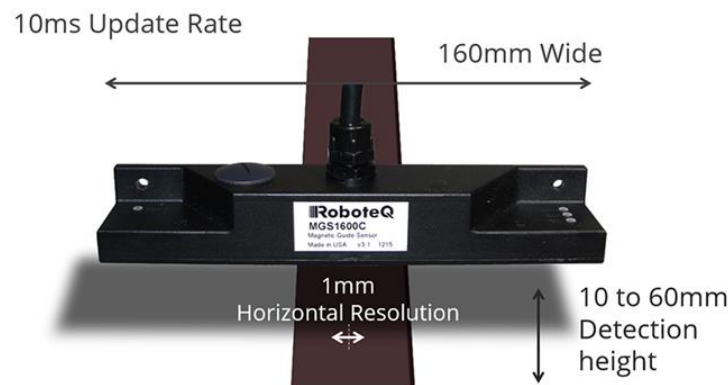
as the prototype of the mobile platform to be developed and participated in the follow-up experimental verification of this study. It should be noted that the specifications, including but not limited to the hardware and software of the AGV, are based on the ground conditions in the laboratory of this research. This AGV, as the mobile platform in this study, aims to realize and validate the corresponding concepts proposed in Chapter 3. In other different manufacturing environments, vehicles of different categories and performances can be used on demand.

4.1.1 Track-Stop Strategy

Looking at the positioning methods commonly used in AGV industry, each has its own advantages and disadvantages in terms of navigation method, cost and accuracy. Considering that the final experiments conducted in this study to verify the effect will be based on the laboratory ground condition and high-precision AM units, the positioning method used needs to be able to match these factors. Magnetic positioning is a rare combination of the precision, cost, flexibility and reliability requirements of large-scale collaborative additive manufacturing technology under this condition. The millimeter-level positioning accuracy lays the foundation for error control, as shown in Figure 4.2. Inexpensive and easy-to-lay magnetic tape guarantees low cost and high flexibility.

Figure 4.2

Specification and Accuracy of Magnetic Tape Following Sensor

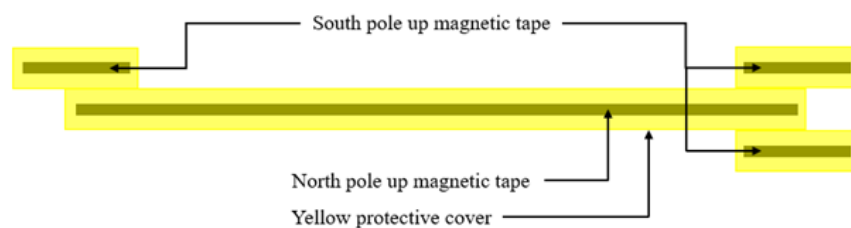


However, for mobile platforms, a single magnetic tape can only control the positioning accuracy in a single axial direction. Only when the mobile platform equipped with the magnetic tape following sensor can accurately travel along the magnetic tape, and can accurately stop at the specified position in this axial direction, can the effective control of the target biaxial axial distance error be achieved.

Therefore, a special magnetic tape setting method was proposed. As shown in Figure 4.3, four magnetic tapes placed in the same orientation form a positioning mark suitable for large-scale collaborative additive manufacturing. The magnetic tapes at both ends have opposite polarities to the longest magnetic tape in the middle, and serve as start and end marks for mobile AM devices to identify and locate. When the magnetic tape tracking sensor installed on the mobile AM device detects the starting point of the positioning mark, the device will start to track the longest magnetic tape and automatically correct the orientation of its path, so that one axial positioning parameter is confirmed. When the sensor detects the end mark, the device slows down and stops exactly at the end of this mark, allowing the positioning parameters of the other axis to be confirmed. A positioning control program suitable for the above logic needs to be developed. Additionally, the setting of the program and tape marks, especially its end points, can be modified or calibrated to minimize distance errors in the X-axis and Y-axis of the mobile AM device until the tolerance range requirements for large-scale collaborative additive manufacturing are met.

Figure 4.3

Magnetic Tape Setting Method



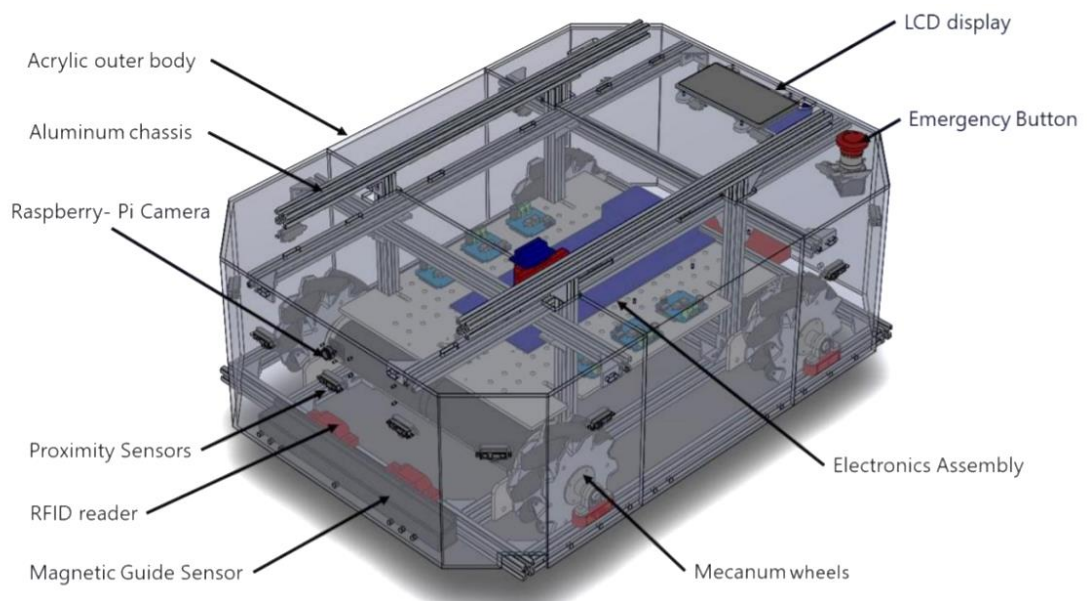
Similar to the selection of the mobile platform, the use of magnetic tape navigation assists to implement the track-stop strategy is only based on the existing laboratory ground conditions. The same method and precision are not necessarily achievable in other different manufacturing environments. But the same concept can also serve other navigation or positioning methods to positioning error correction.

4.1.2 Development of AGV Prototype Structure

In order to reduce costs, this research uses the AGV prototype developed by previous master students in the laboratory to support students to actively learn skills in the field of smart manufacturing. The main frame of the AGV is constructed from standard-sized aluminum profiles, and the outer casing is covered with acrylic plastic. The large-capacity lithium battery and the high-torque stepper motor equipped with Mecanum wheels together provide the driving power for the vehicle. Inside this AGV, a variety of different types of sensors and electronic components are preset, as shown in Figure 4.4.

Figure 4.4

Components of the Modular AGV Prototype



As a modular mobile platform, the robust and flexible structure of the AGV prototype provides the basis for the subsequent development and adaptation of AM units. Some of the necessary sensors and controller systems were activated and reconfigured to meet the requirements for navigation and some categories of error control capabilities. At the same time, some additional components are also added to ensure the adaptability of the other two modular parts. After these settings and modifications, the structural characteristics of the AGV are as follows.

- Aluminum profile frame provides large load capacity
- Mecanum wheel provides flexible movement
- High-torque stepper motor with encoder provides both output and rotation closed-loop detection
- Two large-capacity lithium batteries supply power for different modular parts respectively
- MPU6050 gyroscope implements motion data detection
- Industrial magnetic tape tracking sensor implements positioning
- Arduino series microcontroller implements data processing and transmission

In terms of structure, considering the need to mount AM unit and angle adjustment system (AAS) in the later stage, the frame of the aluminum profile is strengthened to improve its load capacity, while keeping the light weight to the maximum extent. Four Mecanum wheels are installed on the four corners of the AGV to ensure the stability of the mobile platform while providing sufficient mobility. In order to improve the accuracy of movement, the stepper motor that controls the Mecanum wheels is equipped with a photoelectric encoder to monitor the output rotation angle at any time, and compensate in time to correct the movement path when the motor loses steps. For weight distribution and stability considerations, two large-capacity lithium batteries are placed at the front and rear ends of the AGV, respectively, to supply power to the AGV, AM unit and AAS. Before the positioning magnetic tape mentioned in Chapter 3 is not detected, the AGV uses common inertial navigation to assist its movement. At this time,

the MPU6050 gyroscope can provide sufficient movement accuracy monitoring capabilities and interfere and correct the path at the appropriate time. The most important thing is that the magnetic tape tracking sensor used to detect the magnetic tape and start the positioning process is accurately installed at the front end of the AGV to avoid the delay of positioning triggering and to eliminate the interference of other structures to the greatest extent. Algorithms for identification and correction of positioning paths will be presented in the following section.

4.1.3 Development of AGV Control System

In order to improve the flexibility of the mobile platform, a hybrid navigation mode is introduced into the control system of the AGV. The AGV travels by traditional inertial navigation until it detects the "track-stop" mark set to enhance positioning. The code for navigation runs in the AGV's main microcontroller, which is the Arduino Due. Four photoelectric encoders and an MPU6050 gyroscope together monitor and correct the AGV's travelling path to guide it to the starting point of the "track-stop" mark.

When the magnetic tape following sensor installed on the front of the AGV detects the starting point of the mark, the positioning process of the "track-stop" logic is officially triggered. The code for the sensor to recognize the tape runs in another microcontroller, the Arduino Mega2560, and feeds the processed data back to the main microcontroller. A program written based on proportional–integral–derivative (PID) control theory carefully guides the AGV to continuously correct the orientation and stop precisely at the end point of the magnetic tape to achieve "positioning error correction" of two types of distance errors and one type of angle error caused by internal causes in Chapter 3. Figure 4.5 shows the code of how the magnetic tape following sensor detects and processes data. Figure 4.6 shows the PID control code for the AGV to correct its movement path.

Figure 4.5

Magnetic Tape Detection Code

```
724 void MGS_Routine()
725 {
726
727     MGS_Analog_Pos = map(analogRead(MGS_ANALOG_POS), 0, 620, 0, 1023); // maps 0 to 3V in MGS sensor to 0 to 1024
728
729     if (MGS_PWM_Pos == 0)
730     { //tape is not detected
731         MGS_Track_Present = 0;
732         MGS_Marker_Left_Detect = 0;
733         MGS_Marker_Right_Detect = 0;
734     }
735     if (MGS_PWM_Pos > 200 && MGS_PWM_Pos < 300)
736     { // tape detected
737         MGS_Track_Present = 1;
738         MGS_Marker_Left_Detect = 0;
739         MGS_Marker_Right_Detect = 0;
740     }
741     if (MGS_PWM_Pos > 450 && MGS_PWM_Pos < 550)
742     { //no tape left marker detected
743         MGS_Track_Present = 0;
744         MGS_Marker_Left_Detect = 0;
745         MGS_Marker_Right_Detect = 1;
746     }
747     if (MGS_PWM_Pos > 700 && MGS_PWM_Pos < 800)
748     { // tape and left marker detected
749         MGS_Track_Present = 1;
750         MGS_Marker_Left_Detect = 0;
751         MGS_Marker_Right_Detect = 1;
752     }
753     if (MGS_PWM_Pos > 950 && MGS_PWM_Pos < 1050)
754     { // no tape right marker detected
755         MGS_Track_Present = 0;
756         MGS_Marker_Left_Detect = 1;
757         MGS_Marker_Right_Detect = 0;
758     }
759     if (MGS_PWM_Pos > 1100 && MGS_PWM_Pos < 1300)
760     { //tape and right marker detected
761         MGS_Track_Present = 1;
762         MGS_Marker_Left_Detect = 1;
763         MGS_Marker_Right_Detect = 0;
764     }
765     if (MGS_PWM_Pos > 1450 && MGS_PWM_Pos < 1550)
766     { //no tape and left and right markers detected
767         MGS_Track_Present = 0;
768         MGS_Marker_Left_Detect = 1;
769         MGS_Marker_Right_Detect = 1;
770     }
771     if (MGS_PWM_Pos > 1700 && MGS_PWM_Pos < 1800)
772     { //tape and left marker and right marker is detected
773         MGS_Track_Present = 1;
774         MGS_Marker_Left_Detect = 1;
775         MGS_Marker_Right_Detect = 1;
776     }
777 }
```

Figure 4.6

Code for PID Control of AGV

```
20 #include "LineFollow.h"
21
22 #define NIVEL_PARA_LINEA 50
23
24 LineFollow::LineFollow(){
25     config(11,5,50,10);
26
27     for(int i=0;i<5;i++){
28         sensor_blanco[i]=0;
29         sensor_negro[i]=1023;
30     }
31 }
32
33 void LineFollow::config(uint8_t KP, uint8_t KD, uint8_t robotSpeed, uint8_t intergrationTime){
34     this->KP=KP;
35     this->KD=KD;
36     this->robotSpeed=robotSpeed;
37     this->intergrationTime=intergrationTime;
38 }
39
40 void LineFollow::calibrRs(){
41     static bool isInitied=false;//So only init once
42     if(isInitied)return ;
43     delay(1000);
44
45     doCalibration(30,500);
46     doCalibration(-30,500);
47     doCalibration(30,500);
48
49     delay(1000);
50     isInitied=true;
51 }
52
53
54 void LineFollow::runLineFollow(){
55     for(int count=0; count<5; count++){
56         {
57             lectura_sensor[count]=map(IRread(count),sensor_negro[count],sensor_blanco[count],0,127);
58             acu=lectura_sensor[count];
59         }
60         //Serial.println(millis());
61         if (acu > NIVEL_PARA_LINEA)
62         {
63             acu/=5;
64
65             int error = ((lectura_sensor[0]<<6)+(lectura_sensor[1]<<5)-(lectura_sensor[3]<<5)-(lectura_sensor[4]<<6))/acu;
66
67             error = constrain(error,-100,100);
68
69             //Calculamos la correccion de velocidad mediante un filtro PD
70             int vel = (error * KP)/10 + (error-last_error)*KD;
71
72             last_error = error;
73
74             //Corregimos la velocidad de avance con el error de salida del filtro PD
75             int motor_left = constrain((robotSpeed + vel),-100,100);
76             int motor_right =constrain((robotSpeed - vel),-100,100);
77
78             //Movemos el robot
79             //motorsWritePct(motor_left,motor_right);
80             motorsWritePct(motor_left,motor_right);
81
82             //Esperamos un poquito a que el robot reaccione
83             delay(intergrationTime);
84
85         }
86         else
87         {
88             motorsStop();
89
90             reportActionDone();
91             //setMode(MODE_SIMPLE);
92         }
93     }
94
95     void LineFollow::doCalibration(int speedPct, int time){
96         motorsWritePct(speedPct, -speedPct);
97         unsigned long beginTime = millis();
98         while((millis()-beginTime)<time)
99             ajusta_niveles();
100         motorsStop();
101     }
102
103     void LineFollow::ajusta_niveles()
104     {
105         int lectura=0;
106
107         for(int count=0; count<5; count++){
108             lectura_IRread(count);
109             if (lectura > sensor_blanco[count])
110                 sensor_blanco[count]=lectura;
111             if (lectura < sensor_negro[count])
112                 sensor_negro[count]=lectura;
113         }
114     }
115 }
```

4.2 Modular AM Unit: Outstretched 3D Printer

In order to adapt to the structure of the existing AGV and support large-scale collaborative additive manufacturing, a modular outstretched 3D printer based on Fused Deposition Modeling (FDM) technology was designed and developed. It should be noted that the core of this kind of modular AM unit lies in the unique outstretched structure and the application of sensors for realizing leveling error correction. The adoption of FDM technology is to better match the current laboratory manufacturing environment, and to verify the corresponding concept in Chapter 3 through experiments. In other different manufacturing environments, different additive manufacturing techniques can be introduced as an alternative.

4.2.1 Zero Value Unifying Strategy

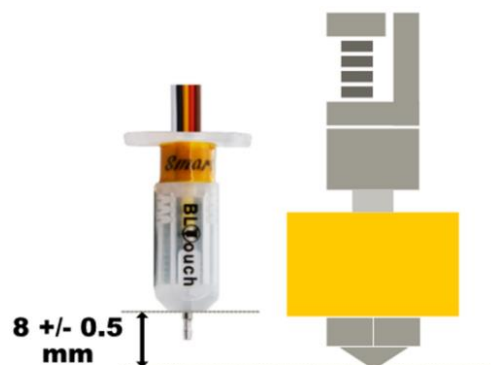
According to the concept statement in Chapter 3, to correct the Z-axis axial distance error, it is only necessary to unify the Z-axis zero value of multiple AM units in their collaborative fabrication region. For most 3D printers, their fabrication region tends to

be fixed. This leads to the fact that the sensor used to calibrate the zero value is usually mounted on a fixed structure, so the 3D printer does not have the flexibility to calibrate at any position.

Therefore, a strategy using the BLTouch sensor to achieve leveling error correction of the Z-axis axial distance error is introduced. BLTouch is a Hall sensor with a micro switch. Unlike the conventional endstop sensor which is mounted on the 3D printer in a fixed position, the BLTouch is mounted in the same direction next to the 3D printer extruder (nozzle) and moves following it, as shown in Figure 4.7. The 3D printer calibrates the zero value by touching the probe of the BLTouch to the surface of the fabrication region. This special homing method makes it possible to correct the Z-axis axial distance errors between large-scale collaborative additive manufacturing devices. When the positioning process of the mobile AM device is completed, as long as multiple devices perform zero value calibration based on the same position or the same height surface in the fabrication region, the home fabrication coordinates of all devices in the Z-axis can be consistent, which also means such distance errors have been minimized.

Figure 4.7

Positional Relationship Between BLTouch and Nozzle



Compared to other sensors, the BLTouch sensor has also been proved to have excellent accuracy and adaptability, as shown in Figure 4.8. In addition, BLTouch also supports height difference detection of surfaces at different positions in the fabrication region to

realize automatic compensation of fillers, which is a supplementary AM error correction outside the scope of this study.

Figure 4.8

Comparison of the Characteristics of Commonly Used Sensors for 3D Printer

| Sensor | BLTouch (Hall) | Proximity | | Micro Switch with SG90 Servo |
|------------------------|-------------------|-------------|-------------|-------------------------------------|
| | | Inductive | Optical | |
| Sensor Type | contact | non-contact | non-contact | contact |
| Standard Deviation | ≤ 0.01 | ≤ 0.2 | ≤ 0.01 | ≤ 0.3 |
| Repeated accuracy | ≤ 1% | ≤ 5% | ≤ 1% | ≤ 5% |
| bed material | Unlimited | Metal | Glass X | Unlimited |
| Max Current | < 300mA | 200mA | 200mA | 300mA |
| Consumption Current | 20mA | 20mA | 20mA | 200mA w/t jitter 20mA w/o jitter |

4.2.2 Development of 3D Printer Prototype Structure

To support large-scale collaborative additive manufacturing, an outstretched 3D printer was designed and developed, as shown in Figure 4.9. Unlike the most common gantry 3D printers, this developed printer has a print arm that can be outstretched and retracted to support the movement of multiple extruders (nozzles) within the same manufacturing space for collaboration. This configuration also ensures that the fabrication region will not interfere with the mobile platform when the printer is mounted on the mobile platform.

Figure 4.9

CAD Model of the Developed Outstretched 3D Printer



The structure of this outstretched 3D printer is based on the most common gantry XYZ structure 3D printers. In order to realize the outstretch and retraction of the extruder (nozzle), the conventional principle of parallel installation of X-axis, Y-axis and Z-axis is banned. An innovative principle of tandem installation of the X-axis, Y-axis and Z-axis is employed. On this 3D printer, the Z-axis is mounted on the Y-axis rail bracket, and the X-axis is mounted on the Z-axis rail bracket, as shown in Figure 4.10. This particular mechanical principle forms the core of the outstretched 3D printer and also enables large-scale collaborative additive manufacturing.

Figure 4.10

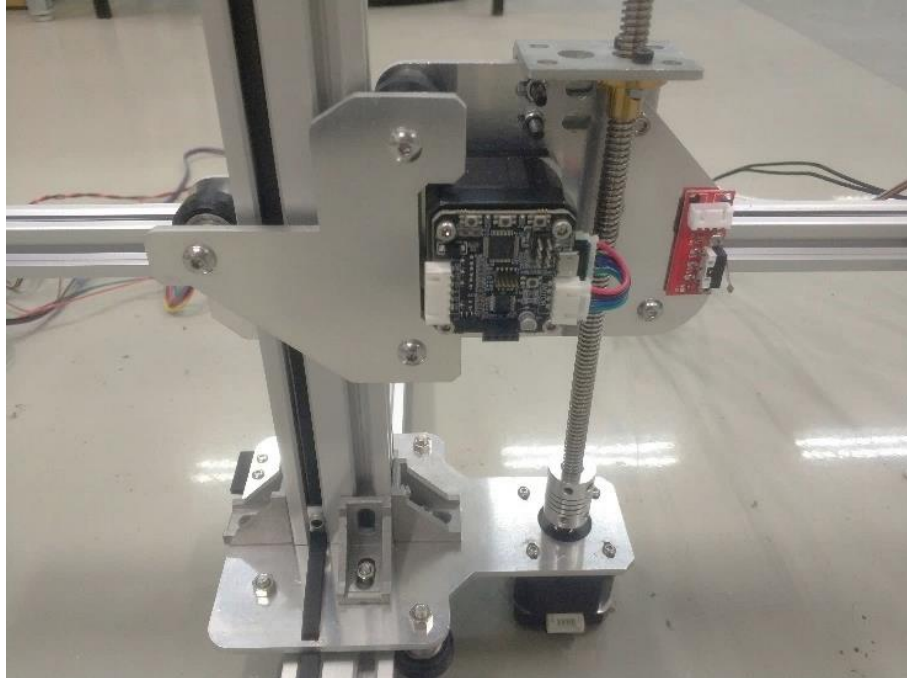
Three-Axis Series Structure



The main structure of the outstretched 3D printer is made of lightweight standard profiles and custom aluminum sheets. Similar to common gantry AM devices, this printer has three translational degrees of freedom that are perpendicular to each other. The axial movements of the 3D printer's X and Y axes are driven by belts, while the Z axis's is driven by a lead screw. Closed-loop stepper motors are introduced to prevent lost steps and enhance printing accuracy. On the other hand, this also ensures that the deviation of the printing results in subsequent experiments does not come from the printer, as shown in Figure 4.11. Necessary sensors are installed to assist with printing and to correct for errors.

Figure 4.11

3D Printer Driver Components



The structural features of this modular outstretched 3D printer prototype are as follows.

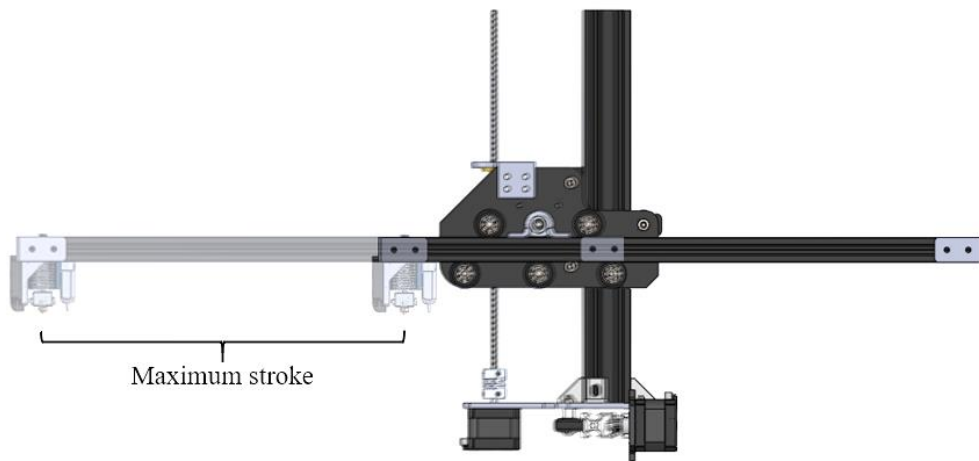
- Outstretched structure enables collaborative additive manufacturing
- Aluminum profiles and brackets form the strong and lightweight frame
- Nema17 stepper motor provides efficient and stable drive
- Multi-wheel guides ensure the stability of the printer
- FDM printing method is high quality and easy to maintain
- 12V power input is easy to obtain and adapt to mobility
- The controller composed of Arduino and RepRap series is efficient and easy to operate

The outstretched arm that translates in the X-axis is the core innovation of this outstretched 3D printer. Aluminum brackets, guide wheels, stepper motors, belts and V-slot profiles make up the outstretched arm structure. Under the premise of ensuring stability, the structure has been extremely simplified to reduce weight and maximize

axial stroke. Figure 4.12 shows the states of the outstretched arm at its minimum and maximum value positions.

Figure 4.12

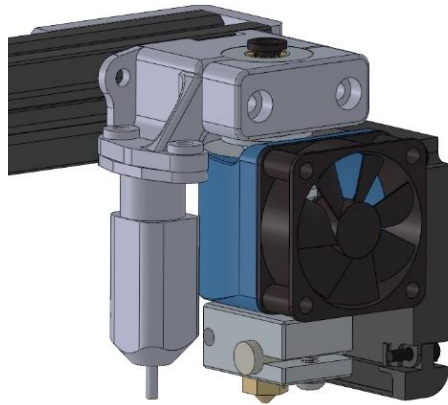
Maximum Stroke of the X-Axis of the Outstretched 3D Printer



The BLTouch sensor used to implement the "zero value unifying" strategy to correct for Z-axis axial distance error during large-scale collaborative additive manufacturing processes is installed next to the nozzle at the end of the outstretched arm, as shown in Figure 4.13. This sensor travels together with the nozzle to maximize detection within the fabrication region. The relative position of the sensor and nozzle has been precisely measured and set in code to ensure that the 3D printer can run properly and conduct zero value calibration.

Figure 4.13

The Structure of the End of the Outstretched Arm



The final specifications and parameters of the hardware of the outstretched 3D printer are set as follows.

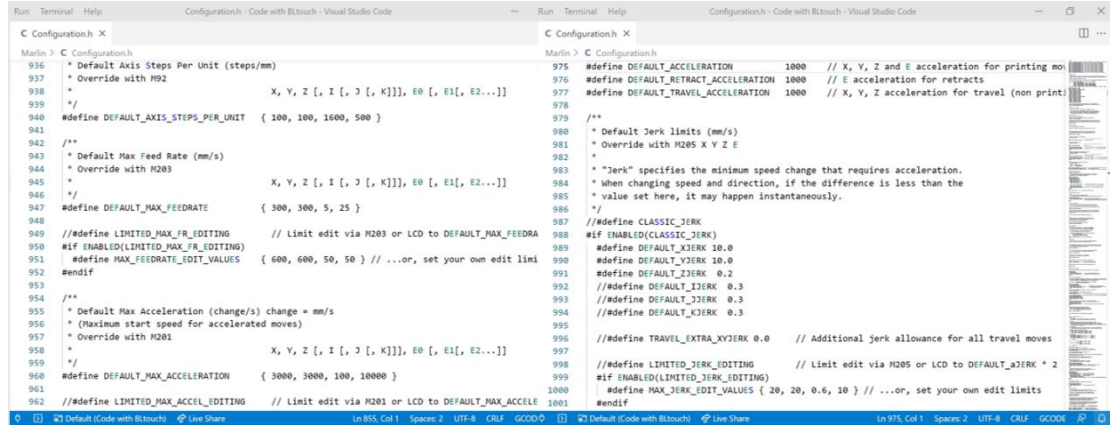
- Maximum printable size of X axis: 250mm
- Maximum printable size of Y axis: 300mm
- Maximum printable size of Z axis: 150mm
- Nozzle inner diameter: 0.4mm
- Filament diameter: 1.75mm

4.2.3 Development of 3D Printer Control System

The controller of this outstretched 3D printer is composed of the Arduino series Mega2560 main control board and the RepRap series RAMPS 1.4 control board. The control code for the 3D printer is based on the open source Marlin firmware. The necessary parameter settings and control logic have been fully defined in the firmware to ensure that the 3D printer can run as planned. Figure 4.14 shows some core printing parameters set in the firmware. A RepRapDiscount series full graphic LCD display is connected to the controller to operate the printer. The UI (user interface) page of this display is shown in Figure 4.15.

Figure 4.14

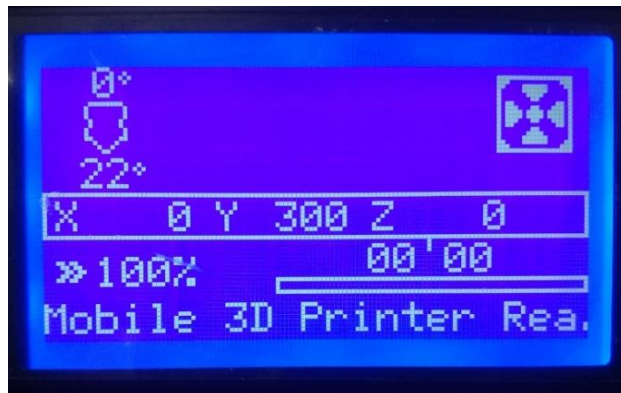
Core Parameters of the Outstretched 3D Printer's Firmware Code



```
936 * Default Axis Steps Per Unit (steps/mm)
937 * Override with M92
938 *
939 */
940 #define DEFAULT_AXIS_STEPS_PER_UNIT { 100, 100, 1600, 500 }
941
942 /**
943 * Default Max Feed Rate (mm/s)
944 * Override with M203
945 *
946 */
947 #define DEFAULT_MAX_FEEDRATE { 300, 300, 5, 25 }
948
949 // #define LIMITED_MAX_FR_EDITING // Limit edit via M203 or LCD to DEFAULT_MAX_FEEDRATE
950 #if ENABLED(LIMITED_MAX_FR_EDITING)
951 #define MAX_FEEDRATE_EDIT_VALUES { 600, 600, 50, 50 } // ...or, set your own edit limits
952 #endif
953
954 /**
955 * Default Max Acceleration (change/s) change = mm/s
956 * (Maximum start speed for accelerated moves)
957 * Override with M201
958 *
959 */
960 #define DEFAULT_MAX_ACCELERATION { 3000, 3000, 100, 10000 }
961
962 // #define LIMITED_MAX_ACCEL_EDITING // Limit edit via M201 or LCD to DEFAULT_MAX_ACCELERATION
963
964 #define DEFAULT_ACCELERATION 1000 // X, Y, Z and E acceleration for printing moves
965 #define DEFAULT_RETRACT_ACCELERATION 1000 // E acceleration for retracts
966 #define DEFAULT_TRAVEL_ACCELERATION 1000 // X, Y, Z acceleration for travel (non print)
967
968 /**
969 * Default Jerk limits (mm/s)
970 * Override with M205 X Y Z E
971 *
972 * "Jerk" specifies the minimum speed change that requires acceleration.
973 * When changing speed and direction, if the difference is less than the
974 * value set here, it may happen instantaneously.
975 */
976 #define CLASSIC_JERK
977 #if ENABLED(CLASSIC_JERK)
978 #define DEFAULT_X_JERK 10.0
979 #define DEFAULT_Y_JERK 10.0
980 #define DEFAULT_Z_JERK 0.2
981 #define DEFAULT_E_JERK 0.3
982 #define DEFAULT_XY_JERK 0.0 // Additional jerk allowance for all travel moves
983 #endif
984 // #define LIMITED_JERK_EDITING // Limit edit via M205 or LCD to DEFAULT_*_JERK * 2
985 #if ENABLED(LIMITED_JERK_EDITING)
986 #define MAX_JERK_EDIT_VALUES { 20, 20, 0.6, 10 } // ...or, set your own edit limits
987 #endif
```

Figure 4.15

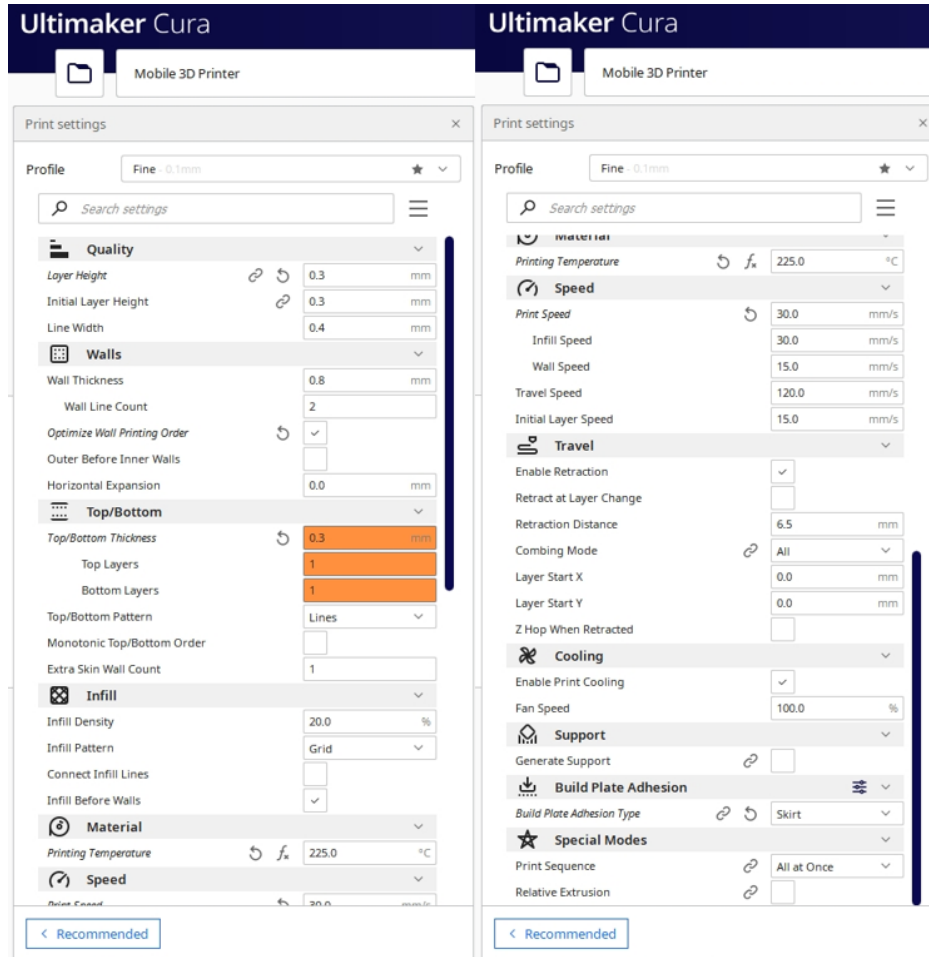
UI of the Outstretched 3D Printer's Display



Before the large-scale collaborative additive manufacturing process, the 3D model of the manufactured object needs to be converted into STL format, and then sliced by professional slicing software. Some of the slicing and printing parameters need to be properly defined in the software to match the structural characteristics of the 3D printer and the printing environment. The Ultimaker Cura slicing software is used in this study, and some of the slicing and printing parameters used for later experiments can be found in Figure 4.16.

Figure 4.16

Slicing and Printing Parameters of Outstretched 3D Printer



4.3 Modular Angle Adjustment System (AAS)

In order to adapt to the structure of the outstretched 3D printer and support large-scale collaborative additive manufacturing, a modular angle adjustment system that automatically performs angle measurement and leveling error correction is designed and developed. The current specification of the modular angle adjustment system is adapted to the developed outstretched 3D printer. In other different manufacturing environments, the system can also be paired with other AM units to achieve leveling error correction of errors, but the load capacity of the system needs to be paid attention to and enhanced when necessary.

4.3.1 Angle Adjustment Strategy

According to the concept statement in Chapter 3, in order to correct the attitude of the AM unit, the key lies in how to release and control the rotational degrees of freedom of the device in X-axis and Y-axis. A mechanical system including sensor, controller and actuator is designed and developed. In this system, the MPU6050 gyroscope is used as a sensor to detect the angle error, the STM32 microcontroller is used as the main controller to analyze the error value and output the execution command, and two stepper motors with encoders are used as the actuator to correct existing angle error of the AM unit through rotation. A rotation control program suitable for the above logic also needs to be developed.

The rotational degrees of freedom of the X-axis and Y-axis of the AM unit can be flexibly controlled, which means that its attitude can be defined at any time. In a large-scale collaborative additive manufacturing process, different manufacturing environments have different attitude requirements for AM units. In generally tilted ground conditions, these AM units might be required to remain tilted. In ground conditions that are generally level but uneven in some of its region, they might be required to remain level. What will not change, however, is that the attitude of each AM unit should be consistent, otherwise collaborative manufacturing cannot be implemented. Therefore, the developed angle adjustment system should have the function of freely setting the target attitude angle, which will be used to match with different manufacturing environments. In addition, the motor should be able to achieve self-locking after completing the leveling error correction of angle error, thereby ensuring the stability of the AM unit during the collaborative manufacturing process.

4.3.2 Development of AAS Prototype Structure

How to transmit the rotational motion output by the motor to the AM unit and make it rotate is the core of the mechanical structure of the system. A mechanical structure in which the output shaft directly drives the AM unit to rotate is proposed to simplify the

structure and reduce the load. Figure 4.17 and Figure 4.18 show the CAD model and practical assembly of the angle adjustment system, respectively.

Figure 4.17

CAD Model of the Angle Adjustment System

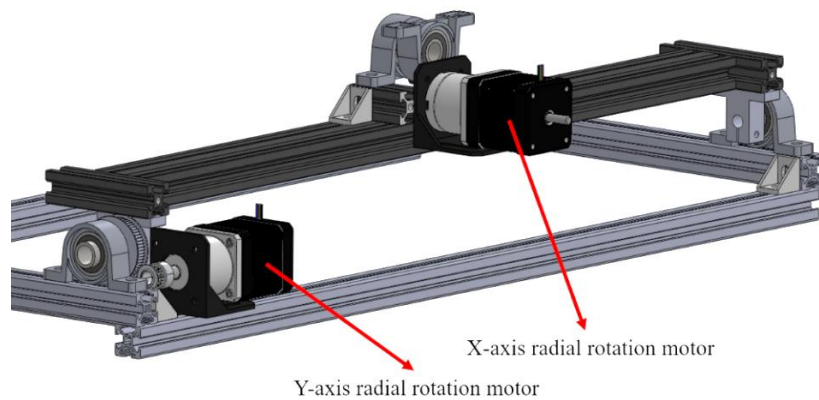
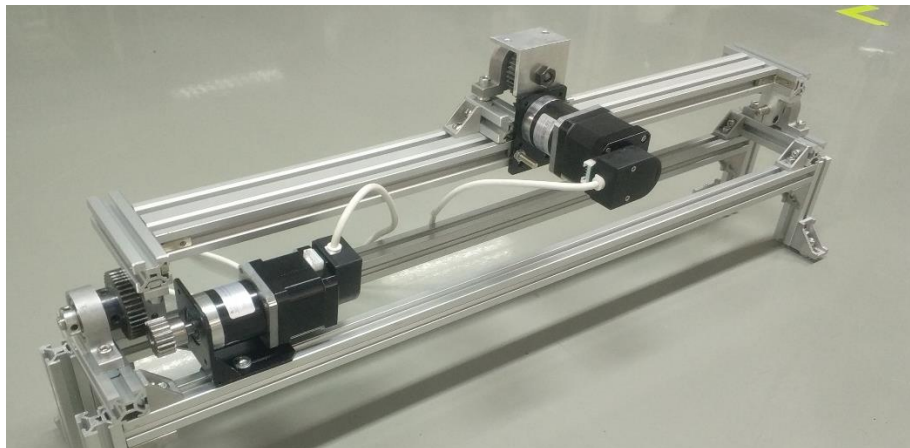


Figure 4.18

Practical Assembly of the Angle Adjustment System

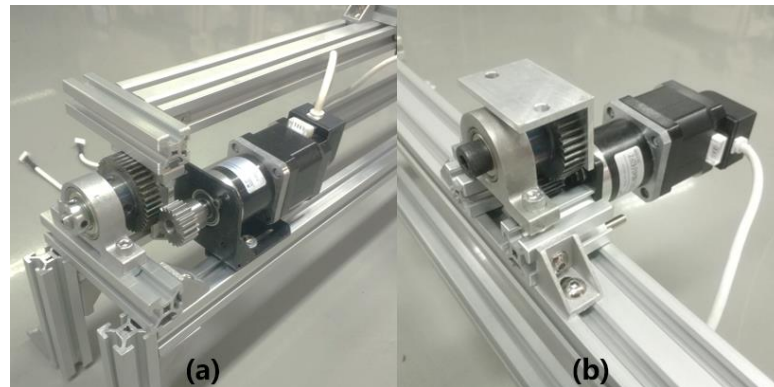


The frame of this angle adjustment system is constructed from standard aluminum profiles. The two ends and the middle of the frame are equipped with mutually vertical bearing blocks, which are respectively connected with the base of the mobile platform and the AM unit to provide the rotational degree of freedom of the X-axis and the Y-

axis. High-torque stepper motors with reducer are installed next to the bearing blocks in two different directions to drive. To further enlarge the torque and optimize the precision of the angle adjustment, A gear set is used as the connection between the output shaft and the driven structure. The other end of the stepping motor is equipped with a photoelectric encoder to detect the rotation angle of the motor, as shown in Figure 4.19. The MPU6050 as a sensor is fixed on the AM unit to obtain its real-time attitude angle. The features of this prototype modular angle adjustment system are as follows.

Figure 4.19

Actuator Layout



Note. (a) Layout of the Y-axis motor, reducer, gear transmission and encoder; (b) Layout of the X-axis motor, reducer, gear transmission, and encoder.

Considering that the entire AM unit needs to be rotated to adjust the attitude angle, the maximum torque needs to be calculated to select the appropriate specification motor. As the AM unit of this study, the gravitational force of the outstretched 3D printer is 24.5 N. When each axis of the printer is at the maximum stroke position, the distance between the center of gravity of the printer and the rotation point where the angle adjustment structure connects to is the farthest, which is 300mm. It can be calculated that the torque required to properly rotate the 3D printer under any circumstances is 7.35 Nm.

After selection, the step angle of the stepper motor selected by the angle adjustment system is 1.8 degrees, and the torque is 0.36 Nm. The reduction ratio of the reducer is 1:14, and the reduction ratio of the gear set is 1:2. It can be calculated that the torque output by the terminal is 10.08 Nm, and the theoretical maximum angle accuracy of the system is 0.064 degrees. Taking into account the laboratory ground conditions for later experiments, the final accuracy of the system is set to 0.1 degrees, and the maximum rotation angle is set to 15 degrees to ensure stable operation.

Finally, the features of this modular angle adjustment system prototype are as follows.

- Aluminum profiles form a strong and lightweight frame
- Stepper motor with reducer provides sufficient torque
- Multi-stage deceleration transmission ensures the precision of angle adjustment
- Photoelectric encoder limits the maximum rotation angle
- MPU6050 gyroscope provides high sensitivity and high precision
- 12V power input is easy to obtain and adapt to mobility
- The controller based on STM32 series microcontroller is efficient and accurate

4.3.3 Development of AAS Control System

The controller of the angle adjustment system is composed of STM32 microcontroller, LV8731 driver, and OLED display. Code written based on PID control theory runs in the main chip and corrects the existing angle error of the AM unit. Figure 4.20 shows some of the key code in the program. In this control program, the target attitude angle that the AM unit needs to achieve can be arbitrarily set to match different collaborative manufacturing conditions. When the system is running, once the encoder detects that the rotation angle in any direction reaches the maximum value, the motor that controls the corresponding direction will stop to avoid overloading or interference. When the angle correction process is over, the program can control the self-locking of the motors to fix the attitude of the AM unit for the next stage of the collaborative additive manufacturing process. The UI page of the controller display is shown in Figure 4.21.

Figure 4.20

Core Code of the AAS Program

```
13 //*****
14 Kinematic Analysis
15 *****/
16 void Kinematic_Analysis(float angle_y,float angle_x)
17 {
18     Target_A = TARGET_A*10*angle_y ;
19     Target_B = TARGET_B*10*angle_x;
20 }
21
22 //*****
23 Main Control Code
24 *****/
25 int EXTI2_IRQHandler(void)
26 {
27     if(INT==0)
28     {
29         EXTI_ClearITPendingBit(EXTI_Line2);
30         Flag_Target=Flag_Target;
31         Reg();
32         Position_A=Read_Encoder(3)/Encoder_Ratio; //Read Encoder
33         Position_B=Read_Encoder(2)/Encoder_Ratio; //Read Encoder
34         Position_C=Read_Encoder(4); //Read Encoder
35         Read_DMP(); //Update
36
37         Motor_A=Position_PID_A(Position_A,Flag); //PD Control for Motor A
38         Motor_B=Position_PID_B(Position_B,Roll); //PD Control for Motor B
39
40         Xianfu_Position();
41
42         Xianfu_Velocity(Max_Velocity,Max_Velocity,Max_Velocity);
43         if(Turn_Off()==0)
44             Set_Pwm(Motor_A,Motor_B,Motor_C);
45         Voltage_Temp=Get_battery_volt();
46         Voltage_Count++;
47     }
48 }
49
50 *****/
51 Function
52 *****/
53 pwm=Kp*e(k)+Ki*E(k)+Kd[e(k)-e(k-1)]
54 *****/
55 int Position_PID_A (int Encoder,int Target)
56 {
57     static float Bias,Pwm,Integral_bias,Last_Bias;
58     Bias=Zero_x-Pitch; //Calculate Error
59     Integral_bias=Bias; //Integral of Error
60     Pwm=Position_KP*Bias+Position_KI*Integral_bias+Position_KD*(Bias-Last_Bias); //Output
61     Last_Bias=Bias;
62     return Pwm;
63 }
64
65 int Position_PID_B (int Encoder,int Target)
66 {
67     static float Bias,Pwm,Integral_bias,Last_Bias;
68     Bias=Zero_y-Roll; //Calculate Error
69     Integral_bias=Bias; //Integral of Error
70     Pwm=Position_KP*Bias+Position_KI*Integral_bias+Position_KD*(Bias-Last_Bias); //Output
71     Last_Bias=Bias;
72     return Pwm;
73 }
74
75 float Position_PID_X (int Encoder,int Target)
76 {
77     static float Bias,Pwm,Integral_bias;
78     Bias=Encoder-Target; //Calculate Error
79     Integral_bias=Bias; //Calculate Error
80     Pwm=anglex_KP*Bias+anglex_KI*Integral_bias+anglex_KD*gyro[0]; //Output
81     Last_Bias=Bias;
82     if(Flag_Stop) Integral_bias=0;
83     return Pwm;
84 }
85
86 float Position_PID_Y (int Encoder,int Target)
87 {
88     static float Bias,Pwm,Integral_bias;
89     Bias=Encoder-Target; //Calculate Error
90     Integral_bias=Bias; //Calculate Error
91     Pwm=angley_KP*Bias+angley_KI*Integral_bias+angley_KD*gyro[1]; //Output
92     Last_Bias=Bias;
93     if(Flag_Stop) Integral_bias=0;
94     return Pwm;
95 }
96
97 //*****
98 PWM Motor Control
99 *****/
100 void Set_Pwm(int motor_a,int motor_b,int motor_c)
101 {
102     int Final_Motor_A,Final_Motor_B,Final_Motor_C;
103     if(motor_a<0) INA=0; //Motor A Direction
104     else INA=1;
105     if(motor_b<0) INB=1; //Motor A Direction
106     else INB=0;
107
108     Final_Motor_A=Linear_Conversion(motor_a); //Linearization
109     Final_Motor_B=Linear_Conversion(motor_b);
110     Final_Motor_C=Linear_Conversion(motor_c);
111     Set_PWM_End(Final_Motor_A,Final_Motor_B,Final_Motor_C);
112 }
113
114 //*****
115 PWM Linearization
116 *****/
117 u16 Linear_Conversion(int motor)
118 {
119     u32 temp;
120     u16 Linear_Moto;
121     temp=1000000/abs(motor);
```

Figure 4.21

UI of the AAS's Display

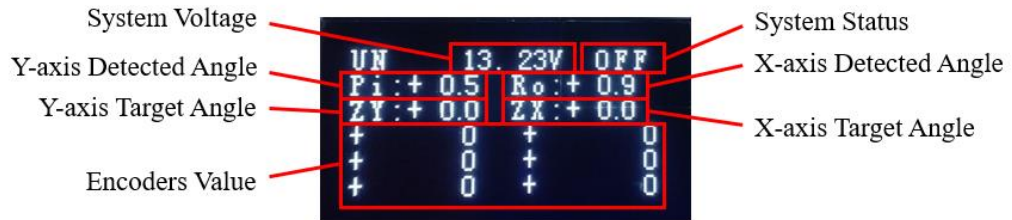


Figure 4.22 and Figure 4.23 are respectively the PID schematic diagram of the system and the response time domain diagram under the current program setting parameters.

Figure 4.22

Control Schematic Diagram of the Angle Adjustment System

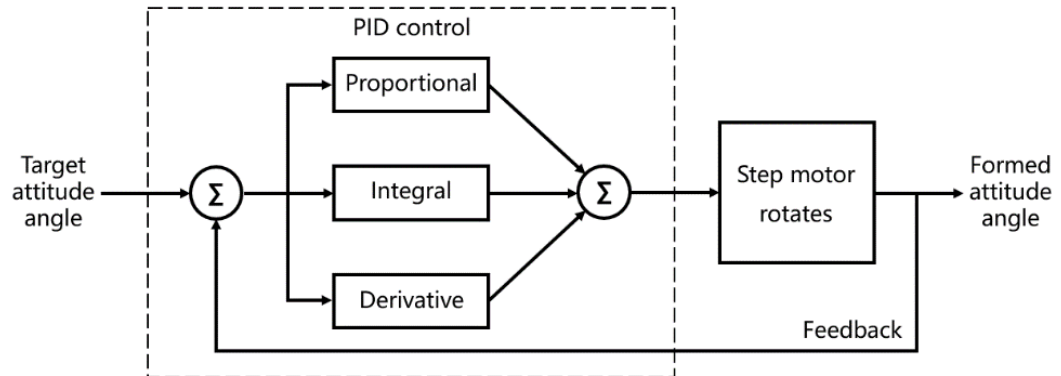
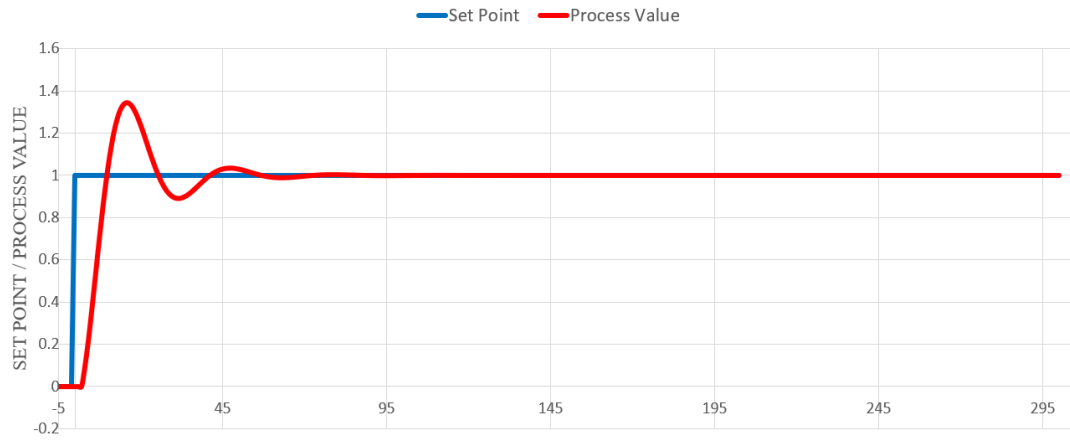


Figure 4.23

Response Time Domain Diagram of Angle Adjustment System



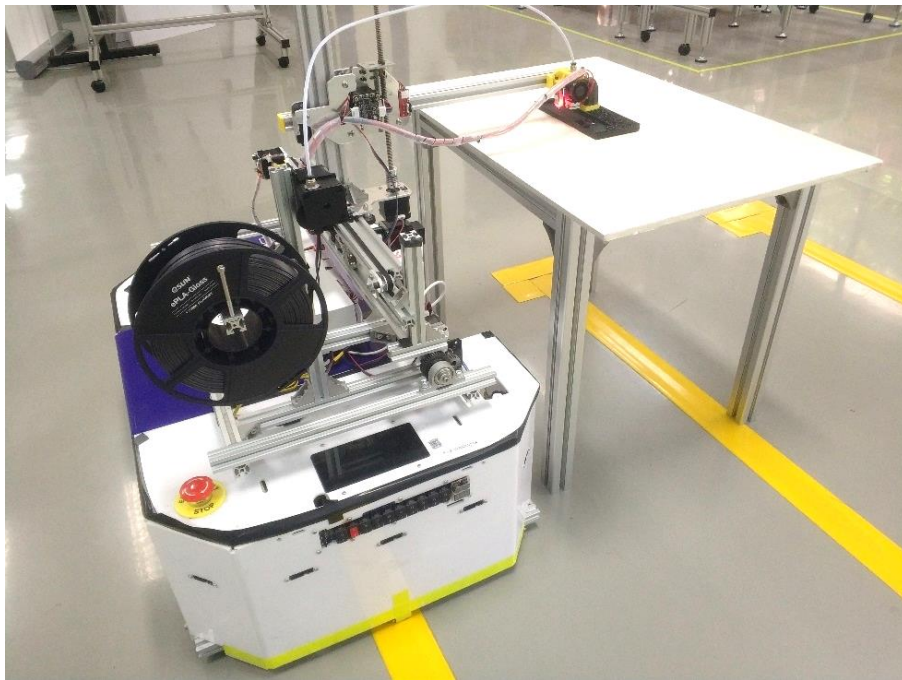
CHAPTER 5

IMPLEMENTATION AND RESULT

According to the design and development in Chapter 4, a real mobile AM device was built in the laboratory, as shown in Figure 5.1. This device has been tested. This chapter will explain the actual operation process and experimental results of the mobile AM device.

Figure 5.1

Physical Construction of Mobile 3D Printer

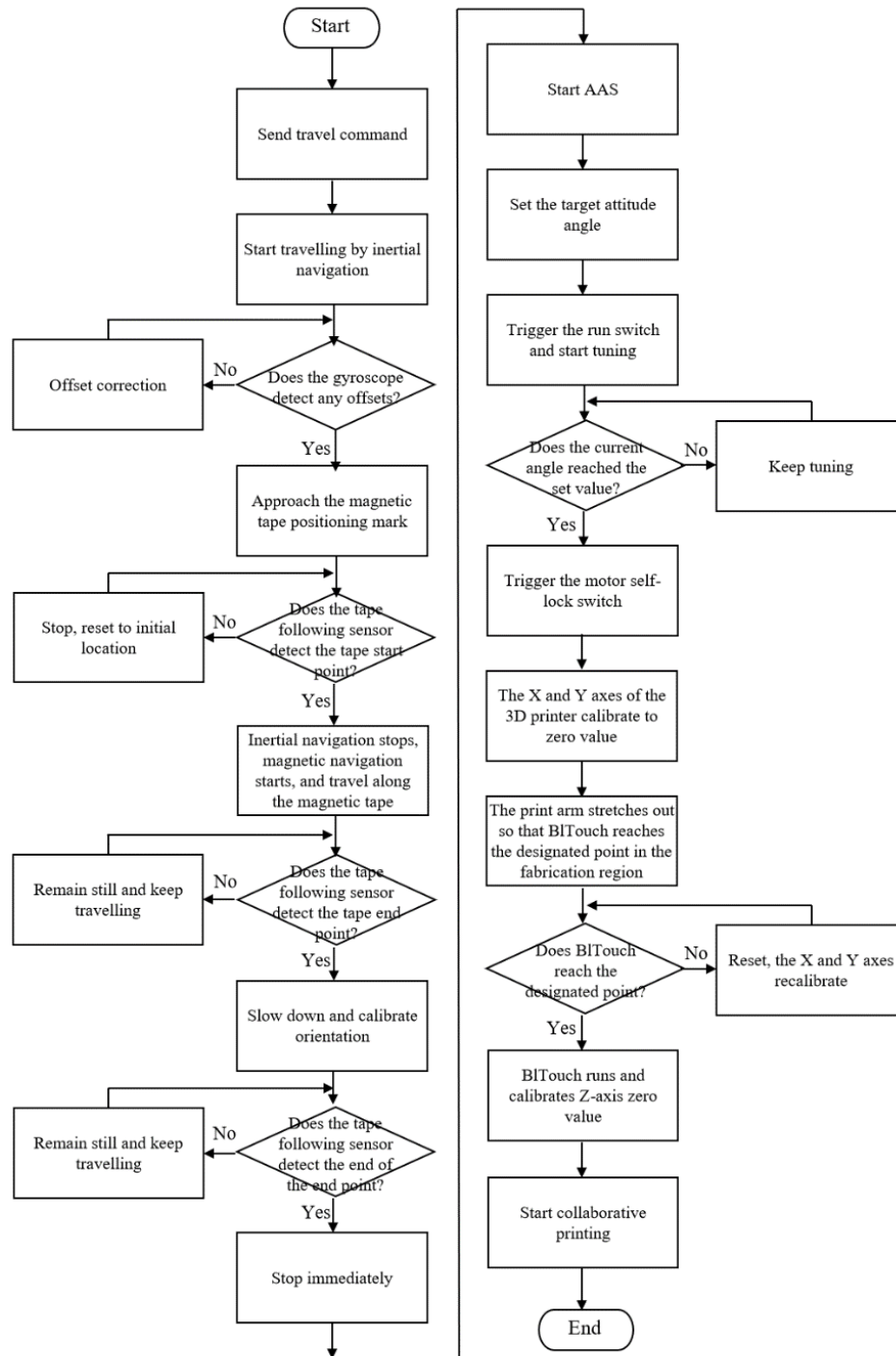


5.1 Operation Process

Chapters 3 and 4 have respectively expounded the concepts of error reduction and the corresponding technical solutions given in this study. However, in the actual implementation process, considering a total of six dimensions of error to be dealt with, a reasonable and orderly process needs to be proposed. Figure 5.2 shows the flow chart of the actual operation of the developed mobile AM device.

Figure 5.2

Operation Process Flow Chart



The developed mobile AM device strictly follows the flow in the flowchart for movement, positioning and error correction. In general, the process of "positioning

error correction" will be carried out first. The stop of the movement of the mobile platform means the termination of the "positioning error correction" process. At this time, in theory, the distance error of the device in the X-axis, Y-axis axial direction and angle error in the Z-axis radial direction have been reduced to the minimum and their corresponding accuracy requirements have been met. Then the process of "leveling error correction" begins. "Angle adjustment" and "zero value unifying" are carried out in sequence to correct the angle errors in the radial direction of the X-axis and Y-axis and the distance error in the axial direction of the Z-axis, respectively. Once the remaining three categories of errors are corrected and meet their respective accuracy requirements, the entire error reduction process ends. When multiple devices have all completed the above process, large-scale collaborative additive manufacturing can be conducted. The final error reduction effect will be directly reflected in the manufactured object and collaboration process.

5.2 Experiment Method and Implementation

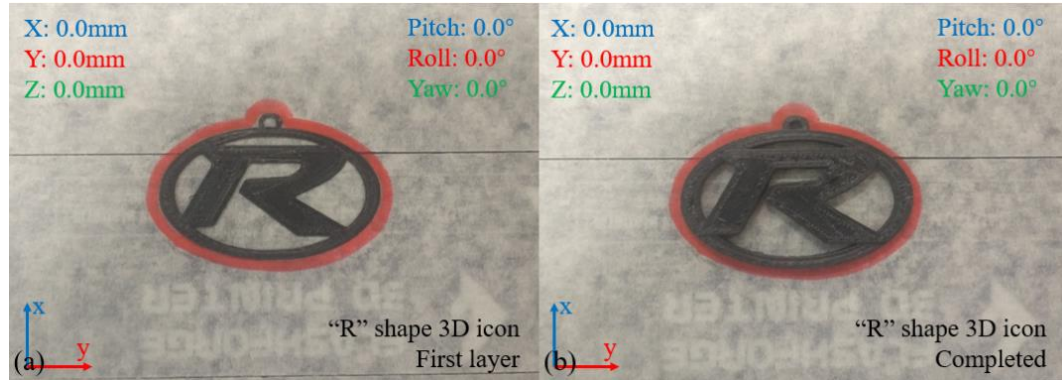
In order to verify that the developed mobile AM device can effectively control errors in large-scale collaborative additive manufacturing, a reasonable experimental method needs to be proposed and implemented. In this section, the inspiration, specific operation method and final result of the conducted experiment will be explained in turn.

5.2.1 Experimental Inspiration

To gain inspiration for the experimental design, a set of 3D printing pre-tests in different manufacturing conditions were conducted to compare practical results. The developed mobile 3D printer is placed at a specific location on flat ground, and the attitude of the 3D printer is manually calibrated. A 3D icon in the shape of an "R" is printed layer by layer. Figure 5.3(a) shows the first layer of the printed object, at the same time its outline is marked with a red marker. Figure 5.3(b) shows the completed printing object. It can be seen that the surface of the first layer of the printed object is flat, the lines are evenly distributed, and its finished product is complete and free of defects. The object printed this time is defined as "standard" and used for subsequent comparisons.

Figure 5.3

Standard Printed "R" Shape 3D Icon

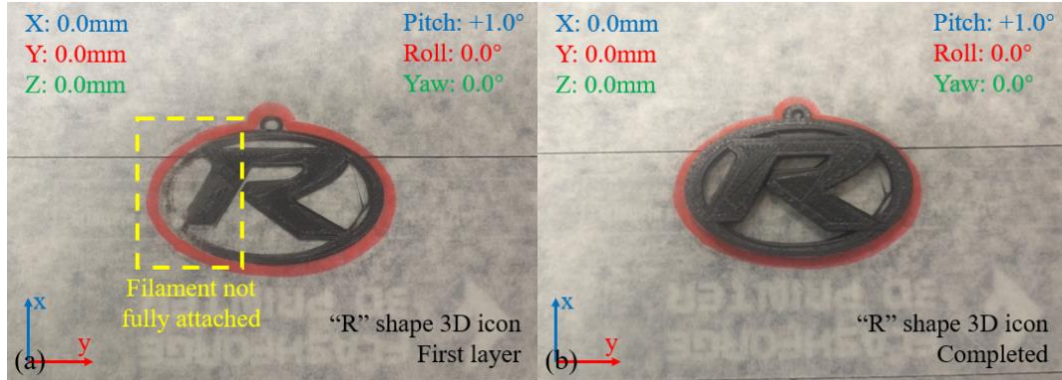


Note. (a) First layer of the standard printed "R" shape icon; (b) Completed status of the standard printed "R" shape icon.

The position of the mobile 3D printer remained the same, and one side of the device was manually raised to create a 1° pitch angle. Another identical "R" shape 3D icon is printed layer by layer. Figure 5.4(a) shows the first layer of the printed object, and Figure 5.4(b) shows the completed printing object. It is obvious that the filaments are not accurately distributed on the side of the device that is not raised, resulting in a missing. This is because when the 3D printer is tilted with the device, the nozzle is too close or even in direct attaches to the surface of the printing platform while printing in some of the regions, so that the filament cannot be smoothly extruded. As the printer is raised layer by layer, the extrusion of the filament gradually returns to normal and the final object is printed.

Figure 5.4

Printed “R” Shape 3D Icon with 1° Pitch Angle

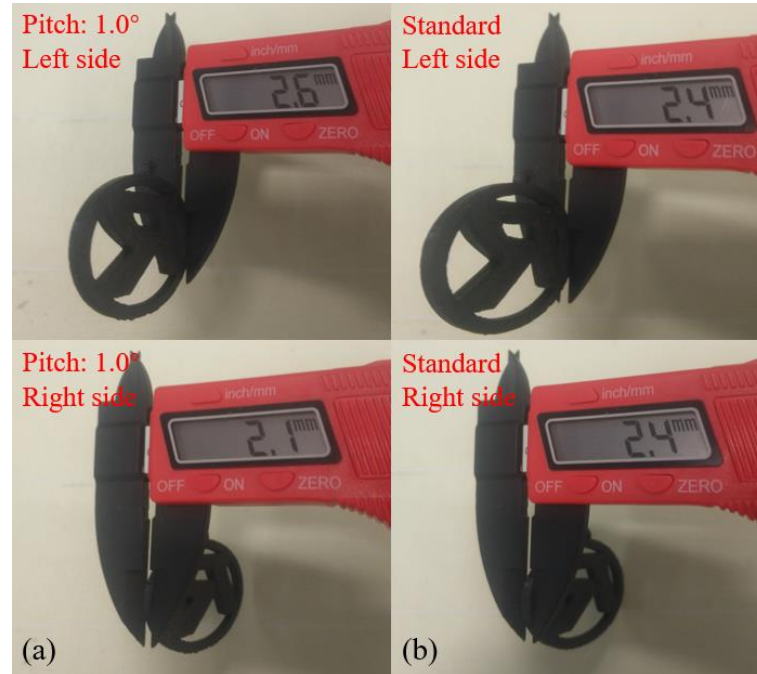


Note. (a) First layer of the printed “R” shape icon with 1° pitch angle; (b) Completed status of the printed “R” shape icon with 1° pitch angle.

Although the same object still has a chance to be printed out when the device is tilted, its actual size needs to be measured and compared with the standard one. Figure 5.5(a) and 5.5(b) show the comparison of the thickness of the two ends of the object with the those of the standard object, respectively. According to the measurement data, it can be clearly found that the objects printed by the device in a tilted state are also tilted.

Figure 5.5

Thickness Comparison Between Two Printed Icons



Note. (a) The comparison of the thickness on both sides of the printed icon with 1° pitch angle; (b) The comparison of the thickness on both sides of the standard printed icon.

Keep the mobile 3D printer with the pitch angle of 1° and print again. This time, in order to prevent the nozzle from attaching to the surface of the printing platform during the printing process, the zero value of the Z-axis of the printer is manually raised. Figure 5.6 shows the comparison of the bottom of the printed object and the one of the standard object this time. It can be found that although the filament can be extruded normally at the bottom this time, the distribution of the filament on the other side is disordered. This is because when this part of region is printed, the distance between the nozzle and the printing platform is too far, and the filament cannot be accurately attached to the surface of the platform.

Figure 5.6

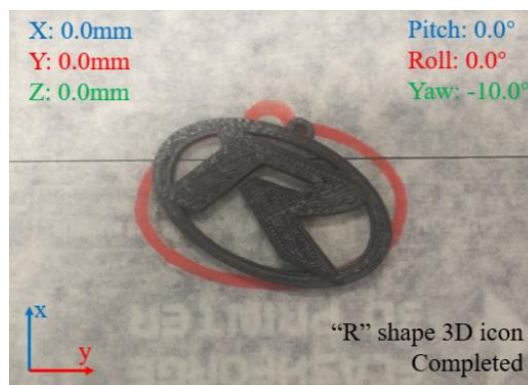
Bottom Comparison Between Two Printed Icons



After returning the mobile 3D printer to the standard attitude, a yaw angle is given. An identical "R" shape 3D icon is printed. As shown in Figure 5.7, the printed object forms an angle relative to the standard position that is the same as the yaw angle of the device.

Figure 5.7

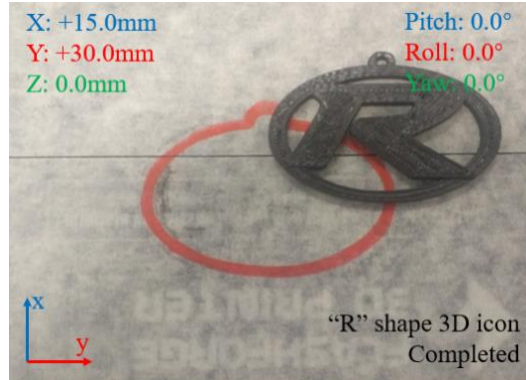
Printed "R" Shape 3D Icon with -10° Yaw Angle



Restore the 3D printer once again and then make it an offset from the standard position. Another printing work is conducted. As shown in Figure 5.8, the position of the printed object is offset from the standard position by the same offset as the overall device.

Figure 5.8

Printed “R” Shape 3D Icon with Certain Distance Error



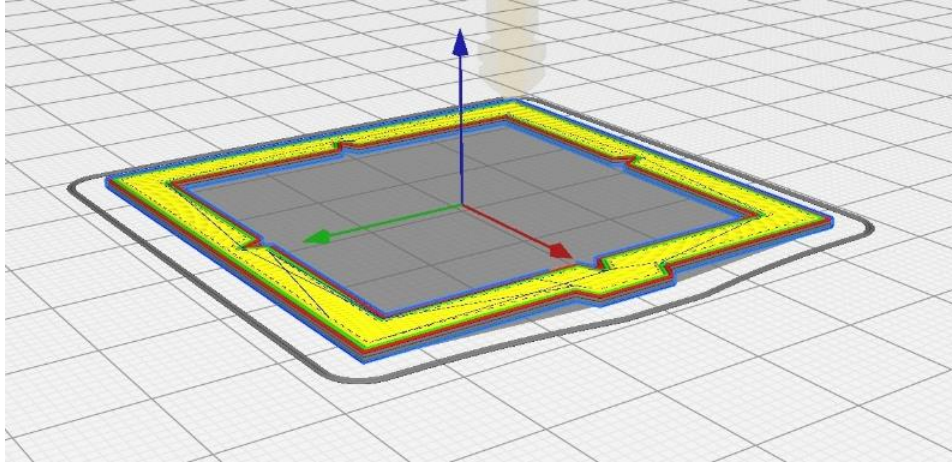
Based on the practical pre-tests described above, an inspiration for setting up the experiment was proposed. It can be confirmed that any distance errors and angle errors produced by mobile AM device will be reflected in the manufactured object accordingly. Therefore, a valid measurement of the manufactured object can reasonably determine the level of error existing in the device. The specific measurement and judgment methods are introduced in the following subsections.

5.2.2 Standard Printed Object

To facilitate measuring the size and position of the printed object, an object of a specified shape will be printed and used for subsequent experiment, as shown in Figure 5.9. The outline of this object is a square with an edge length of 50 mm. One of its edges is marked to determine the orientation of the print. The inside of it is cut out of another smaller size square, and it has a mark in the middle of each edge for easy measurement. A total of three layers of filaments are accumulated layer by layer to form its structure. In theory, the thickness of this sheet-like object should be 0.9 mm.

Figure 5.9

Sliced Model of the Printed Object for Experiment



In the laboratory, a designated manufacturing region and corresponding device positioning marks have been set, as shown in Figure 5.10. The developed mobile 3D printer will travel to the positioning point, correct the error, and then conduct the manufacturing process according to the established flow. Before conducting an experiment, a criterion needs to be set against which the results of subsequent experiments can be compared. Therefore, the mobile 3D printer is manually placed on the designated positioning points. Its positions and attitudes in all directions are strictly manually calibrated to ensure that errors do not exist. A standard experimental object was printed as shown in Figure 5.11. All of its dimensional parameters have been measured to be the same as theoretical values. Its position and orientation are also marked on the printing platform for later comparison and measurement.

Figure 5.10

Physical Fabrication Setting

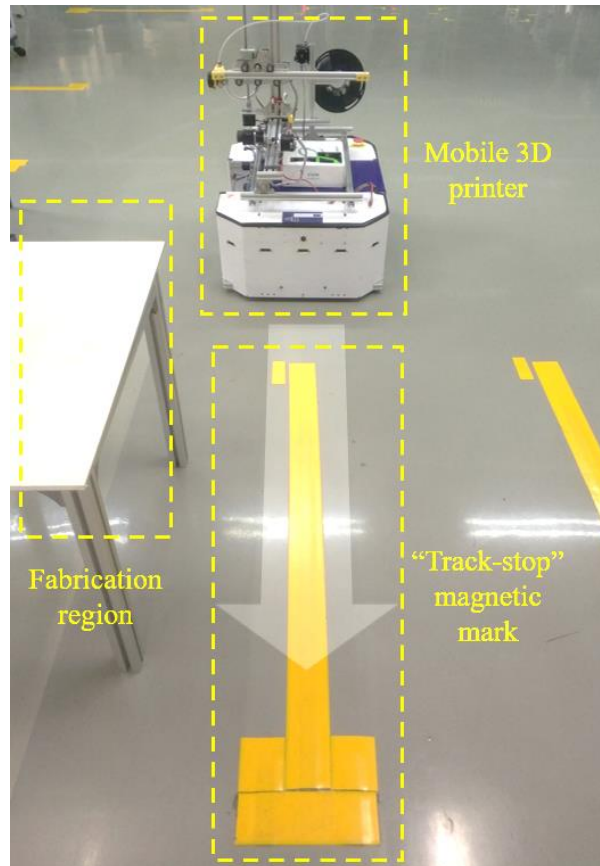
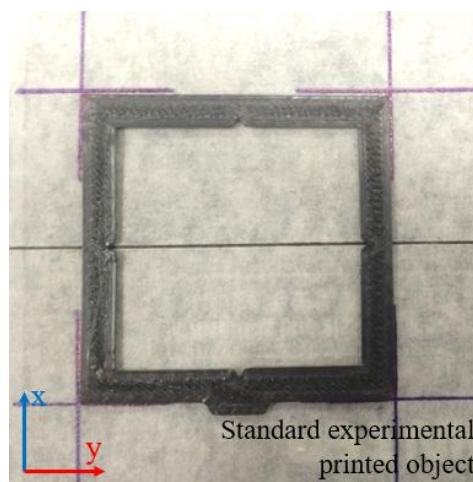


Figure 5.11

Standard Experimental Printed Object

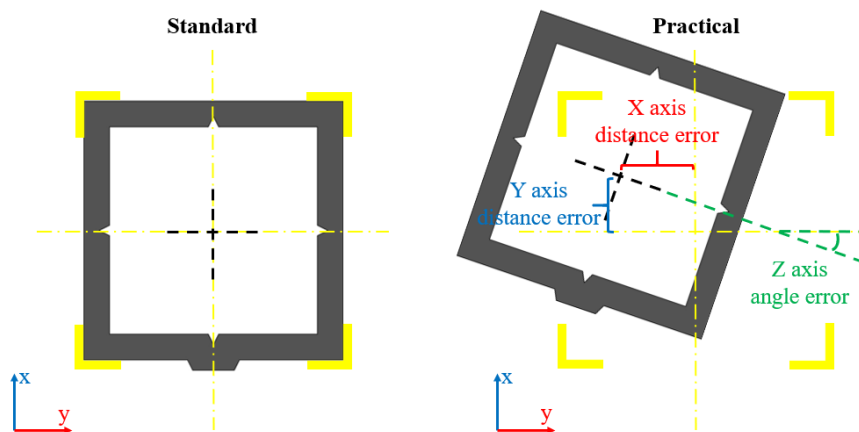


5.2.3 Judgment of “Positioning Errors”

Combining the actual printing effect in the previous subsection and the error analysis in Chapter 3, it can be known that the three positioning errors that need to be corrected will not affect the shape and size of the printed object, but only affect its position and orientation. Therefore, when the printing is completed, it is only necessary to measure the position and orientation of the printed object and compare them with the standard parameters, and then three categories of errors of the mobile 3D printer can be obtained, which is the distance error of the X-axis and the Y-axis, and the angle error of the Z-axis. Figure 5.12 shows how these three errors are measured. The marks inside the printed object can be connected during the actual measurement to facilitate data collection. In the subsequent data recording process, in order to reflect the corresponding attitude angle of the mobile 3D printer, the angle error of the Z axis is also referred as the yaw angle of the device.

Figure 5.12

Measurement of Positioning Errors Produced by "Internal Causes"



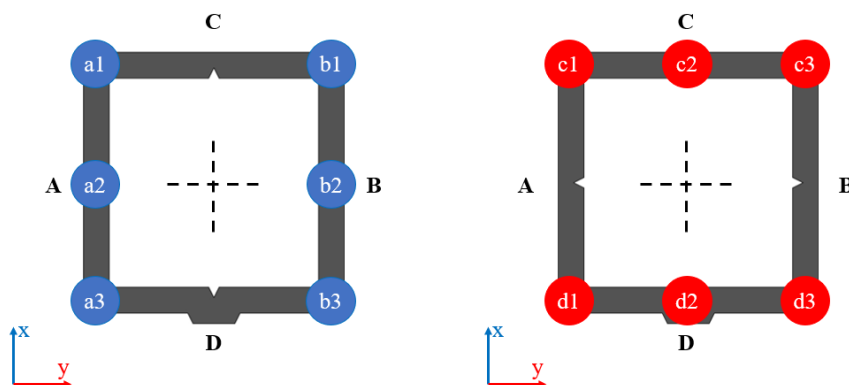
5.2.4 Judgment of “Leveling Errors”

Combining the actual printing effect in the previous subsection and the error analysis in Chapter 3, it can be known that the three leveling errors that need to be corrected will affect the shape and size of the printed object, especially in terms of thickness. Therefore, the measurement and comparison of different positions of the printed object

and the overall thickness can directly reflect the dimensions of these three categories of errors. As shown in Figure 5.13, after the orientation of the printed object is unified, its edges are named A, B, C, and D respectively. Take three points on each edge to measure the thickness and calculate the average value to represent the printing thickness of each edge. The difference between the thicknesses of edge A and edge B can reflect the size of the X-axis angle error. Similarly, the difference between the thicknesses of side C and side D can reflect the size of the Y-axis angle error. The overall thickness of the printed object can be calculated by averaging all measured points. The difference between the thickness and the standard one can reflect the size of the Z-axis distance error. In the subsequent data recording process, the thickness difference between edge A and edge B is directly referred as the angle error of X-axis, and the thickness difference of edge C and edge D is directly referred as the angle error of Y-axis. The overall thickness is directly referred as the Z-axis distance error.

Figure 5.13

Measurement of Leveling Errors Produced by "External Causes"



5.2.5 Potential Radom Error

Random error in the operation of the developed mobile 3D printer need to be determined before formally conducting the experiment. The mobile 3D printer is placed and fixed at the specific target location. In order to eliminate system errors to the greatest extent, the position and attitude of the device are manually calibrated to reach

the set value, without the proposed error correction concept, strategy and corresponding mechanism being introduced. The standard experimental printing object was printed ten times in this state. According to the measurement method already introduced, various parameters of the ten printed objects were measured to determine the dimension of random error. Table 5.1 shows the error values for each printed object and the mean value.

Table 5.1

Results of the Random Error Tests

| No. | X-axis distance error (mm) | Y-axis distance error (mm) | Yaw/Z-axis angle error (°) | Thickness difference between edge A and B/X-axis angle error (mm) | Thickness difference between edge C and D/Y-axis angle error (mm) | Overall thickness difference /Z-axis distance error (mm) |
|--------|----------------------------|----------------------------|----------------------------|---|---|--|
| Test1 | 0.0 | 0.0 | 0.0 | 0.0 | 0.0 | 0.0 |
| Test2 | 0.0 | 0.0 | 0.0 | 0.033 | 0.0 | 0.013 |
| Test3 | 0.0 | -0.1 | 0.0 | 0.0 | 0.0 | 0.0 |
| Test4 | 0.0 | 0.0 | 0.0 | 0.0 | 0.0 | 0.0 |
| Test5 | 0.0 | 0.0 | 0.0 | 0.0 | -0.034 | -0.013 |
| Test6 | 0.0 | 0.0 | 0.0 | 0.0 | 0.0 | 0.0 |
| Test7 | 0.0 | 0.0 | 0.0 | 0.0 | 0.0 | 0.0 |
| Test8 | 0.0 | 0.0 | 0.0 | 0.0 | 0.0 | 0.0 |
| Test9 | 0.0 | 0.0 | 0.0 | 0.0 | 0.0 | 0.0 |
| Test10 | 0.1 | 0.0 | 0.0 | 0.0 | 0.0 | 0.0 |
| Mean | 0.01 | -0.01 | 0.0 | 0.003 | -0.003 | 0.0 |

According to the data shown in the table, it can be seen that random error does exist, but based on the current experimental conditions, accurate distribution regular pattern

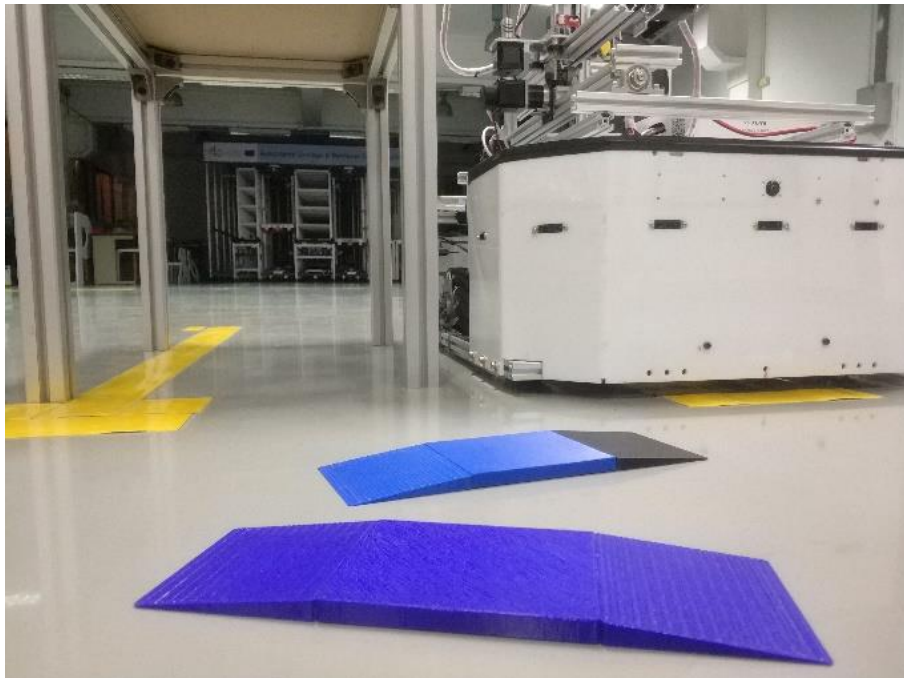
and factors which caused errors cannot be summarized. In general, the value of the random error is universally very small, and it does not affect the result of the experiment at all. Therefore, potential random error will not be considered during data generalization for subsequent experiment. The conditions, quantities, variables and control groups of subsequent experiment will also be optimized to avoid random error to the greatest extent.

5.2.6 Experimental Condition Setting

In this experiment, two artificial slopes as shown in Figure 5.14 will be laid to simulate slightly uneven ground conditions. When the two slopes were placed under different wheels of the developed mobile 3D printer, the device produced a slight angle error of around 1° - 1.5° in different directions.

Figure 5.14

Artificial Slopes

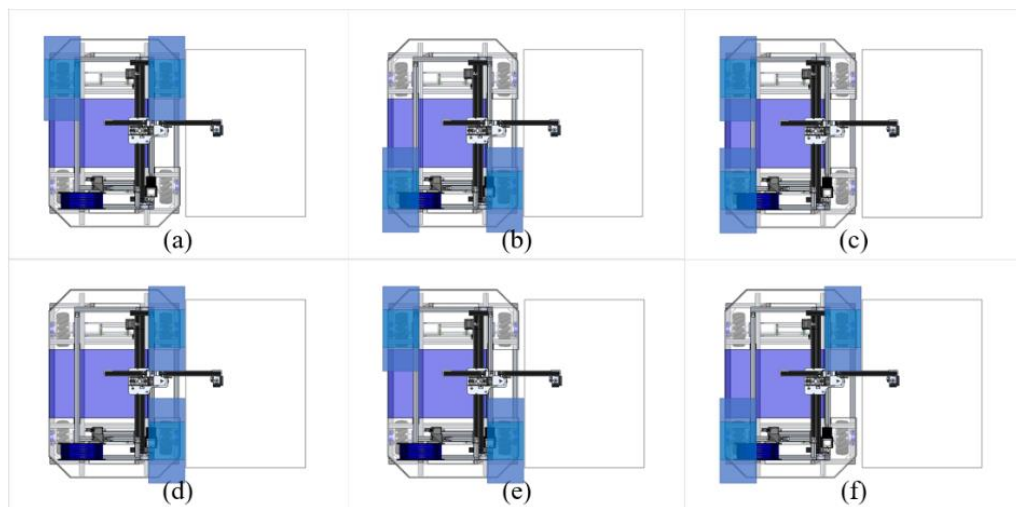


After permutations and combinations, the two slopes can provide a total of six different ground conditions for the mobile 3D printer, as shown in Figure 5.15. In the experiment,

each experimental group will print under these six different conditions. In order to ensure the reliability and validity of the experimental data, under each condition of the same group, the experiment will be performed three times, and the data of each time will be recorded and compared with the corresponding data of other groups.

Figure 5.15

Six Different Ground Conditions Created by Slope Placement



Note. (a) Slopes being placed at the bottom of the left front wheel and right front wheel; (b) Slopes being placed at the bottom of the left rear wheel and right rear wheel; (c) Slopes being placed at the bottom of the left front wheel and left rear wheel; (d) Slopes being placed at the bottom of the right front wheel and right rear wheel; (e) Slopes being placed at the bottom of the left front wheel and right rear wheel; (f) Slopes being placed at the bottom of the right front wheel and left rear wheel.

5.2.7 Experimental Variable Setting

In order to verify that the proposed concepts of "positioning error correction" and "leveling error correction" can effectively control the error within the tolerance range and support large-scale collaborative additive manufacturing, the developed mobile 3D printer will conduct four sets of printing experiments. The variables for these four experiments are set as follows.

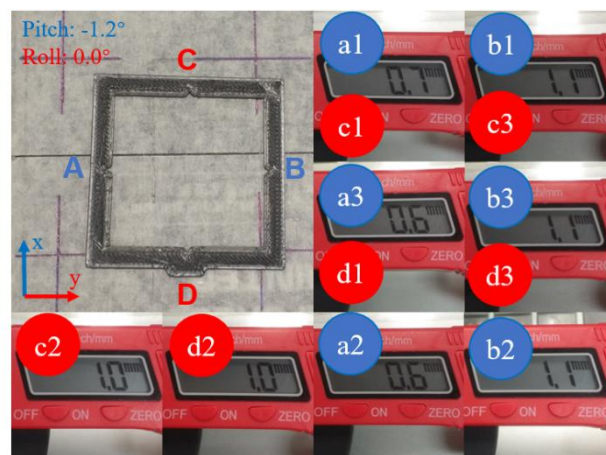
- Conduct travelling and printing without "positioning error correction" and "leveling error correction"
- Conduct travelling and printing with "positioning error correction", and without "leveling error correction"
- Conduct travelling and printing with "leveling error correction", and without "positioning error correction"
- Conduct travelling and printing together with "positioning error correction" and "leveling error correction"

5.3 Result

Figure 5.16 and Figure 5.17 respectively show two typical printing and measurement results without and with "positioning error correction" and "leveling error correction" are introduced under the same ground condition. Due to the large number of experiments, all experimental measurement data will be listed in the table instead of in the form of figures.

Figure 5.16

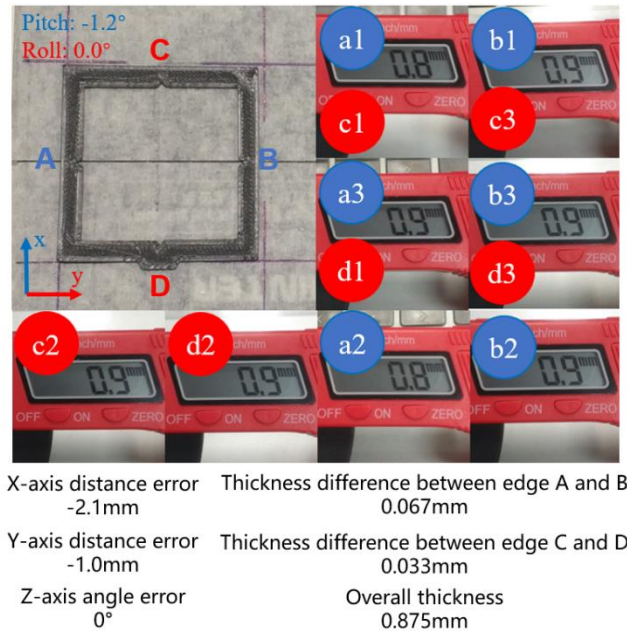
Printing and Measurement Results Under Ground Condition without "Positioning Error Correction" and "Leveling Error Correction"



| | |
|---------------------------------|--|
| X-axis distance error -3.8mm | Thickness difference between edge A and B 0.467mm |
| Y-axis distance error +5.1mm | Thickness difference between edge C and D 0.033mm |
| Z-axis angle error 0.9° | Overall thickness 0.9mm |

Figure 5.17

Printing and Measurement Results Under Ground Condition with "Positioning Error Correction" and "Leveling Error Correction"



The tables below show the error results of the developed mobile 3D printers under six different experimental conditions before and after the intervention of "positioning error correction" and "leveling error correction". Note that in all the tables below, XD refers to X-axis distance error; YD refers to Y-axis distance error; ZA refers to Z-axis angle error; Pitch refers to the pitch angle value read by the sensor in the current state; Row refers to the row angle value read by the sensor in the current state; XA refers to X-axis angle error, which is the thickness difference between edge A and B; YA refers to Y-axis angle error, which is the thickness difference between edge C and D; ZD refers to Z-axis distance error, which is the overall thickness difference; AVG refers to the average value. All distance and angle data are taken as absolute values for ease of comparison.

Table 5.2

Results of Slopes Being Placed at the Bottom of the Left Front Wheel and Right Front Wheel of the Mobile 3D Printer

| Variable | No. | XD (mm) | YD (mm) | ZA (°) | Pitch (°) | Row (°) | XA (mm) | YA (mm) | ZD (mm) |
|---|-----------|------------|------------|-----------|--------------|------------|------------|------------|------------|
| Without "positioning error correction" and "leveling error correction" | Test 1 | 16.3 | 3.5 | 2.8 | 1.3 | 0.0 | 0.567 | 0.033 | 0.017 |
| | Test 2 | 2.8 | 8.1 | 0.8 | 1.2 | 0.1 | 0.466 | 0.033 | 0.008 |
| | Test 3 | 9.8 | 1.0 | 2.1 | 1.2 | 0.0 | 0.467 | 0.033 | 0.025 |
| | AVG | 9.6 | 4.2 | 1.9 | 1.2 | 0.0 | 0.500 | 0.033 | 0.017 |
| With "positioning error correction", without "leveling error correction" | Test 1 | 1.3 | 0.8 | 0.0 | 1.2 | 0.0 | 0.567 | 0.034 | 0.017 |
| | Test 2 | 0.8 | 0.0 | 0.0 | 1.2 | 0.0 | 0.367 | 0.034 | 0.017 |
| | Test 3 | 2.5 | 0.4 | 0.1 | 1.3 | 0.0 | 0.500 | 0.034 | 0.034 |
| | AVG | 1.5 | 0.4 | 0.0 | 1.2 | 0.0 | 0.478 | 0.034 | 0.022 |
| Without "positioning error correction", with "leveling error correction" | Test 1 | 8.6 | 2.0 | 1.3 | 0.0 | 0.0 | 0.000 | 0.033 | 0.008 |
| | Test 2 | 4.3 | 3.5 | 1.0 | 0.0 | 0.0 | 0.000 | 0.033 | 0.008 |
| | Test 3 | 1.6 | 1.5 | 0.4 | 0.0 | 0.0 | 0.000 | 0.033 | 0.008 |
| | AVG | 4.8 | 2.3 | 0.9 | 0.0 | 0.0 | 0.000 | 0.033 | 0.008 |
| With "positioning error correction" and "leveling error correction" | Test 1 | 2.4 | 0.5 | 0.0 | 0.0 | 0.0 | 0.033 | 0.000 | 0.008 |
| | Test 2 | 1.8 | 1.5 | 0.0 | 0.0 | 0.0 | 0.033 | 0.000 | 0.008 |
| | Test 3 | 1.6 | 0.2 | 0.0 | 0.0 | 0.0 | 0.000 | 0.000 | 0.000 |
| | AVG | 1.9 | 0.7 | 0.0 | 0.0 | 0.0 | 0.022 | 0.000 | 0.006 |

Table 5.3

Results of Slopes Being Placed at the Bottom of the Left Rear Wheel and Right Rear Wheel of the Mobile 3D Printer

| Variable | No. | XD (mm) | YD (mm) | ZA (°) | Pitch (°) | Row (°) | XA (mm) | YA (mm) | ZD (mm) |
|---|-----------|------------|------------|-----------|--------------|------------|------------|------------|------------|
| Without "positioning error correction" and "leveling error correction" | Test 1 | 6.7 | 2.6 | 1.7 | 1.4 | 0.0 | 0.600 | 0.167 | 0.075 |
| | Test 2 | 11.1 | 3.9 | 1.3 | 1.3 | 0.0 | 0.433 | 0.133 | 0.009 |
| | Test 3 | 4.0 | 4.7 | 0.3 | 1.3 | 0.0 | 0.500 | 0.100 | 0.017 |
| | AVG | 7.3 | 3.7 | 1.1 | 1.3 | 0.0 | 0.511 | 0.133 | 0.033 |
| With "positioning error correction", without "leveling error correction" | Test 1 | 1.3 | 0.4 | 0.1 | 1.3 | 0.0 | 0.500 | 0.133 | 0.042 |
| | Test 2 | 0.7 | 0.6 | 0.0 | 1.3 | 0.0 | 0.467 | 0.100 | 0.042 |
| | Test 3 | 1.4 | 0.3 | 0.0 | 1.2 | 0.0 | 0.367 | 0.133 | 0.025 |
| | AVG | 1.1 | 0.4 | 0.0 | 1.3 | 0.0 | 0.445 | 0.122 | 0.036 |
| Without "positioning error correction", with "leveling error correction" | Test 1 | 4.2 | 5.1 | 0.8 | 0.0 | 0.0 | 0.000 | 0.033 | 0.008 |
| | Test 2 | 2.7 | 6.0 | 0.5 | 0.0 | 0.0 | 0.033 | 0.033 | 0.000 |
| | Test 3 | 16.9 | 2.7 | 2.3 | 0.0 | 0.0 | 0.000 | 0.000 | 0.017 |
| | AVG | 7.9 | 4.6 | 1.2 | 0.0 | 0.0 | 0.011 | 0.022 | 0.008 |
| With "positioning error correction" and "leveling error correction" | Test 1 | 0.2 | 0.2 | 0.0 | 0.0 | 0.0 | 0.033 | 0.033 | 0.000 |
| | Test 2 | 1.1 | 1.0 | 0.0 | 0.0 | 0.0 | 0.033 | 0.033 | 0.017 |
| | Test 3 | 1.0 | 0.0 | 0.0 | 0.0 | 0.0 | 0.000 | 0.033 | 0.008 |
| | AVG | 0.8 | 0.4 | 0.0 | 0.0 | 0.0 | 0.022 | 0.033 | 0.008 |

Table 5.4

Results of Slopes Being Placed at the Bottom of the Left Front Wheel and Left Rear Wheel of the Mobile 3D Printer

| Variable | No. | XD (mm) | YD (mm) | ZA (°) | Pitch (°) | Row (°) | XA (mm) | YA (mm) | ZD (mm) |
|---|-----------|------------|------------|-----------|--------------|------------|------------|------------|------------|
| Without "positioning error correction" and "leveling error correction" | Test 1 | 6.2 | 2.0 | 0.8 | 0.0 | 1.3 | 0.166 | 0.400 | 0.008 |
| | Test 2 | 14.7 | 8.3 | 2.8 | 0.0 | 1.3 | 0.067 | 0.367 | 0.008 |
| | Test 3 | 5.3 | 3.6 | 0.6 | 0.1 | 1.4 | 0.000 | 0.533 | 0.017 |
| | AVG | 8.7 | 4.6 | 1.4 | 0.0 | 1.3 | 0.078 | 0.433 | 0.011 |
| With "positioning error correction", without "leveling error correction" | Test 1 | 0.0 | 1.2 | 0.1 | 0.0 | 1.2 | 0.100 | 0.366 | 0.050 |
| | Test 2 | 0.9 | 1.0 | 0.1 | 0.0 | 1.3 | 0.033 | 0.500 | 0.000 |
| | Test 3 | 0.5 | 0.2 | 0.0 | 0.0 | 1.4 | 0.200 | 0.567 | 0.042 |
| | AVG | 0.5 | 0.8 | 0.1 | 0.0 | 1.3 | 0.111 | 0.478 | 0.031 |
| Without "positioning error correction", with "leveling error correction" | Test 1 | 8.1 | 1.8 | 0.9 | 0.0 | 0.0 | 0.066 | 0.033 | 0.008 |
| | Test 2 | 2.9 | 4.6 | 0.3 | 0.0 | 0.0 | 0.033 | 0.000 | 0.008 |
| | Test 3 | 7.7 | 3.7 | 1.5 | 0.0 | 0.0 | 0.000 | 0.000 | 0.017 |
| | AVG | 6.2 | 3.4 | 0.9 | 0.0 | 0.0 | 0.033 | 0.011 | 0.011 |
| With "positioning error correction" and "leveling error correction" | Test 1 | 0.6 | 0.7 | 0.0 | 0.0 | 0.0 | 0.033 | 0.066 | 0.008 |
| | Test 2 | 1.3 | 0.6 | 0.1 | 0.0 | 0.0 | 0.000 | 0.000 | 0.000 |
| | Test 3 | 0.2 | 0.6 | 0.1 | 0.0 | 0.0 | 0.000 | 0.000 | 0.000 |
| | AVG | 0.7 | 0.6 | 0.1 | 0.0 | 0.0 | 0.011 | 0.022 | 0.003 |

Table 5.5

Results of Slopes Being Placed at the Bottom of the Right Front Wheel and Right Rear Wheel of the Mobile 3D Printer

| Variable | No. | XD (mm) | YD (mm) | ZA (°) | Pitch (°) | Row (°) | XA (mm) | YA (mm) | ZD (mm) |
|---|-----------|------------|------------|-----------|--------------|------------|------------|------------|------------|
| Without "positioning error correction" and "leveling error correction" | Test 1 | 5.6 | 2.3 | 0.3 | 0.1 | 1.3 | 0.200 | 0.466 | 0.000 |
| | Test 2 | 12.3 | 7.4 | 1.4 | 0.0 | 1.4 | 0.300 | 0.600 | 0.025 |
| | Test 3 | 14.2 | 10.6 | 2.1 | 0.0 | 1.3 | 0.167 | 0.500 | 0.017 |
| | AVG | 10.7 | 6.8 | 1.2 | 0.0 | 1.3 | 0.222 | 0.522 | 0.014 |
| With "positioning error correction", without "leveling error correction" | Test 1 | 1.2 | 0.5 | 0.0 | 0.0 | 1.4 | 0.167 | 0.600 | 0.008 |
| | Test 2 | 0.8 | 0.2 | 0.1 | 0.0 | 1.3 | 0.200 | 0.500 | 0.025 |
| | Test 3 | 0.6 | 1.4 | 0.0 | 0.0 | 1.4 | 0.167 | 0.600 | 0.008 |
| | AVG | 0.9 | 0.7 | 0.0 | 0.0 | 1.4 | 0.178 | 0.567 | 0.014 |
| Without "positioning error correction", with "leveling error correction" | Test 1 | 8.5 | 5.9 | 0.7 | 0.0 | 0.0 | 0.033 | 0.033 | 0.000 |
| | Test 2 | 9.7 | 1.7 | 1.1 | 0.0 | 0.0 | 0.000 | 0.033 | 0.008 |
| | Test 3 | 6.6 | 7.2 | 0.1 | 0.0 | 0.0 | 0.033 | 0.000 | 0.008 |
| | AVG | 8.3 | 4.9 | 0.6 | 0.0 | 0.0 | 0.022 | 0.022 | 0.006 |
| With "positioning error correction" and "leveling error correction" | Test 1 | 1.4 | 0.9 | 0.0 | 0.0 | 0.0 | 0.000 | 0.000 | 0.017 |
| | Test 2 | 0.0 | 1.0 | 0.0 | 0.0 | 0.0 | 0.033 | 0.000 | 0.008 |
| | Test 3 | 0.8 | 0.4 | 0.2 | 0.0 | 0.0 | 0.033 | 0.000 | 0.008 |
| | AVG | 0.7 | 0.8 | 0.1 | 0.0 | 0.0 | 0.022 | 0.000 | 0.011 |

Table 5.6

Results of Slopes Being Placed at the Bottom of the Left Front Wheel and Right Rear Wheel of the Mobile 3D Printer

| Variable | No. | XD (mm) | YD (mm) | ZA (°) | Pitch (°) | Row (°) | XA (mm) | YA (mm) | ZD (mm) |
|---|-----------|------------|------------|-----------|--------------|------------|------------|------------|------------|
| Without "positioning error correction" and "leveling error correction" | Test 1 | 13.7 | 4.6 | 2.3 | 1.0 | 1.3 | 0.300 | 0.600 | 0.025 |
| | Test 2 | 17.2 | 9.6 | 2.4 | 1.0 | 1.3 | 0.300 | 0.467 | 0.025 |
| | Test 3 | 27.7 | 6.5 | 3.2 | 0.9 | 1.3 | 0.266 | 0.466 | 0.050 |
| | AVG | 19.5 | 6.9 | 2.6 | 1.0 | 1.3 | 0.289 | 0.511 | 0.033 |
| With "positioning error correction", without "leveling error correction" | Test 1 | 0.7 | 0.8 | 0.1 | 1.0 | 1.2 | 0.233 | 0.567 | 0.100 |
| | Test 2 | 1.0 | 0.6 | 0.0 | 0.9 | 1.3 | 0.133 | 0.467 | 0.000 |
| | Test 3 | 1.8 | 1.2 | 0.1 | 1.0 | 1.3 | 0.233 | 0.367 | 0.017 |
| | AVG | 1.2 | 0.9 | 0.1 | 1.0 | 1.3 | 0.200 | 0.467 | 0.039 |
| Without "positioning error correction", with "leveling error correction" | Test 1 | 8.9 | 4.4 | 0.9 | 0.0 | 0.0 | 0.000 | 0.033 | 0.008 |
| | Test 2 | 20.2 | 15.1 | 0.8 | 0.0 | 0.0 | 0.033 | 0.033 | 0.017 |
| | Test 3 | 3.9 | 11.7 | 0.2 | 0.0 | 0.0 | 0.000 | 0.033 | 0.025 |
| | AVG | 11.0 | 10.4 | 0.6 | 0.0 | 0.0 | 0.011 | 0.033 | 0.017 |
| With "positioning error correction" and "leveling error correction" | Test 1 | 1.6 | 1.0 | 0.2 | 0.0 | 0.0 | 0.033 | 0.033 | 0.000 |
| | Test 2 | 1.4 | 0.4 | 0.2 | 0.0 | 0.0 | 0.066 | 0.000 | 0.000 |
| | Test 3 | 1.4 | 0.9 | 0.1 | 0.0 | 0.0 | 0.000 | 0.000 | 0.000 |
| | AVG | 1.5 | 0.8 | 0.2 | 0.0 | 0.0 | 0.033 | 0.011 | 0.000 |

Table 5.7

Results of Slopes Being Placed at the Bottom of the Right Front Wheel and Left Rear Wheel of the Mobile 3D Printer

| Variable | No. | XD (mm) | YD (mm) | ZA (°) | Pitch (°) | Row (°) | XA (mm) | YA (mm) | ZD (mm) |
|---|-----------|------------|------------|-----------|--------------|------------|------------|------------|------------|
| Without "positioning error correction" and "leveling error correction" | Test 1 | 11.5 | 8.8 | 1.8 | 1.0 | 1.3 | 0.367 | 0.433 | 0.050 |
| | Test 2 | 3.8 | 5.6 | 0.6 | 0.9 | 1.3 | 0.233 | 0.434 | 0.067 |
| | Test 3 | 9.7 | 4.9 | 0.8 | 0.9 | 1.4 | 0.433 | 0.533 | 0.025 |
| | AVG | 8.3 | 6.4 | 1.1 | 0.9 | 1.3 | 0.344 | 0.467 | 0.047 |
| With "positioning error correction", without "leveling error correction" | Test 1 | 0.7 | 0.3 | 0.2 | 0.9 | 1.2 | 0.067 | 0.367 | 0.059 |
| | Test 2 | 1.3 | 1.0 | 0.1 | 0.9 | 1.2 | 0.400 | 0.300 | 0.042 |
| | Test 3 | 2.1 | 1.2 | 0.2 | 1.0 | 1.3 | 0.434 | 0.467 | 0.058 |
| | AVG | 1.4 | 0.8 | 0.1 | 0.0 | 0.0 | 0.033 | 0.000 | 0.008 |
| Without "positioning error correction", with "leveling error correction" | Test 1 | 10.3 | 19.2 | 0.2 | 0.0 | 0.0 | 0.000 | 0.033 | 0.008 |
| | Test 2 | 14.8 | 2.1 | 2.0 | 0.0 | 0.0 | 0.033 | 0.000 | 0.008 |
| | Test 3 | 24.3 | 3.3 | 2.7 | 0.0 | 0.0 | 0.000 | 0.000 | 0.000 |
| | AVG | 16.5 | 8.2 | 1.6 | 0.0 | 0.0 | 0.011 | 0.011 | 0.005 |
| With "positioning error correction" and "leveling error correction" | Test 1 | 1.4 | 0.8 | 0.1 | 0.0 | 0.0 | 0.033 | 0.000 | 0.008 |
| | Test 2 | 0.9 | 1.0 | 0.1 | 0.0 | 0.0 | 0.000 | 0.000 | 0.017 |
| | Test 3 | 1.1 | 0.5 | 0.1 | 0.0 | 0.0 | 0.033 | 0.033 | 0.017 |
| | AVG | 1.1 | 0.8 | 0.1 | 0.0 | 0.0 | 0.022 | 0.011 | 0.014 |

It should be noted that, according to the analysis of error sources in Chapter 3 and the pre-tests in this chapter, in all the parameters listed in the above tables, except for "pitch" and "roll", which are automatically read by the system, the remaining six parameters are all the final error values obtained after experimental measurement and calculation, and correspond to the six categories of error in the three-dimensional space one-to-one. The values of these six categories of data can intuitively reflect the size of the corresponding distance error and angle error.

According to the listed table results, it is easy to know that under each different ground conditions, the introduction of "positioning error correction" and "leveling error correction" can effectively reduce the errors caused by "internal factors" and "external factors", respectively. Multiple sets of tests have proved that the developed device has high reliability and validity in error controlling. In addition, by comparing the printing results under different manufacturing conditions, it can be found that the more uneven the ground, the more significant the error reduction by the device. To visualize the extent to which the concepts of "positioning error correction" and "leveling error correction", Table 5.8 lists the average values of printing result for all manufacturing conditions in which the experiment was conducted.

Table 5.8*Average Values of Printing Result*

| | XD (mm) | YD (mm) | ZA (°) | XA (mm) | YA (mm) | ZD (mm) |
|--|------------|------------|-----------|------------|------------|------------|
| Without "positioning error correction" and "leveling error correction" | 10.683 | 5.433 | 1.550 | 0.324 | 0.350 | 0.026 |
| With "positioning error correction", without "leveling error correction" | 1.100 | 0.667 | 0.050 | 0.241 | 0.278 | 0.025 |
| Without "positioning error correction", with "leveling error correction" | 9.117 | 5.633 | 0.967 | 0.015 | 0.022 | 0.009 |
| With "positioning error correction" and "leveling error correction" | 1.117 | 0.683 | 0.083 | 0.022 | 0.013 | 0.007 |

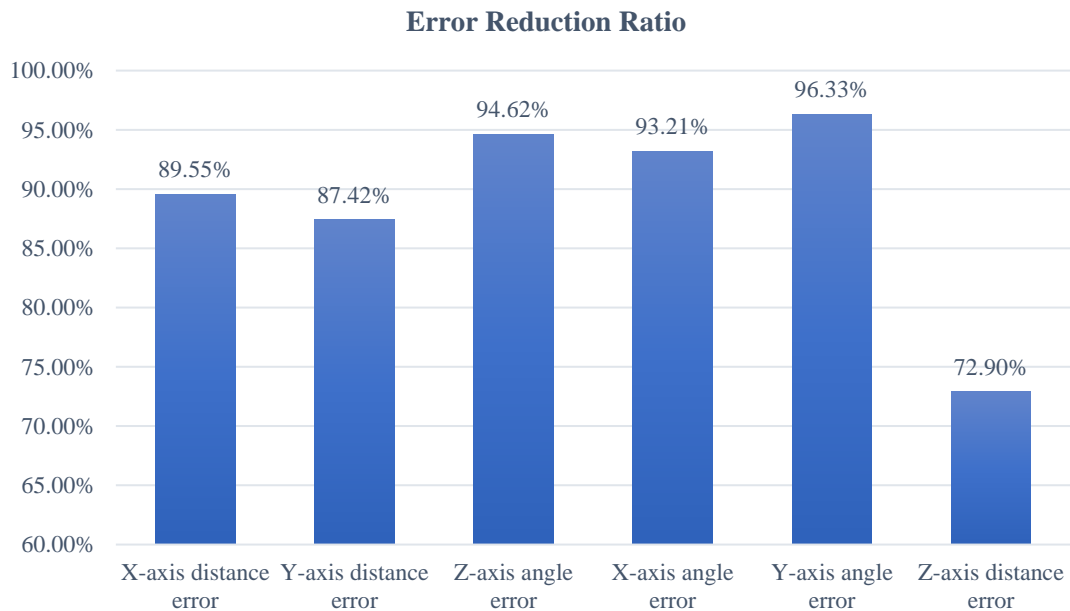
In this table, the separate introduction of the concepts of "positioning error correction" and "leveling error correction" and the introduction of both have very little difference in the values corresponding to the reduced errors, so analysis of variance (ANOVA) was used to verify whether there is a significant difference between them. Raw data for each pairwise corresponding group were performed in Excel by one-factor ANOVA. After the verification of the F test and the P value test, it can be known that there is no significant difference in the effect of "positioning error correction" and "leveling error correction" introduced separately and simultaneously on the error reduction.

By comparing the average error results before and after "positioning error correction" and "leveling error correction" are introduced into the developed mobile 3D printer, it

can be seen that the gaps under each category of error are huge. The reduced error value has been controlled to a quite low level, which basically meets the error tolerance range of various collaborative manufacturing processes. Figure 5.18 shows the ratio of error value reduction after the introduction of "positioning error correction" and "leveling error correction". For large-scale collaborative additive manufacturing, this level of improvement is effective and hugely meaningful.

Figure 5.18

Error Reduction Ratio



CHAPTER 6

CONCLUSION AND RECOMMENDATIONS

6.1 Conclusion

The main objective of this research is to design and develop a mobile 3D printer, which is towards supporting large-scale collaborative additive manufacturing in practical fabrication environments. In order to achieve this objective, some reasonable technical solutions were proposed, and the causes of various categories of errors were analyzed and classified one by one. The concepts of "positioning error correction" and "leveling error correction" were introduced and combined with the technical solutions to control the two types of errors produced by "internal cause" and "external cause", respectively. According to the corresponding strategies, specific structural design and technical means were adopted to achieve error correction. A series of experiments have been conducted and verified the validity of the concepts in practical applications.

The developed mobile 3D printer consists of multiple modular systems that can be flexibly operated simultaneously or separately. In addition, the proposed concepts and strategies are equally applicable to other large-scale collaborative additive manufacturing conducted using different AM devices and fabrication conditions, and can be regarded as an optimized solution to improve the existing problems of this technology.

6.2 Recommendations

Although the concepts of "positioning error correction" and "leveling error correction" have been successfully introduced into large-scale collaborative additive manufacturing and have been shown to reduce errors indirectly caused by mobility, there are still some defects and space for optimization. One aspect is about the hardware. At present, the technical methods proposed for the corresponding concept combine the consideration of cost and efficiency, so the terminal precision is limited. However, in fact, there is

still room for improvement in the accuracy and stability of practical applications. Another aspect is about the software. Due to the modular characteristic of the current prototype being developed, there are multiple independent control systems, which can make the operation slightly complicated when conducting large-scale collaborative additive manufacturing. After the proposed concepts are formally applied to any product, an integrated control logic and system may need to be developed.

REFERENCES

- Guo, N., Leu, M.C. (2013). Additive manufacturing: technology, applications and research needs. *Frontiers of Mechanical Engineering*, 8, 215–243.
<https://doi.org/10.1007/s11465-013-0248-8>
- Sun, H., Peng, X., Yu, Z., Li, H., Zhang, S., Wu, Y., Fu, G. (2019). Design and application of multi-nozzle 3D printing teaching aids. *Mechanical Engineer & Automation*, 215, 110-112.
- Agranoff, R., McGuire, M. (2003). Inside the matrix: Integrating the paradigms of intergovernmental and network management. *International Journal of Public Administration*, 26(12), 1401–1422.
- Ranaweera, S. (2019). [Development of collaborative additive manufacturing]. Asian Institute of Technology.
- Shen, H., Pan, L., Qian, J. (2019). Research on large-scale additive manufacturing based on multi-robot collaboration technology. *Additive Manufacturing*, 30, p. 100906. <https://doi.org/10.1016/j.addma.2019.100906>
- Eric, B., Clement, G. (2015). Large-scale 3D printing with a cable-suspended robot. *Additive Manufacturing*, 7, 27-44.
<http://dx.doi.org/10.1016/j.addma.2015.05.001>
- Hunt, G., Mitzalis, F., Alhinai, T., Hooper, P.A., Kovac, M. (2014, May 31-July 7). 3D printing with flying robots. International Conference on Robotics & Automation, Hong Kong Convention and Exhibition Center, Hong Kong, China.
- Marques, L.G., Williams, R.A., Zhou, W. (2017). A mobile 3D printer for cooperative 3D printing. Proceedings of the 28th Annual International Solid Freeform Fabrication Symposium – An Additive Manufacturing Conference.
- Poudel, L., Zhou, W., Sha, Z. (2020). A generative approach for scheduling multi-robot cooperative three-dimensional printing. *Journal of Computing and*

- Information Science in Engineering, 20(6), p. 0611011.
<https://doi.org/10.1115/1.4047261>
- Zhang, X., Li, M., Lim, J.H., Weng, Y., Tay, Y.W.D., Pham, H. (2018). Large-scale 3D printing by a team of mobile robots. *Automation in Construction*, 95, 98-106.
<https://doi.org/10.1016/j.autcon.2018.08.004>
- Kevin, S., Thomas, B., Sebastien, G., Alexandre, A., Elodie, P., Benoit, F. (2018). Improvement of the mobile robot location dedicated for habitable house construction by 3D printing. *International Federation of Automatic Control*, 51-11, 716-721. <https://doi.org/10.1016/j.ifacol.2018.08.403>
- ISO/ASTM 52900. Additive manufacturing-General principles-Terminology. Geneva: International Organisation for Standardisation. Retrieved October 28, 2021, from <https://scholar.google.com/>
- Gibson, I., Rosen, D.W., Stucker, B. (2015). *Additive manufacturing technologies: 3D printing, rapid prototyping, and direct digital manufacturing*. 2nd ed.. New York: Springer-Verlag New York. <https://doi.org/10.1007/978-3-030-56127-7>
- Kruth, J.P., Leu, M.C., Nakagawa, T. (1998). Progress in additive manufacturing and rapid prototyping. *CIRP Annals*, 47(2), 525-540.
[https://doi.org/10.1016/S0007-8506\(07\)63240-5](https://doi.org/10.1016/S0007-8506(07)63240-5)
- Gao, W., Zhang, Y., Ramanujan, D., Ramani, K., Chen, Y., Williams, C.B., Wang, C.L., Shin, Y.C., Zhang, S. (2015). The status, challenges, and future of additive manufacturing in engineering. *Computer-Aided Design*, 69, 65-89.
<https://doi.org/10.1016/j.cad.2015.04.001>
- Winkless, L. (2015). Is additive manufacturing truly the future? *Metal Powder Report*, 70(5), 229-232. <https://doi.org/10.1016/j.mprp.2015.05.003>
- Petrovic, V., Gonzalez, J.V.H., Ferrando, O.J., Gordillo, J.D., Puchades, J.R.B., Grinan, L.P. (2011). Additive layered manufacturing: sectors of industrial application shown through case studies. *International Journal of Production Research*, 49(4), 1061-1079. <https://doi.org/10.1080/00207540903479786>
- Albar, A., Chougan, M., Kheetan, M.J., Swash, M.R., Ghaffar, S.H. (2020). Effective extrusion-based 3D printing system design for cementitious-based materials.

Results in Engineering, 6, p. 100135.

<https://doi.org/10.1016/j.rineng.2020.100135>

Gosselin, C., Duballet, R., Roux, P., Gaudilliere, N., Dirrenberger, J., Morel, P. (2016). Large-scale 3D printing of ultra-high performance concrete-a new processing route for architects and builders. *Materials and Design*, 100, 102-109. <https://doi.org/10.1016/j.matdes.2016.03.097>

Zuo, Z., Gong, J., Huang, Y., Zhan, Y., Gong, M., Zhang, L. (2019). Experimental research on transition from scale 3D printing to full-size printing in construction. *Construction and Building Materials*, 208, 350-360. <https://doi.org/10.1016/j.conbuildmat.2019.02.171>

Barnett, E., Gosselin, C. (2015). Large-scale 3D printing with a cable-suspended robot. *Additive Manufacturing*, 7, 27-44. <https://doi.org/10.1016/j.addma.2015.05.001>

Xiao, J., Ji, G., Zhang, Y., Ma, G., Mechtcherine, V., Pan, J., Wang, L., Ding, T., Duan, Z., Du, S. (2021). Large-scale 3D printing concrete technology: Current status and future opportunities. *Cement and Concrete Composites*, 122, p. 104115. <https://doi.org/10.1016/j.cemconcomp.2021.104115>

Mechtcherine, V., Nerella, V.N., Will, F., Nather, M., Otto, J., Krause, M. Large-scale digital concrete construction-CONPrint3D concept for on-site, monolithic 3D-printing. *Automation in Construction*, 107, p. 102933. <https://doi.org/10.1016/j.autcon.2019.102933>

Lu, S.C., Elmaraghy, W., Schuh, G., Wilhelm, R. A scientific foundation of collaborative engineering. *CIRP Annals*, 56(2), 605-634. <https://doi.org/10.1016/j.cirp.2007.10.010>

3D-Proto. (2014). Pt.1: Dual “parking” extruder for a Prusa i3 RepRap 3D printer / by 3D-Proto. <https://www.youtube.com/watch?v=9VlvsebqdhU>

Colgate, J.E., Peshkin, M.A., Wannasuphoprasit, W. (1996). [Cobots: Robots for collaboration with human operators]. Northwestern University.

Simoës, A.C., Soares, A.L., Barros, A.C. (2020). Factors influencing the intention of managers to adopt collaborative robots (cobots) in manufacturing

- organizations. *Journal of Engineering and Technology Management*, 57, p. 101574. <https://doi.org/10.1016/j.jengtecman.2020.101574>
- Bui, H., Pierson, H.A., Nurre, S.G., Sullivan, K.M. (2019). Tool path planning optimization for multi-tool additive manufacturing. *Procedia Manufacturing* 39, 457-464. <https://doi.org/10.1016/j.promfg.2020.01.389>
- Stillstrom, C., Jackson, M. (2007). The concept of mobile manufacturing. *Journal of Manufacturing Systems*, 26(3-4), 188-193. <https://doi.org/10.1016/j.jmsy.2008.03.002>
- Keating, S.J., Leland, J.C., Cai, L., Oxman, N. (2017). Toward site-specific and self-sufficient robotic fabrication on architectural scales. *Science Robotics*, 2(5). <https://doi.org/10.1126/scirobotics.aam8986>
- Kenger, Z.D., Koc, C., Ozceylan, E. (2021). Integrated disassembly line balancing and routing problem with mobile additive manufacturing. *International Journal of Production Economics*, 235, p. 108088. <https://doi.org/10.1016/j.ijpe.2021.108088>